Bacterial Microflora of the Cold-Water Coral *Lophelia pertusa* (Scleractinia, Caryophylliidae)

Bakterielle Mikroflora der Kaltwasser-Koralle *Lophelia pertusa* (Scleractinia, Caryophylliidae)

Dissertation
zur Erlangung des akademischen Grades
Doctor rerum naturalium (Dr. rer. nat.)
der
Mathematisch-Naturwissenschaftlichen Fakultät
der
Christian-Albrechts-Universität zu Kiel

vorgelegt von
Sven Christopher Neulinger

Kiel, im April 2008

Referentin: Prof. Dr. Karin Lochte

Korreferentin: Prof. Dr. Tina Treude

Tag der Disputation: 10. Juni 2008

Zum Druck genehmigt: 10. Juni 2008

…….

(Der Dekan)

"I am a firm believer that without speculation there is no good and original observation."

Charles Robert Darwin (1809-1882)

in a letter to Alfred Russel Wallace, 22 December 1857

Index

Summary

The pseudocolonial coral *Lophelia pertusa* (Scleractinia, Caryophylliidae) is a eurybathic, stenothermal cosmopolitan cold-water species. It occurs in two colour varieties, white and red. *L. pertusa* builds vast cold-water coral reefs along the continental margins, which are among the most diverse deep-sea ecosystems. Microbiology of *L. pertusa* has been in scientific focus for only a few years. The question whether the coral holds a host-specific bacterial community is not finally answered. Possible implications of the two colour varieties for microbial colonisation must be taken into account. Bio imaging can reveal the in-situ location of bacterial groups on and possible interactions with the coral. The present study aimed at investigating these aspects, drawing a more comprehensive picture of community structure, taxonomy, and in-situ location of *L. pertusa*-hosted microbes.

Bacteria on coral samples from the Trondheimsfjord (Norway) were characterised by the culture-independent 16S rDNA- and rRNA-based techniques T-RFLP, cloning and sequencing, and CARD-FISH. *L. pertusa* revealed a high microbial richness. Clone sequences were dominated by *α-* and *γ-Proteobacteria*. Other abundant taxa were *Bacteroidetes*, *Actinobacteria*, *Verrucomicrobia*, *Firmicutes*, and *Planctomycetes*. The bacterial community of *L. pertusa* differed conspicuously from that of the environment, but was not 'specific' *sensu stricto*. It was rather divided into a tissue-bound fraction that was spatially constant within the sampling area and a "liquid-associated" fraction in the mucus and gastric fluid varying with location and colour variety of its host. Parallels to other coral-bacterial associations suggested existence of certain 'cold-water coral-specific' bacterial groups *sensu lato*. *L. pertusa*-associated bacteria appeared to play a significant role in the alimentation of their host by degradation of sulphur compounds, cellulose, chitin, and end products of the coral's anaerobic metabolism. Different bacterial groups in red and white *L. pertusa* could explain the dissimilar dispersal of these two phenotypes by different nutritional strategies. Some microbes were regarded as opportunistic pathogens, others might even be connected to coral colouring. Filamentous bacteria in the gastrocoel were identified as bona fide TM7, whose tight binding to the endoderm implied exchange of metabolites with their host. A novel *Mycoplasma* species on the nematocyst batteries of the coral tentacles was proposed as "*Candidatus* Mycoplasma corallicola". This organism appeared to be a commensal that profits from the leakage of dissolved organic substances during prey capture activity of *L. pertusa*.

Kurzfassung

Lophelia pertusa (Scleractinia, Caryophylliidae) ist eine eurybathe, stenotherme Kaltwasserkoralle. Sie tritt als rote und weiße Farbvarietät auf. *L. pertusa* bildet ausgedehnte Kaltwasserriffe entlang der Kontinentalränder, die zu den artenreichsten Lebensräumen der Tiefsee zählen. Die Mikrobiologie von *L. pertusa* steht erst seit wenigen Jahren im Fokus des wissenschaftlichen Interesses. Die Frage, ob die Koralle eine wirtsspezifische Bakteriengemeinschaft beherbergt, ist nicht endgültig beantwortet. Mögliche Auswirkungen der unterschiedlichen Farbvarietäten auf die bakterielle Besiedlung der Koralle sind zu berücksichtigen. Bildgebende Verfahren können Aufschluss über die genaue Lage der Bakteriengruppen und mögliche Wechselwirkungen mit der Koralle geben. Ziel der dieser Arbeit ist es, diese Aspekte zu untersuchen und ein umfassenderes Bild der Struktur, Taxonomie und Verteilung der Bakteriengemeinschaft auf *L. pertusa* zu zeichnen.

Bakterien von Korallenproben aus dem Trondheimsfjord (Norwegen) wurden mit den kulturunabhängigen, auf 16S-rDNA und rRNA basierenden Methoden T-RFLP, Klonen und Sequenzierung, sowie CARD-FISH charakterisiert. *L. pertusa* wies eine reiche Bakterienflora auf. Klon-Sequenzen wurden von *a-* und *γ-Proteobacteria* dominiert. Klone von *Bacteroidetes*, *Actinobacteria*, *Verrucomicrobia*, *Firmicutes* und *Planctomycetes* waren ebenfalls zahlreich. Die Bakteriengemeinschaft von *L. pertusa* unterschied sich deutlich von jener der Umgebung, war jedoch nicht ‚spezifisch' i. e. S. Sie war unterteilt in eine innerhalb des untersuchten Gebietes konstante gewebeassoziierte Fraktion, sowie eine „flüssigkeitsassoziierte" Fraktion in Schleim und Gastralflüssigkeit. Letztere variierte abhängig von Standort und Farbe des Wirtes. Parallelen zu anderen Korallen-Bakterien-Assoziationen legten die Existenz ‚kaltwasserkorallen-spezifischer' Bakteriengruppen i. w. S. nahe. Die Bakterien auf *L. pertusa* schienen durch Abbau von Schwefelverbindungen, Zellulose, Chitin und Endprodukten des anaeroben Wirtsmetabolismus eine wichtige Rolle für die Ernährung der Koralle zu spielen. Unterschiedliche bakterienbedingte Ernährungsstrategien in roten und weißen *L. pertusa* könnten das abweichende Verbreitungsmuster dieser beiden Phänotypen erklären. Neben opportunistischen Pathogenen wurden auch Bakterien entdeckt, die für die Farbgebung der Koralle verantwortlich sein könnten. Fadenförmige Bakterien auf dem Endoderm, identifiziert als bona fide TM7, könnten Metabolite mit ihrem Wirt austauschen. Auf den Nematocysten der Tentakel profitierte „*Candidatus* Mycoplasma corallicola" offenbar kommensal von gelösten organischen Substanzen, die beim Beutefang von *L. pertusa* freigesetzt werden.

1 Introduction

1.1 The Cold-Water Coral *Lophelia pertusa*

The pseudocolonial scleractinian coral *Lophelia pertusa* (Linnaeus 1758) belongs to the family Caryophylliidae (Wells 1956). Though it is commonly referred to as a 'deep-water' or 'deep-sea' coral, this does not mean that it lives exclusively in deep oceanic water masses, but describes the ability of the coral to thrive at greater water depths in a cold and dark environment: Occurrence of this species is rather defined by temperature (4-12°C; preferred range, 6-8°C), salinity (~35-37 PSU), and dissolved oxygen (~3-5 $ml \cdot l^{-1}$) (Freiwald 1998, 2002). The coral grows from 39 m on the Tautra reef in the Norwegian Trondheimsfjord (Hovland and Risk 2003) down to 3000 m in the Atlantic (Squires 1959). In fact, *L. pertusa* inhabits shallow water only in Norwegian fjords (Strømgren 1971) because of the low depth of the thermocline (Freiwald et al. 1997). *L. pertusa* is thus a rather eurybathic, but stenothermal *cold-water* species, occurring in areas characterised by high biological production and vigorous hydrodynamic regimes (Rogers 1999).

The species occurs in two colour varieties (Fig. 1): white (transparent) and red (also referred to as "pink") (Dons 1944; Strømgren 1971). The question whether these two phenotypes differ genetically is still open, though the molecular phylogeny of *L. pertusa* and its population structure in the NE Atlantic have been addressed quite recently: The coral population in the NE Atlantic should not be considered panmictic (random-mating) but instead forms distinct offshore and fjord populations. The recruitment of sexually produced larvae appears to be strongly local (Le Goff-Vitry et al. 2004).

Like all scleractinian corals from such environments, *L. pertusa* has no algal endosymbionts and is thus termed 'azooxanthellate'. Stony corals lacking zooxanthellae are commonly called 'ahermatypic' (non-reef-building), as opposed to their 'hermatypic' relatives in shallow tropical waters. This denomination, however, disregards the ability of *L. pertusa* to build vast and complex thicket frameworks in the bathyal zone along the continental margins (Fig. 2). Though *L. pertusa*'s average linear extension rate of 5.5 $mm \cdot yr^{-1}$ (Mortensen and Rapp 1998) is far less than that of branching warm-water corals (100-200 $mm \cdot yr^{-1}$) (Buddemeier and Kienze 1976), its extreme long-

evity of estimated 200-366 years allows the coral to build colonies up to 1.5 m in height (Wilson 1979). Post-glacial *Lophelia* reefs developed over periods of 1,000-10,000 years (Rogers 1999).

Fig. 1: Red and white colour variety of *L. pertusa* growing entwined together with associated sponges at Tautraryggen (Tautra sill) in the Trondheimsfjord, Norway. Photo by courtesy of Erling Svensen (http://www.uwphoto.no).

Cold-water corals do not build large continuous reef structures like, e.g., the Great Barrier Reef off the East coast of Australia or the Belize Barrier Reef in the Caribbean Sea, but form rather discontinuous patches and banks. Nonetheless, the overall area covered by cold-water reefs exceeds by far the extent of their tropical coral reef counterparts (magenta areas in Fig. 2).

L. pertusa is the dominant coral in the NE Atlantic, forming giant carbonate mounds and reef patches along the continental margin from the North Cape to the Straits of Gibraltar (Mortensen et al. 1995; Freiwald 1998; Freiwald et al. 1999; Freiwald 2002). The coral is most abundant on the continental shelf in mid Norway at 200-400 m depth with largest densities along the continental break and on edges of shelf-crossing trenches (Fosså et al. 2002). Illustration of known cold-water coral reef locations (red points in Fig. 2) might convey the impression that the main

distribution of *L. pertusa* is confined to the North Atlantic. However, this appears to be merely a consequence of intensive research and mapping effort in this ocean region. As shown by the predictive distribution of *L. pertusa* (orange and yellow areas in Fig. 2), the species is rather assumed to be an abundant cosmopolitan, fringing the margins of all continents.

The importance of *L. pertusa* in reef-forming processes with respect to lithification was discussed, e.g., by Reitner (1993), and recently by Noé et al. (2005). Despite that, cold-water coral reefs have long been neglected in calculations of global carbonate production. $CaCO_3$ flux is 4%–12% of that in tropical reefs, and a preliminary global estimate indicates that cold-water coral $CaCO_3$ production could add >1% to the total marine $CaCO_3$ production (Lindberg and Mienert 2005). Given their assumed widespread occurrence (Fig. 2), cold-water reefs might constitute a significant carbonate sink.

Cold-water reefs are among the most diverse deep-sea ecosystems with more than 980 invertebrate species known to be associated with cold-water corals, belonging to a broad range of taxa: Foraminifera, Cnidaria, Nemertini, Polychaeta, Crustacea, Gastropoda, Bivalvia, and Ophiuroidae (Echinodermata) (Buhl-Mortensen and Mortensen 2004). Obviously, also sponges (Porifera) occur at least on some *Lophelia* reefs (Fig. 1). Though most of these organisms are not found exclusively on *Lophelia* banks, many of them are much less common in other habitats (Mortensen 2001).

Unfortunately, cold-water reefs are also highly endangered by human impact: Because the coral thickets provide habitat particularly for some commercially important fish and crustacean species (Roberts and Hirshfield 2004), they are sought grounds for industrial fishing. In the past, *Lophelia* reefs were exploited by long-line and gillnet fisheries (Fosså et al. 2002). While these traditional methods caused only limited damage to the coral framework, introduction of bottom trawling in the 20th century led to considerable reef destruction (Fosså et al. 2002; Hall-Spencer et al. 2002). Due to their slow growth (see above), recovery of cold-water reefs from these massive impacts is likely to be in the order of decades or even centuries (Roberts and Hirshfield 2004).

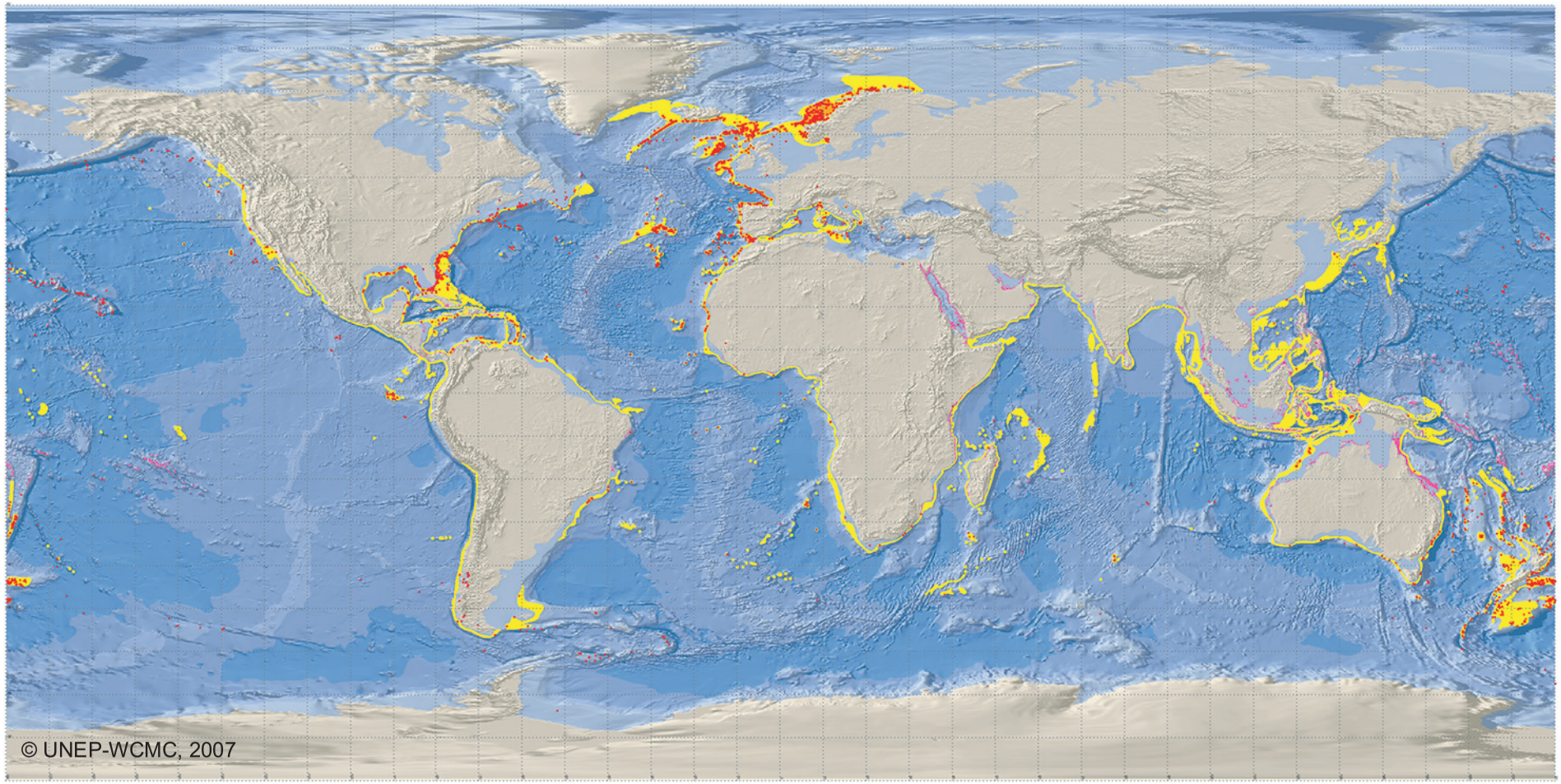

Fig. 2: Global distribution of known cold-water coral reefs (red), predictive distribution of *L. pertusa* (orange, very likely occurrence; yellow, conceivable occurrence), and distribution of warm-water reefs (magenta). Source: World Conservation Monitoring Centre of the United Nations Environment Programme (UNEP-WCMC). The map was modified graphically after compilation with the UNEP-WCMC IMapS tool (http://bure.unep-wcmc.org/marine/coldcoral/viewer.htm).

1.2 Coral-Associated Bacteria

Interactions between warm-water corals and bacteria have been observed for over seventy years: Yonge (1937) and Franzisket (1970) noticed that bacterial digestion of mucus could interfere with coral respirometric measurements. Corals are able to feed on bacteria from the water column (DiSalvo 1971). Sieburth (1975) described bacterial "lawns" covering the tissue surface of the ahermatypic coral *Astrangia danae*. Ducklow and Mitchell (1979) showed that the external mucus layer of certain stony reef corals is inhabited by communities of heterotrophic bacteria; population levels of these bacteria seem to be controlled by some host corals, and show response to stresses applied to the host. Santavy (1995) observed bacteria-filled ovoids in Caribbean *Porites astreoides* samples. Carbon source utilisation patterns of bacteria isolated from the mucus of various Caribbean corals exhibited species-specific mucus-associated microbial communities (Ritchie and Smith 1997).

It is still under debate whether such bacterial-anthozoan assemblages are specific and of ecological importance. Nevertheless, there are copious examples that microbes do not just dwell passively on a coral, but have noticeable impact on their host – for both its advantage and disadvantage: The observation that many tropical corals ingest their own mucus (Coles and Strathmann 1973) indicates that they take advantage from the ability of the mucus-inhabiting bacteria to scavenge low-concentrated nutrients (Knowlton and Rohwer 2003). Experiments suggest that bacterially driven nitrification takes place in the tissue of living hermatypic corals (Wafar et al. 1990). Diazotrophic bacteria in reef-building stony corals benefit from organic carbon excreted by the coral tissue, supplying their hosts with nitrogen-containing compounds (Williams et al. 1987; Shashar et al. 1994; Lesser et al. 2004). Hermatypic warm-water corals live in close symbiosis with dinoflagellate algae of the genus *Symbiodinium*, known as 'zooxanthellae', which are located intracellularly in the coral. In the oligotrophic, nutrient-limited environment of the tropical coral reef, both nitrogen fixation and nitrification – as a pathway of nitrogen recycling (Wafar et al. 1990) – are favourable for these zooxanthellae.

Among endolithic microborers inhabiting the corallum (=coral skeleton) of the Indo-Pacific shallow-water species *Porites lobata*, bacteria were shown to be responsible for breakdown of the organic skeletal matrix (DiSalvo 1969). More recently, the cyanobacterium *Plectonema terebrans* was found in both live and dead specimens of the same coral (Lukas 1974; Le Campion-Alsumard et

al. 1995). In the latter case, the consequence for the host can be considered ambivalent: On the one hand, *P. terebrans* weakens the internal structure of its host through biocorrosion; on the other hand, the coral may benefit from the nitrogen-fixing activity of the cyanobacterium as shown for other coral-diazotroph associations (Williams et al. 1987; Lesser et al. 2004). Hermatypic corals are prone to numerous bacterially induced diseases, among which are Coral Bleaching (Banin et al. 2000a; Banin et al. 2000b), Black Band Disease (Cooney et al. 2002; Frias-Lopez et al. 2002; Richardson and Kuta 2003), and White Plague (Bythell et al. 2002; Denner et al. 2003). Microbial surface fouling is another detrimental threat. Accordingly, many scleractinians and other anthozoans use antibiotic compounds to make chemical war on bacteria (Slattery et al. 1995; Koh 1997; Kelman et al. 1998; Wilsanand et al. 1999; Kelman et al. 2006). This kind of antagonism is fairly common in nature. Yet, it is stunning that substances produced in certain corals show activity against potentially pathogenic marine bacteria, but not against the associated microbes from the animal's tissue and mucus (Kelman et al. 1998). Thus, one may be apt to think that corals are able to differentiate between "enemy" and "friend". But, as Kelman et al. (1998) and Knowlton and Rohwer (2003) point out, the source of antimicrobial activity could again be the coral-associated bacteria themselves.

In recent years, molecular genetics has been increasingly applied to investigate the diversity and specificity of associations between bacteria and tropical reef corals. The culture-independent analysis of ribosomal RNA genes (16S rDNA) revealed a richness in prokaryotic gene sequence patterns comparable to that of the eukaryotic coral reef community (Rohwer et al. 2001; Frias-Lopez et al. 2002; Rohwer et al. 2002). These studies showed that coral-associated bacteria were not only different to water-column bacteria, but that different coral species harbour dissimilar bacterial communities, even when physically adjacent. Moreover, microbial patterns of the same coral species separated by time and space remained similar. These investigations strongly suggest that coral-bacterial associations are non-random.

1.3 Aims of this Study

Though bacteria may be of similar great ecological significance for *L. pertusa* as described above for warm-water scleractinians, the microbiology of this coral has been in scientific focus for only a few years. Microbial aspects of the bioerosion patterns in *L. pertusa* skeletons were presented by

Beuck and Freiwald (2005). Beside some preliminary investigations on *L. pertusa*-associated bacteria (Kellogg and Stone 2004; Kellogg 2006), Yakimov et al. (2006) were the first to publish phylogenetic data on metabolically active microbes in Mediterranean specimens of this coral. By means of clone libraries derived from reversely transcribed bacterial 16S rRNA, the authors could show that the sampled coral specimens sheltered a microbial community different from that of dead corals, sediment, or surrounding water. Spatial variation of the bacterial community on *L. pertusa* from the Mingulay-reefs in the Sea of the Hebrides was only recently observed by Großkurth (2007). The author also reported evidence for both antimicrobial and growth-stimulating factors that may permit *L. pertusa* to influence composition of its epibacterial community. Latest contribution was made by Schöttner et al. (2008), who characterised and compared the microbial consortia of *L. pertusa* by means of ARISA (Automated Ribosomal Intergenic Spacer Analysis) (Fisher and Triplett 1999). The authors found that various parts (surface, skeleton, mucus) of corals from in-situ (fjord slope, Norway) and ex-situ (maintenance tank) environments, ambient seawater, and proximal sediment each exhibited distinct community profiles. This suggested special relations between bacteria and the different habitats. All these studies show that living *L. pertusa* hosts special bacterial associations which are unlike those of the environment, and probably actively influenced by the coral. The associations appear to differ both with the partitioning of their host and with its habitat.

One prerequisite to call an observed coral-microbial association truly 'specific' is spatial constancy. Thus, the next step in understanding the microbiology of *L. pertusa* is to compare coral-associated bacteria not only from different stations within the *same* geographic region, but also from *different* geographic regions. Moreover, the existence of two colour phenotypes in *L. pertusa* and their possible implications for microbial colonisation must be taken into account. Finally, bio imaging can reveal the in-situ location of bacterial groups on the coral, providing insights in possible microbe-host interactions.

The present study aimed at investigating these points, drawing a more comprehensive picture of community structure, taxonomy, and in-situ location of *L. pertusa*-hosted microbes. Therefore, the following objectives were posed:

(1) Comparison of the bacterial assemblages of *L. pertusa* from the Trondheimsfjord in Norway with those of the surrounding environment. This fjord is a high-latitude environment comparable to those locations examined by the two latest studies (see above) but comprising the coral's shallowest habitat (Hovland and Risk 2003). It was thus important to know whether *L. pertusa* from that region harbours special bacteria as well.

(2) Determination of the variability of these assemblages with the coral's location in the Trondheimsfjord and with its colour variety, respectively.

(3) Identification of the dominant bacterial groups associated with *L. pertusa* and their potential ecological role.

(4) Locating the (tissue-associated) bacteria on *L. pertusa* by in-situ imaging.

Answers to these questions should illuminate the relations between *L. pertusa* and its associated bacteria. In particular, the issue whether this association is specific and implications for coral ecology (nutrition, health, dispersal, and colouring) were to be discussed.

1.4 General Strategy

Microbial variability on *L. pertusa* from the Trondheimsfjord was addressed by the following strategy: Sampling sites had to feature healthy cold-water corals that were not noticeably influenced by human activity. To account for intra-regional variability, sites were sampled that lay at least a few kilometres apart from each other, and at different depths. At each location, red and white corals were recovered to assess inter-phenotypic bacterial variance. To get a suitable number of parallels for reliable statistics, three coral colonies were randomly collected per station with three branches of healthy polyps sampled per colony. Thus, 9 samples per station and 27 samples in total were acquired with about equal numbers of red and white *L. pertusa* branches. To test whether bacteria found in *L. pertusa* were also ubiquitously present in the environment, water and sediment samples were taken from the adjacency of the corals.

The Trondheimsfjord in mid Norway was chosen as sampling region for the following reasons: Healthy and undisturbed *L. pertusa* reefs are known to grow at various locations within the fjord, including its shallowest habitat on the Tautra reef (Hovland and Risk 2003). Infrastructure of

Trondhjem Biological Station facilitated flexible land-based operation. The remotely operated vehicle (ROV) "Minerva" of the Norwegian University of Science and Technology in Trondheim was an ideal tool for the recovery of corals from deep locations. With the chartered research vessel "Vita" providing a dynamic positioning system, precise navigation of the ROV was ensured.

Marine prokaryotes are known for their extremely poor culturability (Amann et al. 1995). To overcome this problem, culture-independent approaches were employed to meet the proposed objectives (→ 1.3):

Objectives (1) and (2) were accomplished by Terminal Restriction Fragment Length Polymorphism (T-RFLP) (Liu et al. 1997) of the bacterial gene for the small ribosomal subunit RNA (16S rDNA). In this method, DNA of complex bacterial communities is amplified by polymerase chain reaction (PCR) with fluorescently labelled primers, and subsequently digested by a restriction enzyme. Bacterial groups differ in number and location of restriction sites on the gene, which results in restriction fragments (RFs) of different number and length for each group. These RFs are separated according to their length by gel electrophoresis in an automated gene sequencer. Only the fluorescently labelled terminal RFs (T-RFs) are detected by the machine, thereby reducing the high complexity of the RF pattern of a multi-species environmental sample. An electropherogram is produced with the T-RF signals that can be regarded as a 'genetic fingerprint' of the microbial community. Comparison of such 'fingerprints' from coral and environmental samples was a means to detect differences and variations in bacterial community patterns.

Detailed phylogenetic analysis (objective (3)) was based on cloning and sequencing of PCR-amplified prokaryotic 16S rDNA. This gene provides an excellent means of identification of bacterial species, as for it large nucleotide sequence databases and powerful tools for sequence comparison exist on the internet. Comparison with closely related organisms and evaluation of common features of a phylogenetic group allows to infer the ecological potential of coral-hosted bacteria, which was also part of objective (3).

The location of tissue-associated bacteria within the coral polyps (objective (4)) was determined by Fluorescence In-Situ Hybridisation (FISH) on coral thin sections. Stony corals exhibit a typical strong tissue autofluorescence that interferes with the signals of fluorescently labelled DNA

probes commonly used to detect bacteria in situ. To surmount this impediment, a special FISH technique named Catalysed Reporter Deposition Fluorescence In-Situ Hybridisation (CARD-FISH) (Schönhuber et al. 1997; Pernthaler et al. 2002) was used. CARD-FISH employs DNA probes labelled with horseradish peroxidase (HRP) at their 5' end. This HRP catalyses the deposition of fluorochrome-coupled tyramide molecules in the vicinity of the probe binding site (a 16S or 23S rRNA molecule). This technique, known as Tyramide Signal Amplification (TSA), provides up to 20-fold brighter signals relative to conventional monolabeled probes (Schönhuber et al. 1997), and thus enables detection of marked cells even against the bright coral tissue background.

2 Materials and Methods

2.1 Location and Sampling

2.1.1 Topographic, Hydrological, and Biological Aspects of the Trondheimsfjord

The Trondheimsfjord is located between 63°30'–64°N and 9°30'–11°30'E on the coast of mid Norway (Fig. 3). From the seaward Agdenes sill with a depth of 195m, three consecutive basins stretch to the inland: The *seaward basin* drops to the maximum depth of the fjord of 617 m immediately behind the Agdenes sill and has a mean depth of 212 m, followed by the large *middle basin* with a maximum depth of 440 m and a mean depth of 130 m. The innermost part, *Beitstadfjord*, is also the shallowest with a maximum depth of 210 m and a mean depth of 86 m (Jacobson 1983; Børsheim et al. 1999). The overall distance from the Agdenes sill to the end of Beitstadfjord is approximately 135 km, making the Trondheimsfjord the third largest in Norway.

Seasonal variation of the fresh water supply from various rivers affects the surface salinity. The less saline surface water is mixed with the more saline water from below while it moves seaward. This produces a residual compensating current below the surface layer known as 'estuarine circulation' (Jacobson 1983). Tidal currents up to 100 $cm \cdot s^{-1}$ at the Agdenes sill and up to 86 $cm \cdot s^{-1}$ at the Tautra sill (separating seaward and middle basin) have been measured (Jacobson 1983). Water masses below the surface layer in the fjord usually change twice a year, through the inflow of deep water in winter and an intermediate coastal water inflow at 20-70 m depth in late summer or early autumn (Jacobson 1983). Measurements of Børsheim et al. (1999) indicate that the water column of the seaward basin is de-stratified in midwinter, and stratification starts in spring. In the seaward fjord, below 100 m depth both temperature and salinity appear to be rather stable (7-8°C and 34-34.7 PSU, respectively) (Jacobson 1983; Børsheim et al. 1999). The euphotic zone of the Trondheimsfjord is not likely to exceed 20 m in depth (Sakshaug and Myklestad 1973).

Two spring blooms of diatoms are persistent from year to year in the area (Sakshaug and Myklestad 1973): The first one starts in March and culminates in early April, nourished mainly by nutrients accumulated during the winter. The second takes place in brackish waters during May-June. This bloom is kept in a physiologically more or less steady state for up to more than one

month apparently related to river floods due to snow melting. Through 'estuarine circulation' (see above) the seaward transport of phytoplankton is compensated for by a continuous replenishment of the populations, as in a chemostat system (Sakshaug and Myklestad 1973). High productivity favours the growth zooplankton, which in turn serves as prey for *L. pertusa* (cf. Kiriakoulakis et al. 2005). The coral occurs on the Agdenes reef complex in the seaward basin and on the Tautra sill. The Tautra reef complex is one of the world's shallowest cold-water coral reefs, reaching up to a depth of only 39 m below the sea surface. Because it has become a target for scuba diving and other activity, the reef has been protected by Norwegian law as a marine nature reserve on an interim basis, as of June 2000 (Fosså et al. 2002; Hovland and Risk 2003).

2.1.2 Sampling and Fixation

L. pertusa specimens were collected at three stations on the Tautra sill and in the seaward basin of the Trondheimsfjord, on 20 and 21 October 2004: (1) 'Tautra' (geographic position, 63°35'34"N, 10°31'4"W; depth, 54 m; temperature, 9.6°C; salinity, 30.1 PSU), (2) 'Stokkbergneset' (63°28'14"N, 9°55'8"W; 264 m; 8.1°C; 31.9 PSU), and (3) 'Røberg' (63°28'36"N, 9°59'43"W; 240 m; 8.1°C; 31.2 PSU). Station 'Tautra' was characterised by silty sediment. The sites 'Stokkbergneset' and 'Røberg', both with rocky steep slope, lay about 30 km further south-west to 'Tautra' at the transition to the sound connecting the seaward fjord basin and Norwegian Sea (Fig. 3). All sampling sites featured apparently healthy coral communities without signs of pollution or other direct human influence.

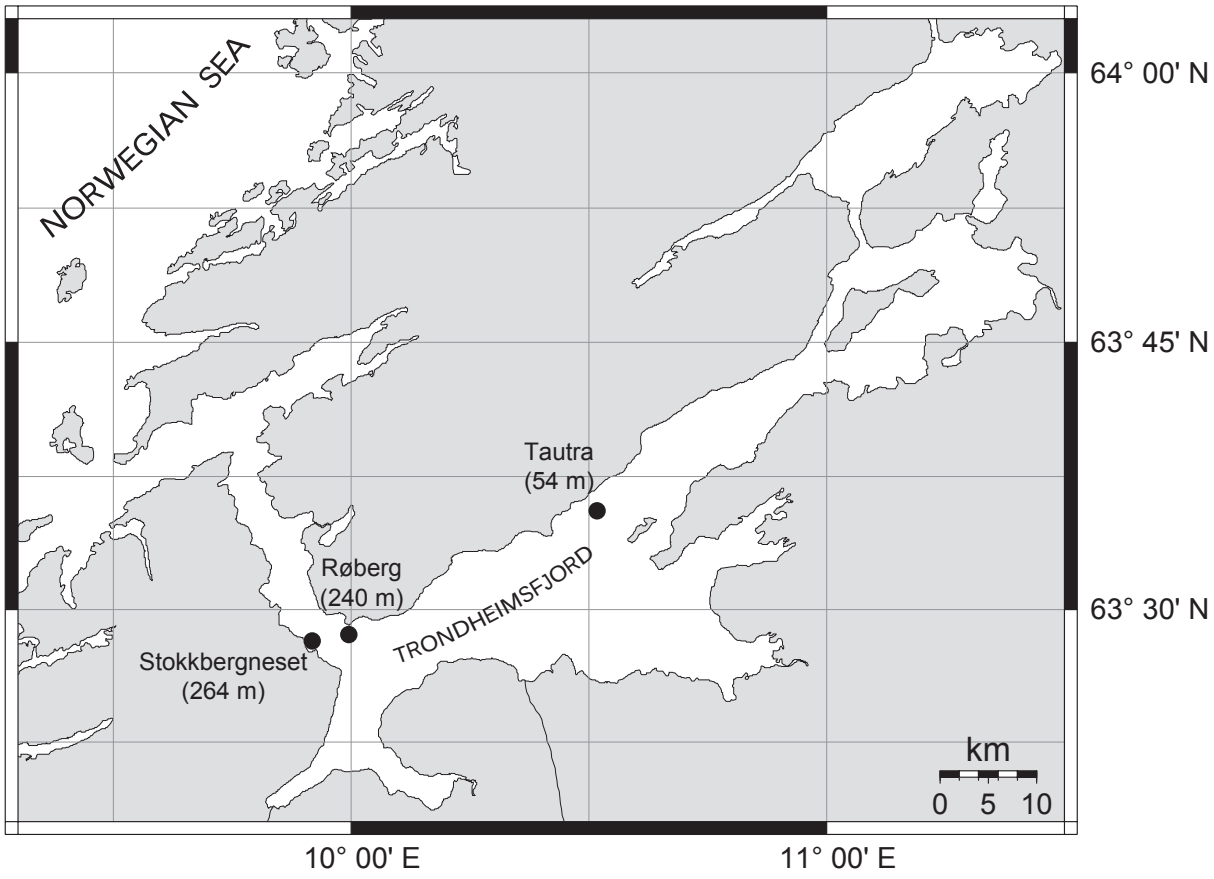

Fig. 3: Map of stations in the Trondheimsfjord (Norway) sampled for this study. The mean sampling depth is given in brackets for each station. (Created with Online Map Creation (OMC; http://www.aquarius.ifm-geomar.de/omc) based on The Generic Mapping Tools (GMT) (Wessel and Smith 1995).)

Sampling was accomplished with the SUB-Fighter 7500 remotely operated vehicle (ROV) "Minerva" from the Norwegian University of Science and Technology (NTNU), Trondheim, in cooperation with the ROV pilots J Järnegren from Trondhjem Biological Station (TBS) and M Ludvigsen from NTNU. A landing net attached to the ROV served as collection device. The net was cleaned after every sampling and also rinsed by the strong water current during the descent of the ROV, so cross-contamination by remains of coral debris and mucus from the previous sampling was unlikely to occur. Moreover, sampling of coral parts that had been in contact with the net was avoided. Three colonies (white and red colour varieties) were randomly collected at each station within a radius of about 10 m around the positions given above, and three living branches with 3-5 polyps were randomly taken per colony, summing up to a total of 27 coral samples (15 white and 12 red). The branches were rinsed with sterile filtered seawater to

remove loosely attached microbes from their surface, and individually put into sterile centrifuge tubes.

All coral samples were incubated in sterile filtered $MgCl_2$ solution to anaesthetise the coral polyps for 30 minutes. Anaesthesia was regarded as beneficial for FISH (→ 2.5) in order to prevent the polyps from full retraction, providing an unobscured view on the tentacles (cf. Bythell et al. 2002). Samples for DNA extraction were frozen at -20°C. Samples for FISH were incubated in a sterile filtered solution of 4% paraformaldehyde in PBS (phosphate-buffered saline: 8.0 g NaCl, 0.2 g KH_2PO_4, 1.15 g Na_2HPO_4, 0.2 g KCl, H_2O ad 1000 ml, pH 8.3) for 5-7 hrs, then transferred into 50% [v/v] ethanol in sterile filtered seawater and frozen at -20°C.

Two samples of surrounding water (1 L each) were collected about 1 m apart from the coral colonies at each station using a Niskin bottle that was attached to the ROV and disengaged remotely. Water samples were cooled to 4°C until return to the laboratory at TBS (4-6 hrs) and filtered through polycarbonate Nucleopore® membrane filters (0.2 µm pore size, ∅ 47 mm) (Whatman). The filters were frozen at -20°C in small Petri dishes. Two sediment samples were taken from the basis of two separate corals from station 'Tautra' and stored at -20°C in sterile centrifuge tubes. It was not possible to collect sediment samples at the other two stations because of their rocky steep slope.

For evaluation of the CARD-FISH method and the applied oligonucleotide probes the following bacterial test strains were used: DSM498 (*γ-Proteobacteria*, *Escherichia coli*); DSM347 (*Firmicutes*, *Bacillus subtilis*); environmental isolate, 98% 16S rDNA sequence similarity to type strain 022-2-10^T (*a-Proteobacteria*, *Erythrobacter vulgaris*); environmental isolate, 99% 16S rDNA sequence similarity to type strain ATCC 25495^T (*Actinobacteria*, *Streptomyces sampsonii*). All strains were cultured on agar plates and harvested during exponential growth phase (by courtesy of A Gärtner). After fixation with 4% formaldehyde in PBS (pH 8.3) at 4°C overnight, bacterial cells were spread onto polycarbonate Nucleopore® membrane filters (0.2 µm pore size, ∅ 47 mm) (Whatman) by vacuum filtration, and frozen at -20°C in small Petri dishes. Sections of these filters were processed the same way as coral thin sections in CARD-FISH (→ 2.5).

Freshly harvested polyps of aquarium-reared *L. pertusa* were used for testing the preparation and CARD-FISH procedure on the coral. These specimens were fixed in PBS with 4% formaldehyde for 5 hrs and immediately decalcified thereafter (→ 2.5).

2.2 DNA Extraction

Whole coral samples were pounded in liquid nitrogen with a mortar and pestle. To avoid carry-over of DNA from consecutive sample treatments, tools were sterilised with 3 M HCl and neutralised with sterile filtered PBS (pH 7.4). DNA was extracted from all sample types with the UltraClean™ Soil DNA Kit (Mo Bio). About 1 g of material (corals/sediment) and approximately one eighth of the polycarbonate filter area (corresponding to the filtrate of about 125 ml seawater) were employed in each extraction, respectively. To minimise DNA shearing, the 'alternative lysis method' proposed by the manufacturer (heating to 70°C instead of vortexing) was applied with 4 times elongated incubation as compared to the manufacturer's protocol.

2.3 T-RFLP

DNA amplification. PCR with template DNA from environmental and coral samples was conducted with the Phusion™ High-Fidelity PCR Kit (Finnzymes) according to manufacturer's instructions, and the *Bacteria*-specific primer 27f (5'-AGAGTTTGATCMTGGCTCAG-3') and universal primer 1492r (5'-GGTTACCTTGTTACGACTT-3'). This primer combination was chosen in order to amplify a broad range of bacterial 16S rDNA sequences. Archaea were not investigated in this study. Primers for T-RFLP were 5'-labelled with the fluorescent dyes 6-FAM (27f) and VIC (1492r), respectively. The total reaction volume was 20 µl, containing 6 µl of template DNA. Since it was impossible to measure the amount of bacterial DNA in the extract (because eukaryotic DNA was present, too), concentration of template DNA was adjusted to obtain clearly visible 16S-rDNA bands on the agarose gel (~10-50 ng per band, estimated by ethidium bromide staining): undiluted DNA extract from coral samples, 1:400 diluted DNA extract from sediment and water samples. PCR conditions were 3 min at 98°C; 35 cycles of: 10 sec at 95°C, 30 sec at 55°C, 45 sec at 72°C; 1 terminal elongation step of 5 min at 72°C. The number of cycles had been adjusted to get a clear signal of coral-derived bacterial PCR products in gel electrophoresis. Since this cycle number was kept constant in the whole assay, the PCR bias

as systematic error remained comparable for all samples. PCR products were obtained from all coral samples but one red from station 'Tautra', resulting in 26 coral PCR products.

Restriction digests. PCR products were purified by excision from a 1% agarose gel in Tris-Acetate-EDTA buffer and subsequent extraction with the NucleoSpin® Extract II Kit (Macherey-Nagel), and eluted from spin columns with 100 µl elution buffer. They were concentrated by conventional isopropanol precipitation and re-suspended with 30 µl elution buffer. The PCR products were digested with two restriction endonucleases commonly used in T-RFLP, Hha I and Alu I, respectively (New England Biolabs). 10 µl of purified PCR product were mixed with 10 µl of restriction enzyme master mix containing 5 U of the respective enzyme. Restriction reactions were incubated for 6 h at 37°C, followed by 20 min at 65°C to denature the enzyme.

Analysis. Restriction products were purified by ethanol precipitation and re-suspended in 12 µl of Hi-Di™ formamide (Applied Biosystems). For determination of fragment lengths ('size calling'), a size standard mix was prepared containing 5.9 µl of Hi-Di™ formamide and 0.1 µl of GeneScan® - 500 [ROX]™ size standard (Applied Biosystems) per sample. 6 µl of the size standard mix were merged with 6 µl of the re-suspended restriction product and denatured at 95°C for 5 min. T-RF signals were detected by capillary electrophoresis on an ABI PRISM® 310 Genetic Analyser with POP-6™ Polymer in a 30 cm capillary (Applied Biosystems) under the following conditions: injection time 15 sec, injection / electrophoresis voltage 15 kV, electrophoresis current ~7 mA, gel temperature 60°C, run time 44 min. Electropherograms were analysed with the program GeneScan® v2.0.2 (Applied Biosystems).

Statistics. Peak data of T-RFs between 30 and 500 nucleotides (nt) and signal intensities ≥50 (arbitrary units) were exported as tabular data from the Genetic Analyser. A data matrix was created from the combined Hha I and Alu I peak data with samples as columns and peak positions (T-RF lengths) as rows. The area under each peak was used as a measure of T-RF abundance, standardised as percentage of total peak area as described by Lukow et al. (2000). Due to rounding errors and minor variations in size determination, the length of defined T-RFs varied by ±1 nt among samples. Peaks were aligned within this range from their expected mean (cf. Lukow et al. 2000). Rows without T-RF data were deleted from the matrix. Two distance matrices were derived from the peak matrix employing (1) Manhattan distances and (2) percent mismatch

distances based on binary (presence – absence) data of peaks. Non-metric Multidimensional Scaling (MDS) was applied to ordinate samples in three dimensions according to the distance matrices. Statistical analyses were performed with (1) average peak numbers of the sample types and (2) the three MDS dimensions as independent variables, and 'sample type', 'station', and 'colour variety' (of the coral samples) as categorical predictors. The Shapiro-Wilk W statistic was used to test the variables for normality. With normally distributed variables, a multivariate analysis of variances (MANOVA) was performed, followed by Duncan's test for post hoc evaluation of significant differences. For non-normally distributed variables, non-parametric Kruskal-Wallis-ANOVA was applied, combined with the Mann-Whitney U test for post hoc evaluation. All statistics were executed with Statistica v6.1 (StatSoft).

2.4 Cloning and Sequencing

DNA amplification. For cloning, DNA extracts of all three stations were pooled according to environmental sample type (water / sediment) and colour variety (corals). In a first step, three parallel PCRs were conducted for each pool (water / sediment / white corals / red corals), each with a total reaction volume of 20 µl containing 6 µl (corals) or 1 µl (water / sediment) of undiluted DNA extract as template. PCR was conducted with the Phusion™ High-Fidelity PCR Kit (Finnzymes) according to manufacturer's instructions and primers 27f and 1492r. PCR conditions were 3 min at 98°C; 20 cycles of: 10 sec at 95°C, 30 sec at 55°C, 45 sec at 72°C; 1 terminal elongation step of 5 min at 72°C. PCR products of the three parallels were pooled and purified as described above (→ 2.3, Restriction digests). Elution from spin columns was done in 25 µl elution buffer. In a second step, the purified PCR products were re-amplified in a total reaction volume of 50 µl containing 6 µl of template DNA (all samples). PCR conditions were 3 min at 98°C; 10 (water / sediment) or 20 (corals) cycles of: 10 sec at 95°C, 30 sec at 55°C, 45 sec at 72°C; 1 terminal elongation step of 5 min at 72°C. This two-step procedure aimed at obtaining high quality PCR products for cloning while reducing formation of chimeric sequences.

Cloning. PCR products were purified and precipitated as described above (→ 2.3, Restriction digests). Cloning was carried out with the TOPO TA Cloning® Kit for Sequencing with One Shot® TOP10 Chemically Competent *E. coli* (Invitrogen). This kit was preferred for its high reliability, but it required DNA inserts with a 3' adenosine overlap for ligation with the cloning

vector. Since the Phusion™ polymerase produces blunt-ended PCR products, a terminal deoxy-adenosine had to be added to the 3' ends of the amplified DNA prior to ligation. For this purpose, the natural non-template-dependent terminal transferase activity of *Taq* polymerase was exploited: PCR products were incubated in 50 µl of 1x ThermoPol buffer (New England Biolabs) with 1 Unit of *Taq* DNA Polymerase (New England Biolabs) and 200 µM dATP (Roche) for 30 min at 72°C. After terminal adenosine addition, PCR products were purified and precipitated as described above (→ 2.3, Restriction digests) and re-suspended with 25 µl elution buffer. Purified products were ligated into the vector, followed by transformation of competent *E. coli* according to manufacturer's instructions. Cells were spread onto LB agar-plates amended with kanamycin (recipe given in the TOPO TA Cloning® Kit manual) and grown at 37°C overnight. Clone forming units were separated into 96-well plates filled with liquid LB medium, and re-grown at 37°C overnight. Cloned 16S rDNA inserts were re-amplified with the primer pair T3 / T7 (contained in the cloning kit). The total reaction volume was 45 µl containing 0.5 µl of *E. coli* cell suspension, 1 U of *Taq* DNA Polymerase (New England Biolabs), 0.1 µM of each primer, 50 µM of each dNTP, and 1x ThermoPol buffer. PCR conditions were 5 min at 95°C; 35 cycles of: 10 sec at 95°C, 30 sec at 55°C, 1 min at 72°C; 1 terminal elongation step of 10 min at 72°C. Aliquots of 5 µl were taken from each PCR product and tested for their correct length (about 1,600 base pairs, including the T3 and T7 priming sites) by agarose gel electrophoresis.

Sequencing. PCR products from clones showing correct length were sequenced at the Institute for Clinical Molecular Biology at Kiel University Hospital (Kiel, Germany). Purification of PCR products and sequencing procedure were as described by Gärtner et al. (2008). Partial sequences were obtained by sequencing with primer 27f. For nearly complete sequences, PCR products were additionally sequenced with primer 1492r, followed by assembling of the two overlapping partial sequences.

Phylogenetic analysis. Sequence data were visually checked for quality issues. Putative chimeric sequences were detected and eliminated using the online tools Chimera Check v2.7 of the Ribosomal Database Project II (RDP II) release 8.1 (Cole et al. 2003) and the Bellerophon chimera detection program (Huber et al. 2004). The sequence classifier of RDP II release 9 (http://rdp.cme.msu.edu/classifier/classifier.jsp) (Cole et al. 2007) and BLAST (Basic Local Alignment Search Tool; http://www.ncbi.nlm.nih.gov/blast/Blast.cgi) (Altschul et al. 1990) were

used for classification of the bacterial sequences and determination of closest relatives. The latter were obtained from the EMBL nucleotide sequence database (http://srs.ebi.ac.uk/) (Kulikova et al. 2004). Data of sequences from this study, their closest relatives, and sequences of coral-associated bacteria from other studies were imported into a sequence library of ARB v2.5b (Ludwig et al. 2004) and aligned according to 16S rRNA secondary structure information. A positional mask was applied that only allowed for unambiguously alignable sequence positions in all following phylogenetic assays. This mask comprised *E. coli* 16S rRNA positions (Brosius et al. 1981) 28-68, 101-183, 220-451, 480-838, 848-1003, 1037-1134, 1140-1440, and 1461-1491. Aligned sequences were incorporated into the phylogenetic 'backbone' tree of the ARB library consisting of over 52,000 sequences, using parsimony as inference method. Sequences were grouped into operational taxonomic units (OTUs) if the proportion of identical sequence positions shared between any two of them was ≥97%, which corresponds approximately to affiliation with the same species (Stackebrandt and Goebel 1994). A rarefaction analysis was conducted, applying the algorithm of Hurlbert (1971) implemented in the program aRarefactWin (http://www.uga.edu/~strata/software/). Theoretical coverage of microbial diversity in the different sample types was estimated from rarefaction curves with the method of Thiel, Neulinger et al. (2007b) (→ Appendix). A maximum likelihood tree with sequences of interest was calculated with 100 bootstrap replicates using the program PHYML (Guindon and Gascuel 2003). To ensure clearness and reliability of this tree, a subset of 133 sequences from the initial ARB alignment was used. This subset contained only reference sequences of relevant OTUs from this study, sequences of coral-associated bacteria from other studies, and reference sequences. An OTU was considered 'relevant' if it (1) comprised at least two sequences from this study that were not from water or sediment clones, or (2) was related to a sequence of a coral-associated bacterium form another study. The corresponding subset of the ARB 'backbone' tree was used as starting tree in PHYML sustaining topology and branch lengths. The most appropriate model of nucleotide substitution for the maximum likelihood calculation was determined with the program ModelGenerator v0.84 (Keane et al. 2006). A detailed phylogeny for classification of *L. pertusa*-hosted *Mycoplasmataceae* was calculated the same way. For comparison of results from cloning and T-RFLP the T-RFs of clone sequences were determined in silico with the tool TRF-CUT (Ricke et al. 2005) integrated in ARB.

Nucleotide sequence accession numbers. Reference clone sequences of all OTUs from *L. pertusa* samples and clone sequences from water and sediment samples obtained in this study were deposited in the EMBL nucleotide sequence database (Kulikova et al. 2004) under accession numbers AM911346-AM911622.

2.5 Fluorescence In-Situ Hybridisation

Decalcification and thin sectioning. The polyps had to be decalcified for CARD-FISH, since the carbonate of the corallum would have hampered thin sectioning as well as epifluorescence microscopy (see below) because of its autofluorescence. Coral branches were decalcified in 20% [w/v] EDTA in PBS (pH 8.3). The solution was changed 2-3 times over two days until the coral skeleton was completely dissolved and polyps remained connected only by the coenosarc. The polyps were then singularised and dehydrated in a graded ethanol/xylene series (ethanol 70% – 90% – 95% – 2×100%, xylene 3×100% [v/v]) at room temperature (RT) for 20 min each step, followed by 2× infiltration in paraffin at 60°C for 10 min each and paraffin embedding in cuboid tin foil molds. Series of 4-5 longitudinal sagittal sections (6-10 µm) of the embedded polyps were immobilised onto SuperFrost Plus slides (Menzel) (2 series per slide). They were de-paraffinated by heating to 60°C and immediate washing in pure xylene and ethanol for 30 sec each step.

Permeabilisation and peroxidase inactivation. Coral thin sections were re-hydrated in ethanol (100% – 70% [v/v]) and H_2O for 30 sec each step. To avoid merging of liquids on the slide, thin sections were framed with a hydrophobic border using a paraffin crayon. Bacterial cell walls were permeabilised by incubation in 100-200 µl lysozyme buffer ($1.355 \cdot 10^6$ U·ml^{-1} lysozyme (Serva), 500 mM EDTA (pH 8.0), 300 mM Tris-HCl (pH 8.0), H_2O ad 100% [v/v]) at 37°C for 2 hrs. After washing with H_2O at RT for 3×1 min, some samples were additionally permeabilised with 100-200 µl achromopeptidase buffer (60 U·ml^{-1} achromopeptidase (Sigma), 10 mM NaCl, 10 mM Tris-HCl (pH 8.0), H_2O ad 100% [v/v]) at 37°C for 1 hr. Slides were again washed with H_2O at RT for 3×1 min and air-dried. For inactivation of endogenous peroxidases, thin sections were incubated in 100-200 µl of 3% [v/v] H_2O_2 at RT for 30 min, followed by washing with H_2O at RT for 3×1 min, air-drying, and storage at -20°C until further processing.

Hybridisation. HRP-labelled oligonucleotide probes (Table 1) were purchased from biomers.net (http://www.biomers.net). The lyophilised probes were rehydrated in H_2O, quantified with a NanoDrop ND-1000 spectrophotometer (Thermo Fisher Scientific), and adjusted to 50 ng·µl^{-1} (probe working solution). The hybridisation buffer consisted of 20-60% [v/v] formamide (depending on the probe, see Table 1), 900 mM NaCl, 20 mM Tris-HCl (pH 8.0), 10% [w/v] dextran sulphate (Sigma), 0.01% [w/v] sodium dodecyl sulphate (SDS), 10% [v/v] blocking solution, and H_2O ad 100% [v/v]. The blocking solution was made of 10% [w/v] blocking reagent for nucleic acid hybridisation (Roche), 1.16% [w/v] maleic acid (Fluka), 150 mM NaCl, and H_2O ad 100% [v/v], pH 7.5. 100-200 µl of a 1:200 [v/v] mixture of probe working solution and hybridisation buffer were spread onto the thin sections.

Table 1: Oligonucleotide probes used in FISH for identification of bacterial populations. Names, targeted taxa, targeted rRNA molecules and sites, and sequences of the probes, and the formamide concentrations in the hybridisation buffer required for specific in-situ hybridisation are stated.

Probe	Target group	Target rRNA	Target site[2)]	Sequence (5'→3')	% formamide	Reference
ALF968	*α-Proteobacteria*	16S	968–985	GGTAAGGTTCTGCGCGTT	45	Neef (1997)
EUB338 I	most *Bacteria*	16S	338–355	GCTGCCTCCCGTAGGAGT	55	Amann et al. (1990)
EUB338 II	*Planctomycetes*	16S	338–355	GCAGCCACCCGTAGGTGT	55	Daims et al. (1999)
EUB338 III	*Verrucomicrobia*	16S	338–355	GCTGCCACCCGTAGGTGT	55	Daims et al. (1999)
GAM42a	*γ-Proteobacteria*	23S	1027–1043	GCCTTCCCACATCGTTT	50	Manz et al. (1992)
BET42a[1)]	*β-Proteobacteria*	23S	1028–1043	GCCTTCCCACTTCGTTT	50	Manz et al. (1992)
HGC236	*Actinobacteria*	16S	236–253	AACAAGCTGATAGGCCGC	30	Erhart et al. (1997)
LGC0355	*Firmicutes*	16S	355–373	GGAAGATTCCCTACTGCTG	45	Hallberg et al. (2006)
LGC0355b	*Mycoplasmataceae*	16S	355–373	GGAATATTCCCTACTGCTG	35	this study
MYC850	*Mycoplasmataceae* from this study	16S	850–867	CGTTAGCTACGCCAGTGA	—[3)]	this study
NON338	— (control)	—	—	ACTCCTACGGGAGGCAGC	55	Wallner et al. (1993)

[1)] Used as unlabeled competitor with probe GAM42a.
[2)] *E. coli* numbering (Brosius et al. 1981).
[3)] No signal with 20% formamide.

Slides were incubated at 35°C for 3-4 hrs in a vapour saturated repository and subsequently washed in Falcon tubes containing 50 ml of washing buffer at 37°C for 5 min. The washing buffer consisted of NaCl (concentration corresponding to the amount of formamide in the hybridisation buffer, see Table 2), 20 mM Tris-HCl (pH 8.0), 5 mM EDTA (pH 8.0), 0.01% [w/v] SDS, and H_2O ad 100% [v/v].

Table 2: Concentration of NaCl in the washing buffer corresponding to the amount of formamide in the hybridisation buffer. Concentrations are determined for stringent washing at 37°C after hybridisation at 35°C.

% formamide in hybridisation buffer	mM NaCl in washing buffer
20	135
25	95
30	64
35	42
40	27
45	16
50	9
55	3
60	0

Tyramide Signal Amplification (TSA). Cyanine 3 (Cy3) and fluorescein tyramide conjugates from TSA™ Tyramide Reagent Packs (PerkinElmer) were dissolved according to the manufacturer's instructions. The amplification buffer contained 10% [v/v] blocking solution (see above), 2 M NaCl, 10% [w/v] dextran sulphate, 0.0015% [v/v] H_2O_2, and PBS (pH 7.3) ad 100% [v/v]. Thin sections were equilibrated with PBS (pH 7.3) at RT for 15 min. 100-200 µl of a 1:500 [v/v] mixture of tyramide solution and amplification buffer were spread onto the thin sections. Incubation of the slides at 46°C for 30 min in a dark, vapour saturated repository was followed by washing with PBS (pH 7.3) at RT for 20 min and H_2O at RT for 3×1 min.

Double hybridisation. Simultaneous marking of bacteria with two different probes was accomplished as follows: After the first signal amplification with Cy3 tyramide HRP was inactivated with H_2O_2 as described above. Then a second hybridisation and signal amplification with fluorescein tyramide was carried out. In a parallel treatment, probe NON338 was used for the second hybridisation to prove that these signals did not result from persisting HRP activity of the first hybridisation.

Mounting. Air-dried thin sections were covered in mountant (80% [v/v] Citifluor AF1 (Citifluor Ltd.), 14% [v/v] VECTASHIELD® Mounting Medium (Vector Laboratories), 1 $\mu g \cdot ml^{-1}$ 4',6'-diamidino-2-phenylindole (DAPI) (Sigma), and PBS (pH 9) ad 100% [v/v]) and stored at -20°C until microscopic analysis.

Microscopy and image processing. Thin sections were viewed on a Leitz DMRB epifluorescence microscope, equipped with filter sets A, N2.1, and I3 (for fluorescence detection of DAPI,

Cy3, and fluorescein, respectively), and 40× and 100× PL FLUOTAR objectives (all from Leica). Image stacks were taken with a digital still camera by advancing the focus layer through the z-axis of the whole thin section in steps of ~2 μm and ~1 μm for the 40× and 100× objective, respectively. Deconvolved composite images were produced from these stacks with the software Helicon Focus v4.21 (Helicon Soft Ltd.). Overlay images for the simultaneous display of fluorescence signals of different dyes were produced with Photoshop® CS (Adobe).

Probe specificity assay. To cross-check specificity of the newly designed probe LGC0355b, a culture of *B. subtilis* DSM347 (which has the probe LGC0355 target site) was hybridised with probes LGC0355 and LGC0355b, respectively, each with 35% formamide. Signal brightness was compared between the two approaches after TSA with Cy3 tyramide. As bacterial cultures harvested during their exponential growth phase have a vast number of ribosomes, even sub-optimal probe binding results in bright fluorescence signals. This makes it difficult to assess brightness differences with the naked eye. Therefore, digital image analysis was employed to compare signal intensities: Of each hybridisation five digital images from filter sections densely covered with bacteria were taken with identical camera settings. Cumulative histograms of pixel brightness values were obtained with ImageJ v1.37 (Rasband 1997-2007). To ensure that results were not biased by dark spaces between the bacterial cells or pixel super saturation, only intermediate brightness values between 80 and 165 (arbitrary units) were taken into account.

3 Results

3.1 T-RFLP

3.1.1 Comparison of Coral and Environmental Samples

T-RFLP, like other PCR-based fingerprinting methods, generates datasets (patterns, electropherograms; Fig. 4) that relate each signal (peak) – in the best case – to a single taxon (Casamayor et al. 2002). T-RFLP analysis of this study yielded such datasets for 26 coral, 6 water, and 2 sediment samples. A total of 517 different electropherogram peak positions were observed. Overlay plots of electropherograms from the three sample types are shown for restriction enzymes Hha I (Fig. 4 a) and Alu I (Fig. 4 b) in combination with primer 27f. The figure gives an impression of what the raw data obtained from the genetic analyser looked like. However, it does neither provide a detailed view due to the limited resolution of the graphic, nor does it allow direct comparison of relative peak intensities. Analyses were therefore solely conducted on the peak matrices.

Comparative values for T-RF profiles of the different sample types are summarised in Table 3. In the peak matrix, 167 (32.3%) peaks belonged exclusively to corals, while the others were shared with sediment (34 peaks, 6.6%), water (49 peaks, 9.5%), or both (78 peaks, 15.1%), summing up to a total of 161 shared peaks (31.1%).

Table 3: Absolute and relative numbers of T-RFLP peaks shared by the respective sample types.

corals only	sediment only	water only	corals + sediment	corals + water	sediment + water	all samples	∑
167	85	74	34	49	30	78	517
32.3%	16.4%	14.3%	6.6%	9.5%	5.8%	15.1%	100.0%

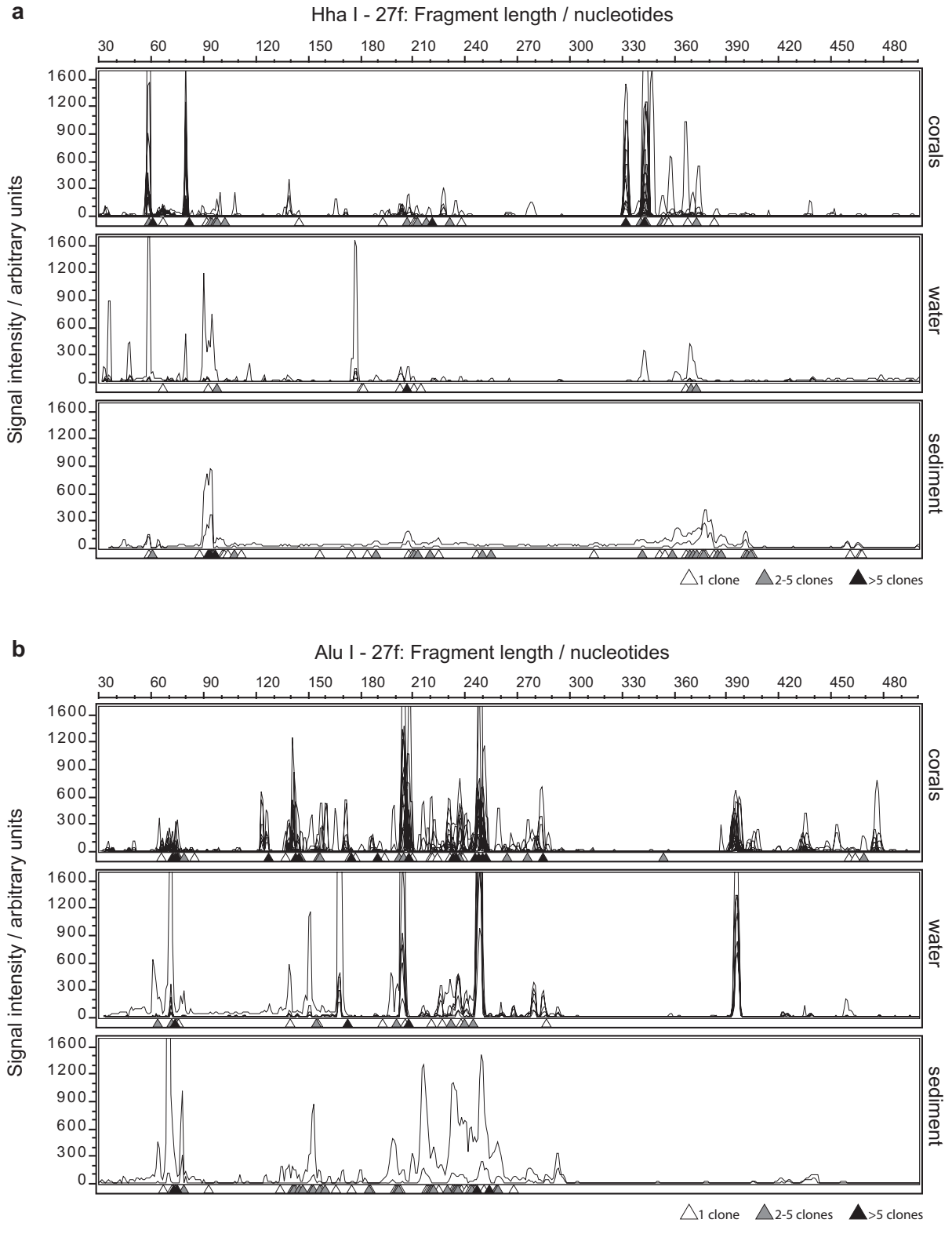

Fig. 4: T-RFLP chromatograms produced by restriction enzymes Hha I (a) and Alu I (b) in combination with primer 27f. All chromatograms of a respective sample type were combined to a single overlay plot to illustrate the overall pattern. T-RFs of clone sequences (→ 3.2.2) as determined by TRF-CUT are indicated as triangles at the respective positions.

The average number of peaks per sample was highest for sediment (150.5), followed by water (83.8), red (54.3) and white (39.4) coral samples. Significance of these differences was tested by Kruskal-Wallis-ANOVA and Mann-Whitney U test, because the distribution of average peak numbers deviated from normality. Kruskal-Wallis-ANOVA indicated significant differences between average peak numbers of the respective sample types ($p < 0.01$). However, the divergence between average peak numbers of red and white coral samples was insignificant according to the Mann-Whitney U test.

Non-metric Multidimensional Scaling (MDS) is used in data visualisation for exploring similarities or dissimilarities between items. In this case the items were coral and environmental samples and the measure of dissimilarity was the Manhattan or percent mismatch distance between any pair of samples based on their T-RFLP peak patterns. Manhattan distance is more robust to outliers than the conventional Euclidean distance measure in the case of normalised peak areas, while percent mismatch measure is particularly suited for binary (presence – absence) data. For comparison of N items a matrix of $N \cdot (N-1)/2$ pairwise distances has to be constructed. A diagram with up to N-1 dimensions would be needed to visualise the distances between all items correctly, which can become impractical for $N > 4$. MDS takes the distance matrix as input and yields a smaller matrix of item 'dimensions', the configuration of which minimises a loss function called 'stress'. Coordinates are plotted in a diagram with 2 or 3 dimensions. Proximity of the items to each other in the diagram indicates how similar they are. The fewer dimensions, the easier it is to interpret the results, but also the worse is the statistical fit. The stress value reported along with each ordination specifies the quality of preservation of the original distance values in the diagram: Following Clarke (1993), stress values < 0.10 indicates an ideal preservation, i.e., the configuration of items is close to their actual distances. A stress value ≤ 0.15 still means a good ordination. Higher values (around 0.20) indicate that the original relations between items are depicted in an exceedingly contorted manner and details of the plot should not be over-interpreted.

MDS is an appropriate means for the exploration of relationships between biological samples, because the method does not assume normal distribution of the raw data. This property is almost never met by biological data in general and T-RFLP patterns in particular. On the other hand, the resulting coordinates often feature normal distribution and can be used as input for further statistical analyses.

For clearness, of the three dimensions calculated by MDS only the two with the most conspicuous differences were plotted in the following diagrams. Coral, water, and sediment samples of all stations were clearly separated from each other by MDS based on normalised peak areas (Fig. 5 a) (stress: 0.10). Data points clustered closely together within their respective sample type with no overlap between different sample types. This separation of coral, water, and sediment samples was corroborated by MANOVA ($p < 0.00$). A similar picture was given by MDS based only on the presence or absence of T-RFs, so-called 'binary' peak data (Fig. 5 b) (stress: 0.05), though this analysis led to greater scattering as compared to MDS based on normalised peak areas. The two more remote sample points in question (one from water and one from sediment) belonged to samples with above-average peak numbers in their T-RFLP profiles. For binary peak data the same clear separation of sample types as for normalised peak data was confirmed by Kruskal-Wallis-ANOVA ($p < 0.00$ for dimensions 1 and 2).

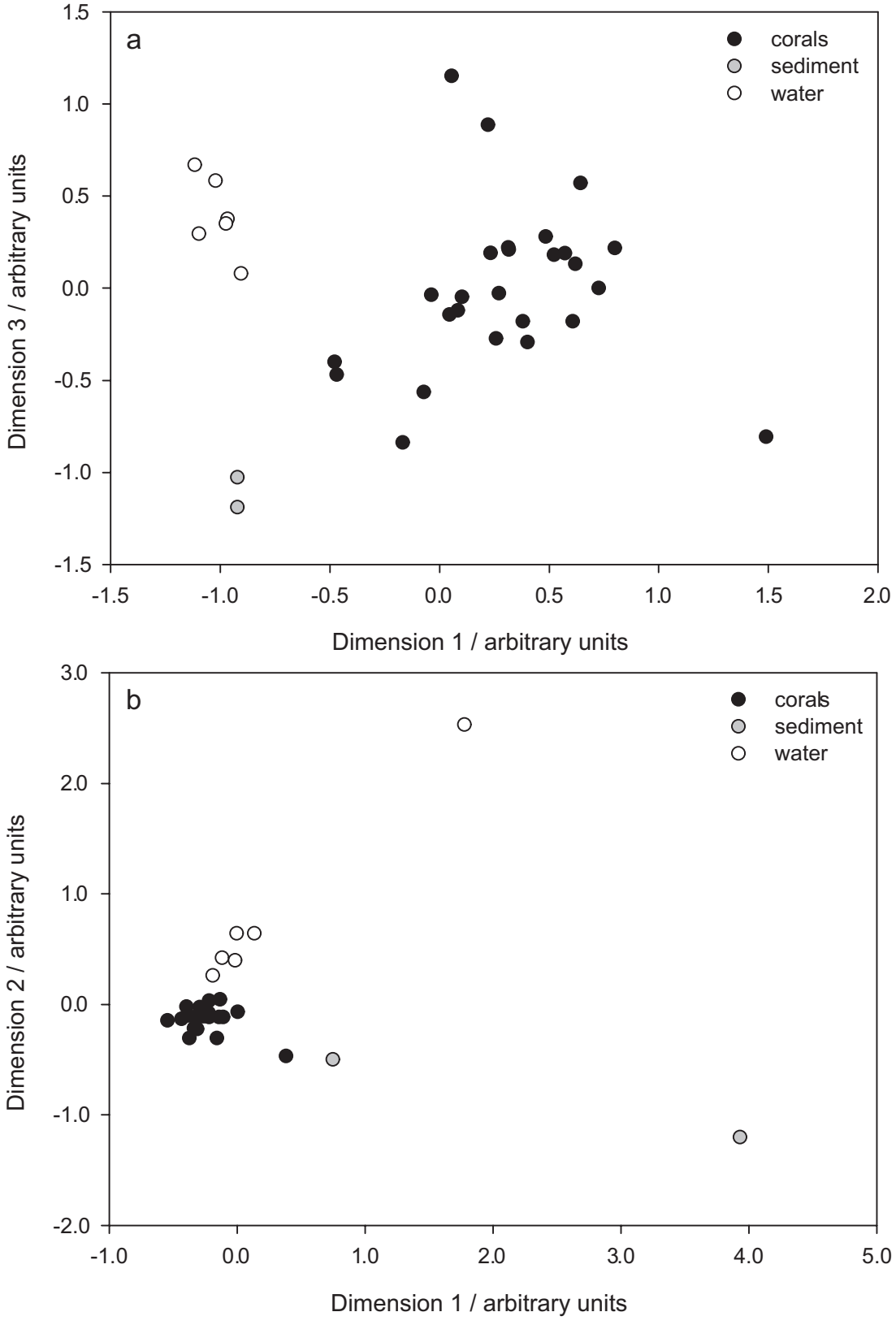

Fig. 5: Multidimensional scaling (MDS) ordination of coral (26 data points), sediment (2 data points), and water samples (6 data points). Ordination was based on Manhattan distances (a) and percent mismatch distances (b) derived from the T-RF peak matrix. For clearness, of the three calculated MDS dimensions only the two with the most conspicuous differences were plotted. Stress values for dimensional downscaling were 0.10 (a) and 0.05 (b), respectively.

3.1.2 Differences between Coral Samples

For analysis of coral samples, T-RFs were divided into two categories: (1) 'rare' peaks occurring in less than one third (<9) of the coral samples (291 T-RFs) and (2) 'consistent' peaks occurring in at least one third (≥9) of the coral samples (37 T-RFs). Fig. 6 illustrates that, though only about one out of nine coral-derived T-RFs was consistent according to the above definition, the second category comprised all dominant peaks (i.e., peaks with highest relative abundance values).

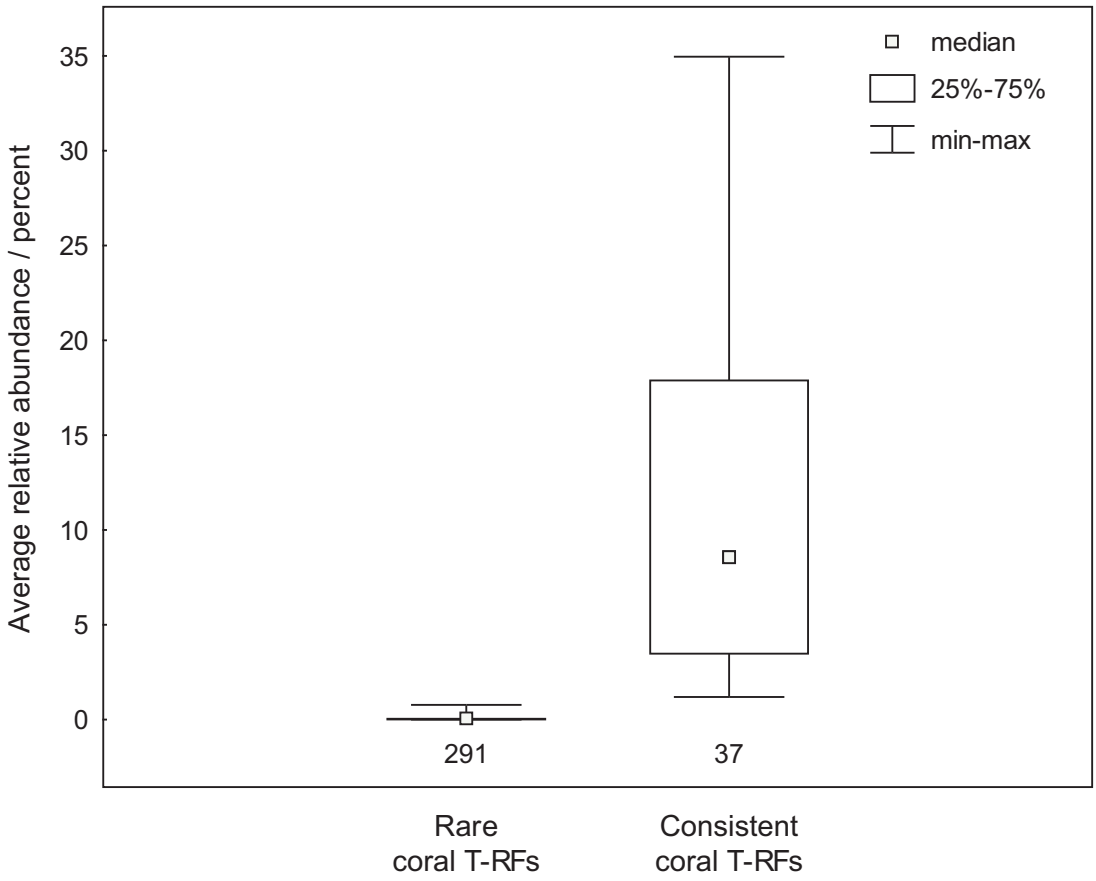

Fig. 6: Distribution of average relative abundances for rare and consistent coral T-RFs. For each distribution the median, central quartiles (25%-75%), and extremes (min-max) are plotted. The number of T-RFs falling into the respective category is stated below the box plots.

MDS dimensions derived from relative abundances of rare peaks (stress: 0.12) (not shown) deviated considerably from normal distribution. Kruskal-Wallis-ANOVA revealed significant differences between stations in dimension 1 ($p < 0.01$). Pairwise comparison by the Mann-Whitney U test denoted the differences between stations 1 and 2 ($p = 0.03$), and between stations 2 and 3 ($p < 0.01$) to be significant. The effect of 'colour variety' was insignificant.

MDS data of consistent peaks (Fig. 7) (stress: 0.09) were approximately normally distributed. With two-way MANOVA the predictor 'station' accounted for a significant difference between corals from different sampling sites (Fig. 7 a) ($p = 0.03$). Post hoc comparison with Duncan's test revealed significant differences between stations 1 and 2 ($p < 0.01$). This is also visible in Fig. 7 a, where values of dimension 2 were mostly positive for coral samples from station 1, while coral samples from station 2 had mostly negative values.

In addition, also dissimilarities between T-RFLP profiles from corals of different colour (Fig. 7 b), denoted by the predictor 'colour variety', were significant ($p = 0.05$). This difference became only clear from two-way MANOVA of MDS coordinates of the coral samples, since it was not as evident from the distribution of sample points as the differences between sampling sites (see above). However, the means of sample coordinates of MDS dimension 2 were more positive for red than for white coral samples (Fig. 8).

The crossover effect 'station' × 'colour variety' that could be evaluated by two-way MANOVA was insignificant.

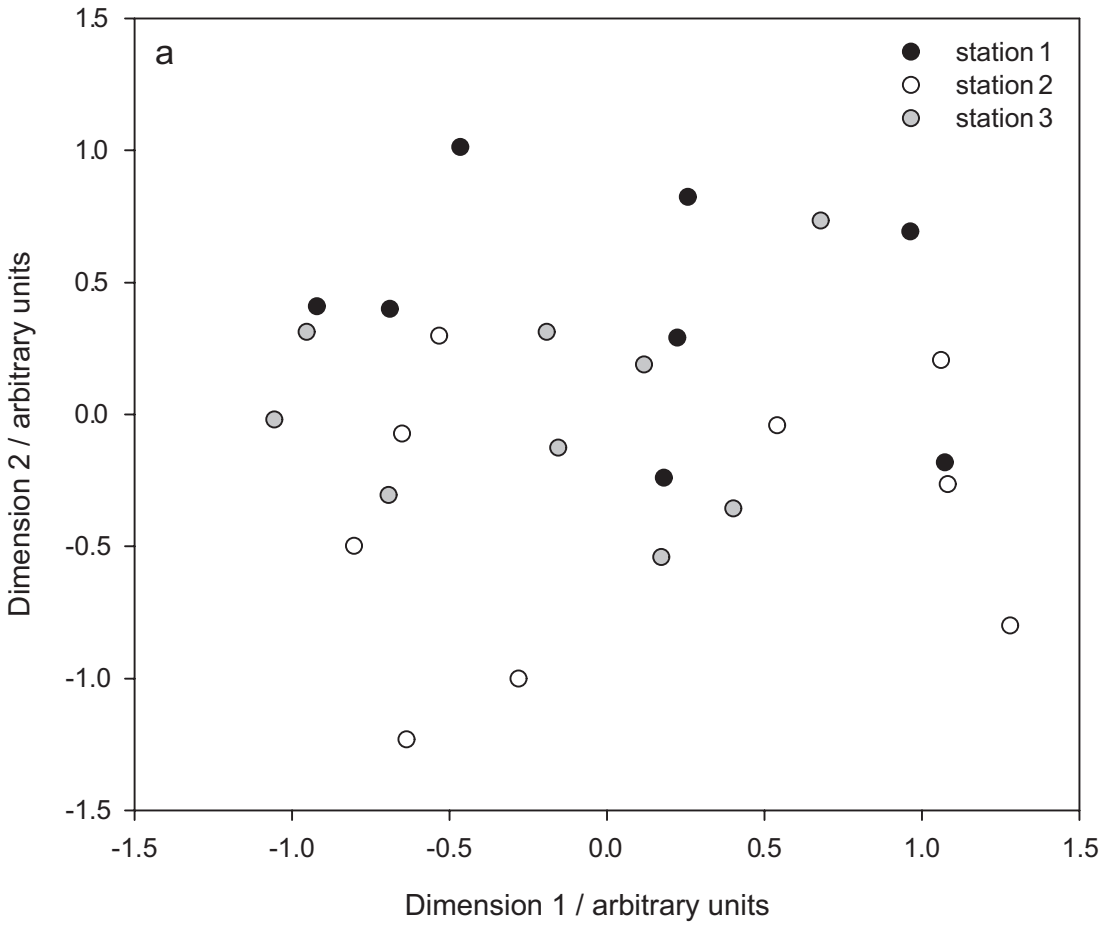

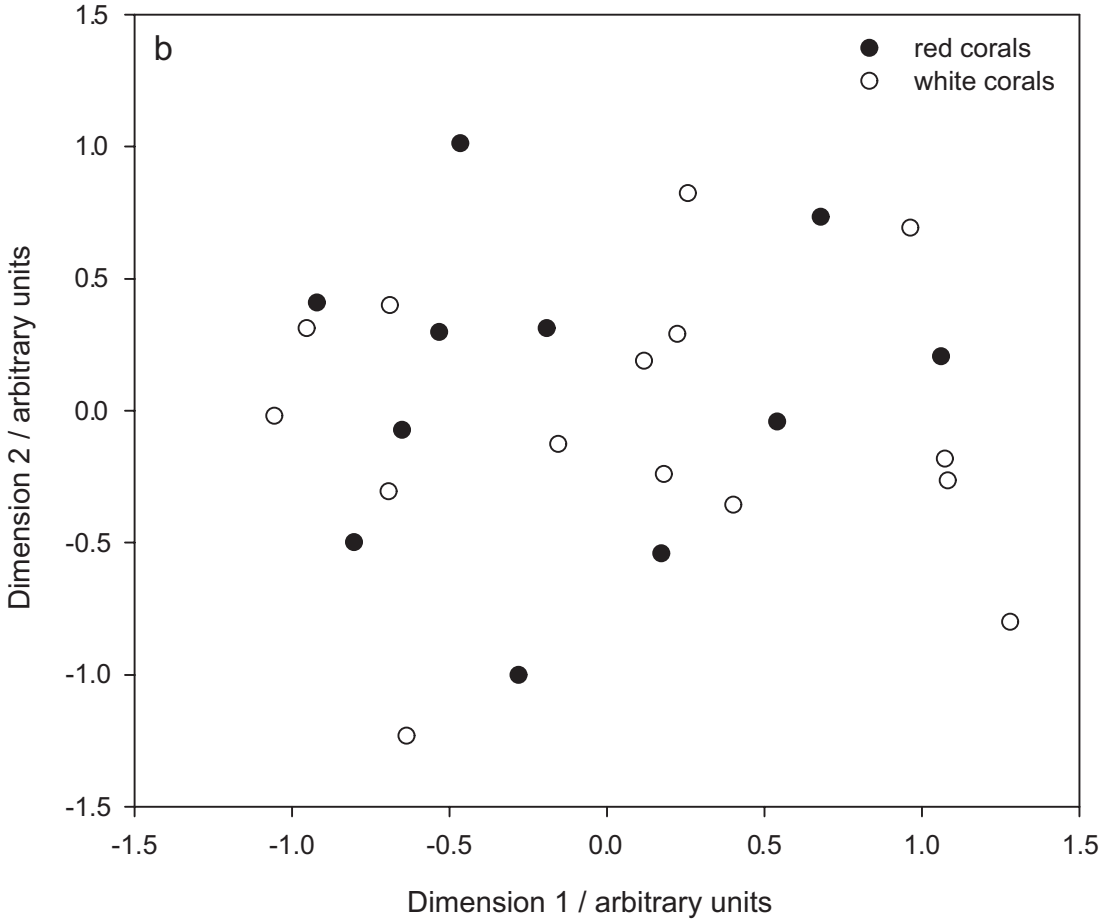

Fig. 7: Multidimensional scaling (MDS) ordination of coral samples (26 data points) based on relative abundances of consistent peaks. The plot is shown twice with samples differentiated into groups from same station (a) and of same colour variety (b), respectively. For clearness, of the three calculated MDS dimensions only the two with the most conspicuous differences were plotted. The stress value for dimensional downscaling was 0.09.

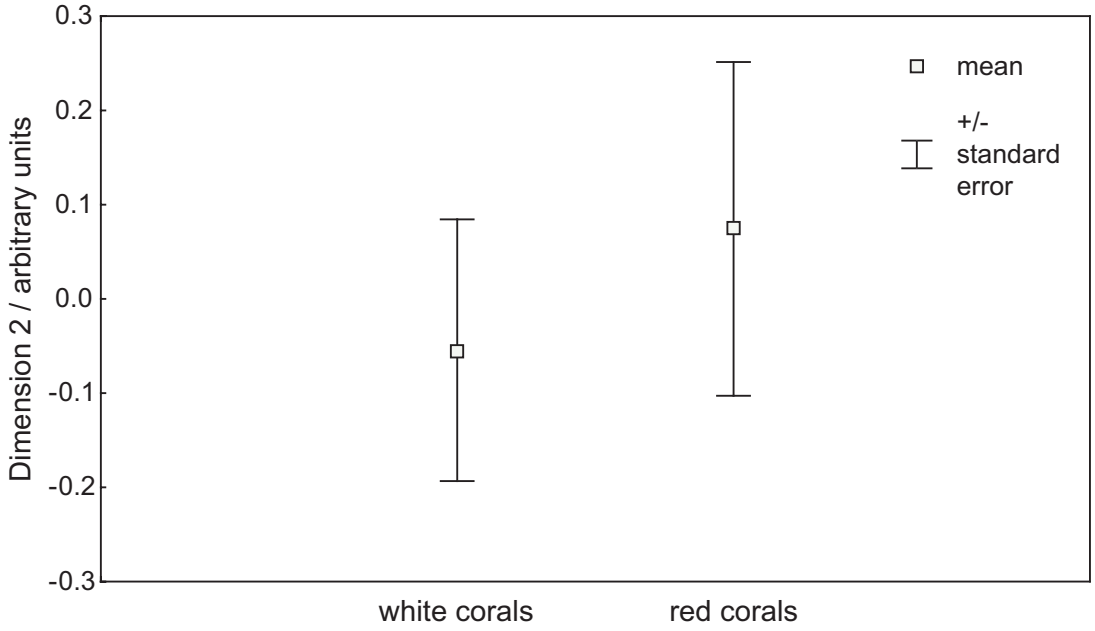

Fig. 8: Summary of the MDS ordination of coral samples differentiated into groups of same colour variety (Fig. 7 b). Means and standard errors of sample coordinates of MDS dimension 2 are given for white and red coral samples.

Corresponding analyses were carried out with MDS dimensions based on (1) rare binary peak data (stress: 0.00), and (2) dominant binary peak data (stress: 0.15) (not shown). Since variables considerably deviated from normal distribution in both cases, Kruskal-Wallis-ANOVA and Mann-Whitney U test were employed to test differences between samples.

In consideration of rare binary T-RF data the predictor 'station' accounted for significant differences between coral samples in dimensions 1 ($p = 0.02$) and 3 ($p = 0.04$). Post hoc comparisons yielded significant differences between stations 1 and 2 (dimension 3; $p < 0.01$), and between stations 2 and 3 (dimension 1; $p = 0.02$). The effect of 'colour variety' was insignificant.

No significant differences were observed for any of the two predictors in consideration of dominant binary T-RF data.

3.2 Cloning and Sequencing

3.2.1 Phylogenetic Analyses

A total of 536 16S rDNA clone sequences passed quality checks and were subjected to phylogenetic analysis: 177 from white corals, 163 from red corals, 71 from water, and 125 from sediment. Length of partial sequences ranged from 294 nt (one sequence) to 902 nt (average, 765 nt). 12 nearly complete sequences from selected bacterial OTUs were retrieved for comparison with FISH probe target sites, design of new FISH probes, and to increase the data basis for phylogenetic calculations. These sequences were 1318 nt to 1421 nt long (average, 1374 nt), and marked by the suffix "full" in the phylogenetic tree (Fig. 11). Based on 97% sequence similarity the number of OTUs found in the respective sample types were 27 (white corals), 54 (red corals), 28 (water), and 74 (sediment). Rarefaction analysis (Fig. 9) assigned highest bacterial OTU richness to the sediment, followed by red *L. pertusa*, water, and white *L. pertusa*. Consequently, theoretical coverage of total bacterial diversity was highest in white *L. pertusa* (83.2%), followed by water (64.7%), sediment (60.3%), and red *L. pertusa* (42.1%). Table 4 summarises these properties of the sequence library.

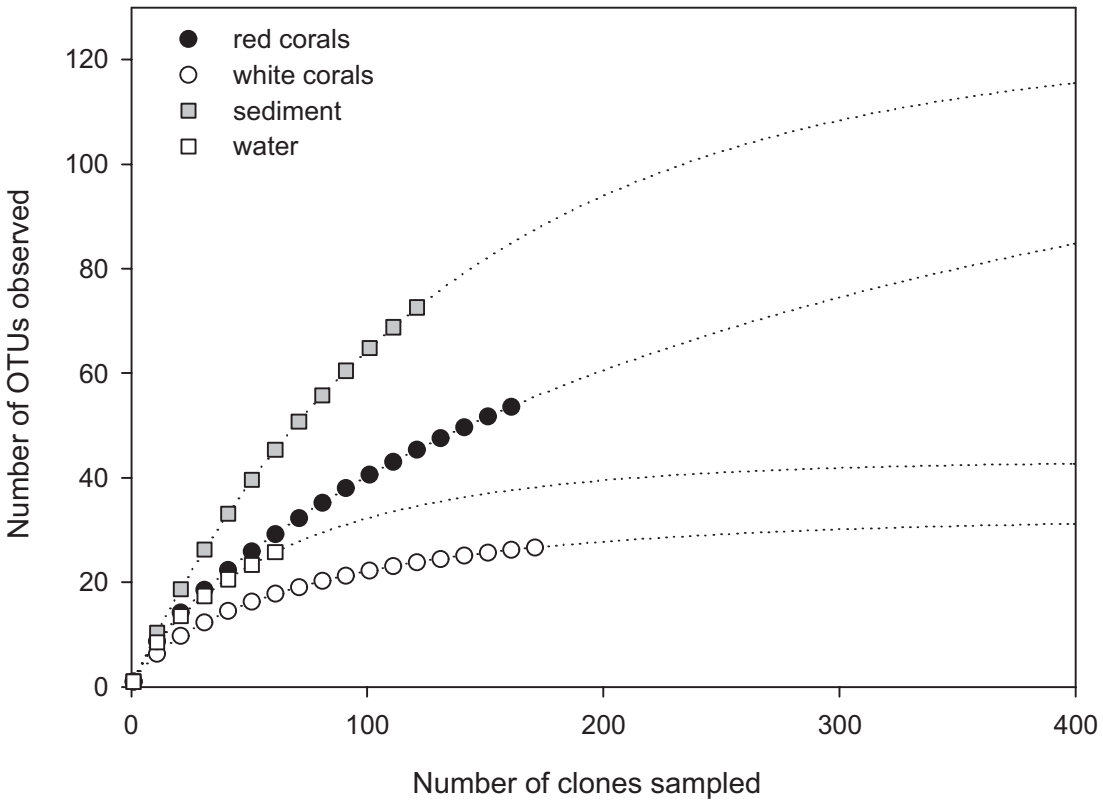

Fig. 9: Rarefaction analysis. The expected number of OTUs is plotted against the number of analysed clones from red and white *L. pertusa*, sediment, and water. Dotted lines mark the extrapolations of the respective rarefaction curves according to the calculation method of Thiel, Neulinger et al. (2007b). The asymptotes of these curves give an estimate of the expected number of OTUs to be found if an infinite number of clones were sampled, which is tantamount to the maximum expectable OTU richness.

Table 4: Summary of properties of the sequence library. For all sample types, the following values are given: Number of analysed clones, number of OTUs based on 97% sequence similarity, and theoretical coverage of total bacterial richness estimated by rarefaction analysis.

	white corals	**red corals**	**water**	**sediment**
no. of clones	177	163	71	125
no. of OTUs	27	54	28	74
coverage	83.2%	42.1%	64.7%	60.3%

Affiliation with bacterial phyla and classes (in case of *Proteobacteria*) and relative abundances of 16S rDNA sequences from corals, water, and sediment are shown in Fig. 10. Qualitative and quantitative differences of the large-scale bacterial community compositions between coral, water, and sediment samples are visible at first sight. Sequences assigned to the phylum *Proteobacteria* constituted the largest fraction, not only in water and sediment but also in both coral colour varieties (64% in white, 50% in red *L. pertusa*). In either case this fraction was dominated by the classes *α-* and *γ-Proteobacteria*. Other major taxa (relative abundance ≥10%) occurring on both coral phenotypes were *Actinobacteria*, *Verrucomicrobia*, *Firmicutes*, and *Planctomycetes*. Some minor taxa (relative abundance <10%) were exclusively found on either colour variety, namely candidate division TM7 on white *L. pertusa* and *δ-Proteobacteria* as well as *Bacteroidetes* on red *L. pertusa*. A small group of cyanobacterial sequences was found on both coral colour varieties but not in the water.

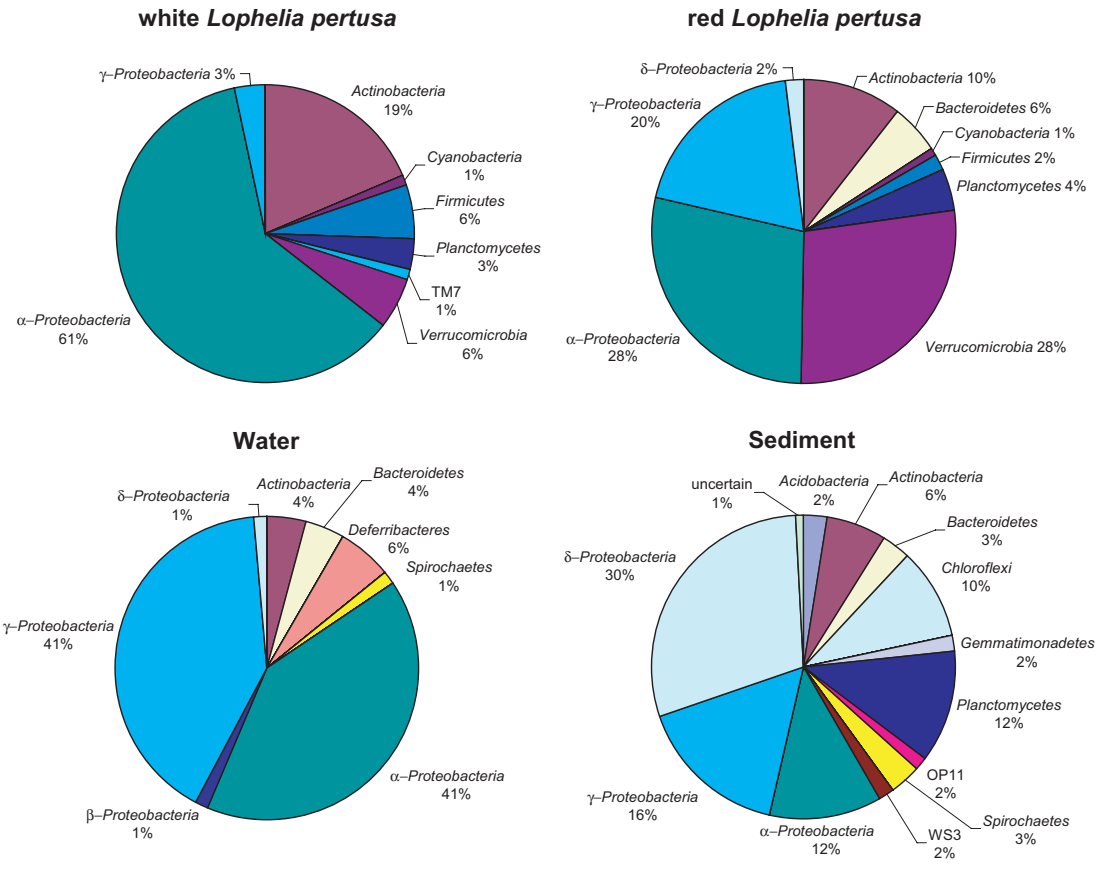

Fig. 10: Affiliation with bacterial phyla and classes (*Proteobacteria*) and relative abundances of 16S rDNA sequences. Data are given separately for red and white *L. pertusa*, water, and sediment. Equal colours in the respective pie charts denote equal taxa.

Detailed analysis on the OTU level revealed that, despite the number of phyla and classes shared among coral colour variations, white and red *L. pertusa* had only twelve OTUs in common. This equals mere 16% of the combined bacterial richness of 75 OTUs for both coral colour varieties. Commonalities between corals and environment were confined to the class *γ-Proteobacteria*, where three OTUs were common to corals and seawater, and one OTU was shared between corals and sediment.

A phylogeny of 133 reference sequences of relevant OTUs is shown in Fig. 11. These OTUs (1) comprised at least two sequences from this study that were not from water or sediment clones or (2) were related to a sequence of a coral-associated bacterium form another study. The phylogenetic tree was based on maximum likelihood calculation according to the GTR+I+G model of nucleotide substitution.

Relevant OTUs affiliated with eight bacterial phyla (*Proteobacteria*, *Bacteroidetes*, *Firmicutes*, *Cyanobacteria*, candidate division TM7, *Actinobacteria*, *Verrucomicrobia*, and *Planctomycetes*). Several sequences published by Yakimov et al. (2006) belonged to three additional phyla (*Gemmatimonadetes*, *Acidobacteria*, and *Nitrospira*) that were exclusively associated with Mediterranean *L. pertusa*. Details on these bacterial groups are presented in the following, emphasising microbes of potential significance for the ecology of *L. pertusa*. Taxonomic classification below the phylum / class level is given for *L. pertusa*-associated OTUs as far it could be reliably determined. For all database sequences their accession numbers and similarity to *L. pertusa*-originating sequences are stated in brackets. In cases with no overlap between a *L. pertusa*-originating and a database sequence the similarity to the closest common relative was determined instead.

a

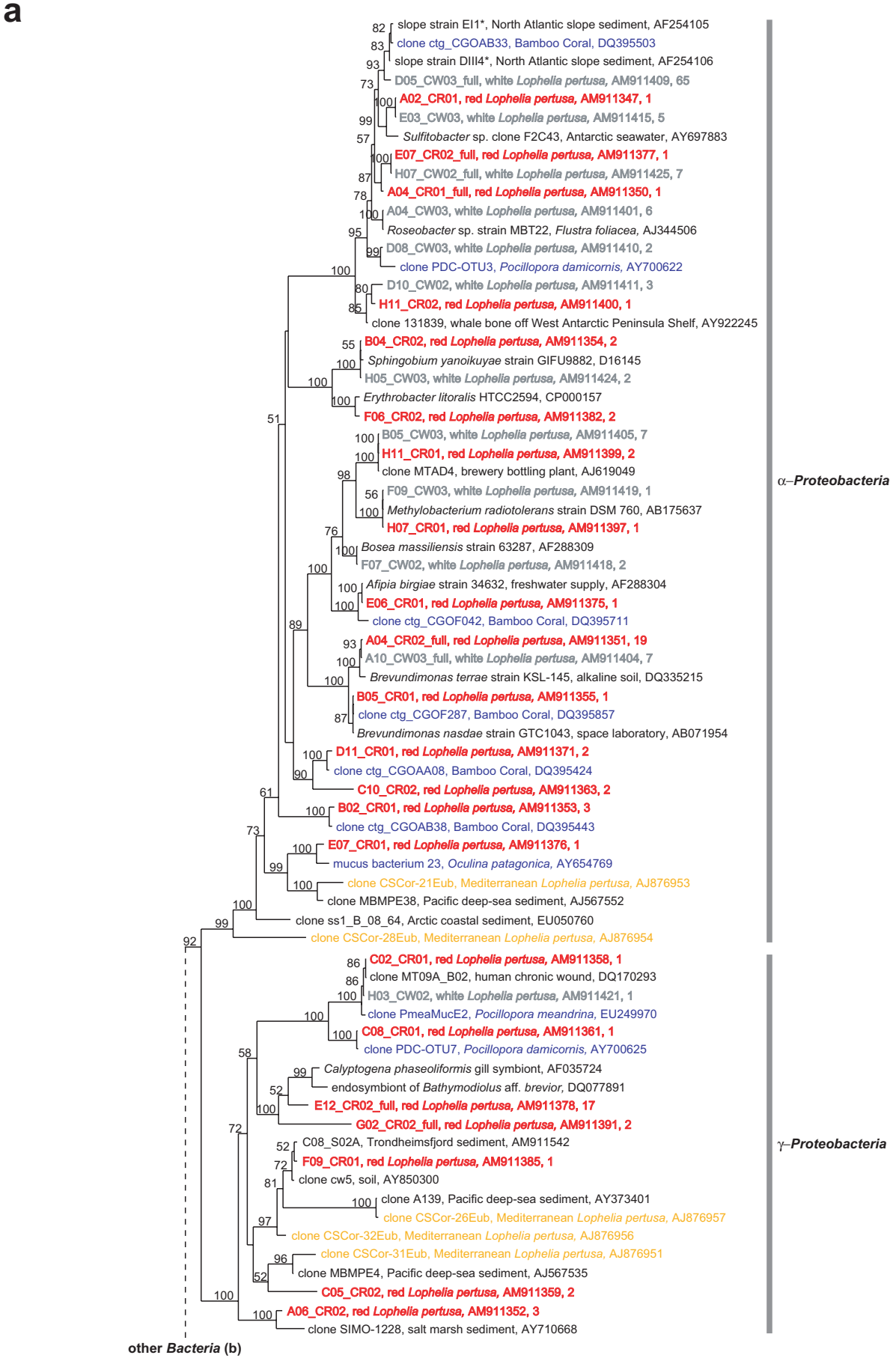
slope strain EI1*, North Atlantic slope sediment, AF254105
clone ctg_CGOAB33, Bamboo Coral, DQ395503
slope strain DIII4*, North Atlantic slope sediment, AF254106
D05_CW03_full, white Lophelia pertusa, AM911409, 65
A02_CR01, red Lophelia pertusa, AM911347, 1
E03_CW03, white Lophelia pertusa, AM911415, 5
Sulfitobacter sp. clone F2C43, Antarctic seawater, AY697883
E07_CR02_full, red Lophelia pertusa, AM911377, 1
H07_CW02_full, white Lophelia pertusa, AM911425, 7
A04_CR01_full, red Lophelia pertusa, AM911350, 1
A04_CW03, white Lophelia pertusa, AM911401, 6
Roseobacter sp. strain MBT22, Flustra foliacea, AJ344506
D08_CW03, white Lophelia pertusa, AM911410, 2
clone PDC-OTU3, Pocillopora damicornis, AY700622
D10_CW02, white Lophelia pertusa, AM911411, 3
H11_CR02, red Lophelia pertusa, AM911400, 1
clone 131839, whale bone off West Antarctic Peninsula Shelf, AY922245
B04_CR02, red Lophelia pertusa, AM911354, 2
Sphingobium yanoikuyae strain GIFU9882, D16145
H05_CW03, white Lophelia pertusa, AM911424, 2
Erythrobacter litoralis HTCC2594, CP000157
F06_CR02, red Lophelia pertusa, AM911382, 2
B05_CW03, white Lophelia pertusa, AM911405, 7
H11_CR01, red Lophelia pertusa, AM911399, 2
clone MTAD4, brewery bottling plant, AJ619049
F09_CW03, white Lophelia pertusa, AM911419, 1
Methylobacterium radiotolerans strain DSM 760, AB175637
H07_CR01, red Lophelia pertusa, AM911397, 1
Bosea massiliensis strain 63287, AF288309
F07_CW02, white Lophelia pertusa, AM911418, 2
Afipia birgiae strain 34632, freshwater supply, AF288304
E06_CR01, red Lophelia pertusa, AM911375, 1
clone ctg_CGOF042, Bamboo Coral, DQ395711
A04_CR02_full, red Lophelia pertusa, AM911351, 19
A10_CW03_full, white Lophelia pertusa, AM911404, 7
Brevundimonas terrae strain KSL-145, alkaline soil, DQ335215
B05_CR01, red Lophelia pertusa, AM911355, 1
clone ctg_CGOF287, Bamboo Coral, DQ395857
Brevundimonas nasdae strain GTC1043, space laboratory, AB071954
D11_CR01, red Lophelia pertusa, AM911371, 2
clone ctg_CGOAA08, Bamboo Coral, DQ395424
C10_CR02, red Lophelia pertusa, AM911363, 2
B02_CR01, red Lophelia pertusa, AM911353, 3
clone ctg_CGOAB38, Bamboo Coral, DQ395443
E07_CR01, red Lophelia pertusa, AM911376, 1
mucus bacterium 23, Oculina patagonica, AY654769
clone CSCor-21Eub, Mediterranean Lophelia pertusa, AJ876953
clone MBMPE38, Pacific deep-sea sediment, AJ567552
clone ss1_B_08_64, Arctic coastal sediment, EU050760
clone CSCor-28Eub, Mediterranean Lophelia pertusa, AJ876954
C02_CR01, red Lophelia pertusa, AM911358, 1
clone MT09A_B02, human chronic wound, DQ170293
H03_CW02, white Lophelia pertusa, AM911421, 1
clone PmeaMucE2, Pocillopora meandrina, EU249970
C08_CR01, red Lophelia pertusa, AM911361, 1
clone PDC-OTU7, Pocillopora damicornis, AY700625
Calyptogena phaseoliformis gill symbiont, AF035724
endosymbiont of Bathymodiolus aff. brevior, DQ077891
E12_CR02_full, red Lophelia pertusa, AM911378, 17
G02_CR02_full, red Lophelia pertusa, AM911391, 2
C08_S02A, Trondheimsfjord sediment, AM911542
F09_CR01, red Lophelia pertusa, AM911385, 1
clone cw5, soil, AY850300
clone A139, Pacific deep-sea sediment, AY373401
clone CSCor-26Eub, Mediterranean Lophelia pertusa, AJ876957
clone CSCor-32Eub, Mediterranean Lophelia pertusa, AJ876956
clone CSCor-31Eub, Mediterranean Lophelia pertusa, AJ876951
clone MBMPE4, Pacific deep-sea sediment, AJ567535
C05_CR02, red Lophelia pertusa, AM911359, 2
A06_CR02, red Lophelia pertusa, AM911352, 3
clone SIMO-1228, salt marsh sediment, AY710668
α–Proteobacteria
γ–Proteobacteria
other Bacteria (b)
0.10

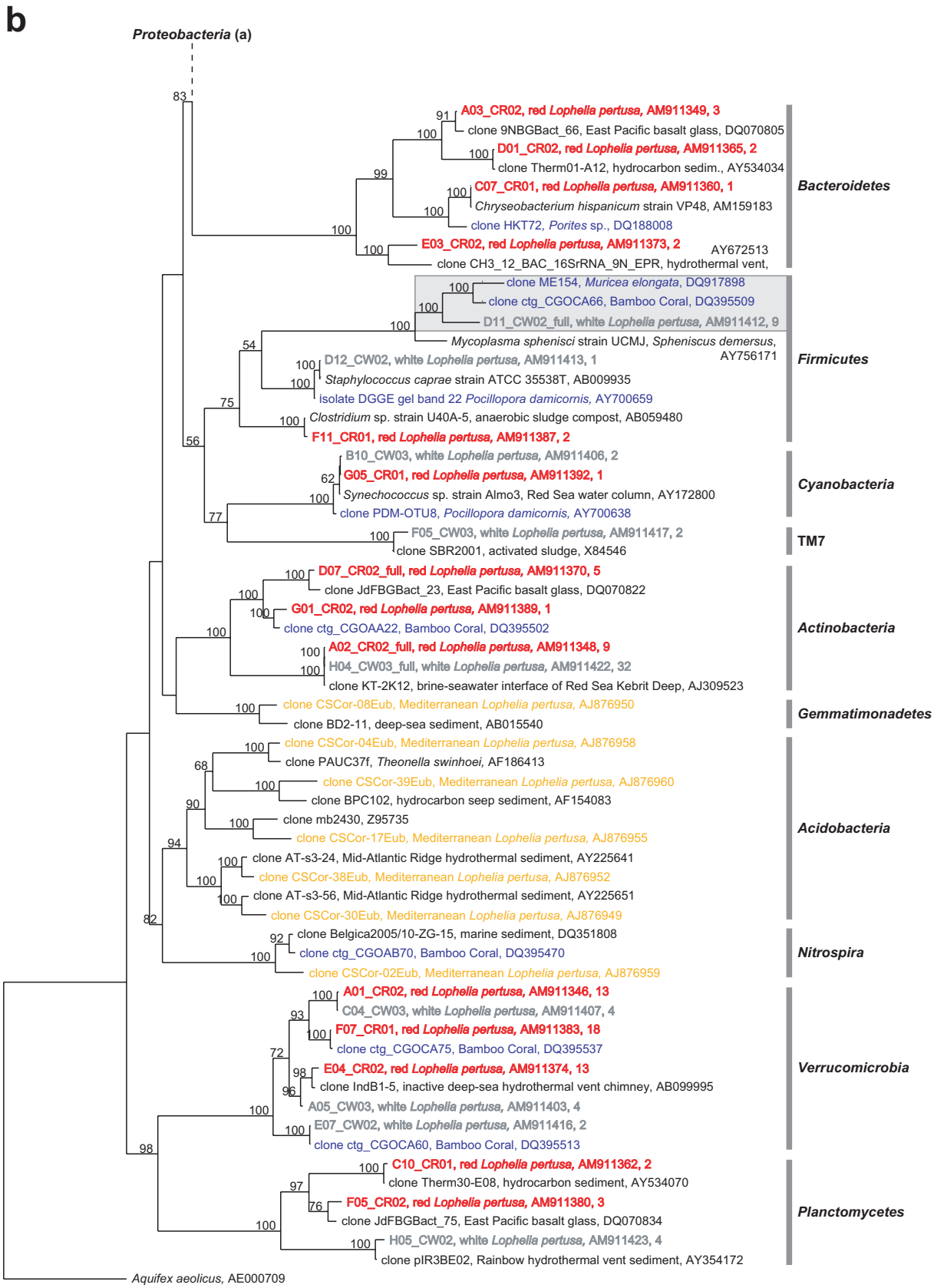
b
Proteobacteria (a)
A03_CR02, red Lophelia pertusa, AM911349, 3
clone 9NBGBact_66, East Pacific basalt glass, DQ070805
D01_CR02, red Lophelia pertusa, AM911365, 2
clone Therm01-A12, hydrocarbon sedim., AY534034
C07_CR01, red Lophelia pertusa, AM911360, 1
Chryseobacterium hispanicum strain VP48, AM159183
clone HKT72, Porites sp., DQ188008
E03_CR02, red Lophelia pertusa, AM911373, 2
clone CH3_12_BAC_16SrRNA_9N_EPR, hydrothermal vent, AY672513
Bacteroidetes
clone ME154, Muricea elongata, DQ917898
clone ctg_CGOCA66, Bamboo Coral, DQ395509
D11_CW02_full, white Lophelia pertusa, AM911412, 9
Mycoplasma sphenisci strain UCMJ, Spheniscus demersus, AY756171
D12_CW02, white Lophelia pertusa, AM911413, 1
Staphylococcus caprae strain ATCC 35538T, AB009935
isolate DGGE gel band 22 Pocillopora damicornis, AY700659
Clostridium sp. strain U40A-5, anaerobic sludge compost, AB059480
F11_CR01, red Lophelia pertusa, AM911387, 2
Firmicutes
B10_CW03, white Lophelia pertusa, AM911406, 2
G05_CR01, red Lophelia pertusa, AM911392, 1
Synechococcus sp. strain Almo3, Red Sea water column, AY172800
clone PDM-OTU8, Pocillopora damicornis, AY700638
Cyanobacteria
F05_CW03, white Lophelia pertusa, AM911417, 2
clone SBR2001, activated sludge, X84546
TM7
D07_CR02_full, red Lophelia pertusa, AM911370, 5
clone JdFBGBact_23, East Pacific basalt glass, DQ070822
G01_CR02, red Lophelia pertusa, AM911389, 1
clone ctg_CGOAA22, Bamboo Coral, DQ395502
A02_CR02_full, red Lophelia pertusa, AM911348, 9
H04_CW03_full, white Lophelia pertusa, AM911422, 32
clone KT-2K12, brine-seawater interface of Red Sea Kebrit Deep, AJ309523
Actinobacteria
clone CSCor-08Eub, Mediterranean Lophelia pertusa, AJ876950
clone BD2-11, deep-sea sediment, AB015540
Gemmatimonadetes
clone CSCor-04Eub, Mediterranean Lophelia pertusa, AJ876958
clone PAUC37f, Theonella swinhoei, AF186413
clone CSCor-39Eub, Mediterranean Lophelia pertusa, AJ876960
clone BPC102, hydrocarbon seep sediment, AF154083
clone mb2430, Z95735
clone CSCor-17Eub, Mediterranean Lophelia pertusa, AJ876955
clone AT-s3-24, Mid-Atlantic Ridge hydrothermal sediment, AY225641
clone CSCor-38Eub, Mediterranean Lophelia pertusa, AJ876952
clone AT-s3-56, Mid-Atlantic Ridge hydrothermal sediment, AY225651
clone CSCor-30Eub, Mediterranean Lophelia pertusa, AJ876949
Acidobacteria
clone Belgica2005/10-ZG-15, marine sediment, DQ351808
clone ctg_CGOAB70, Bamboo Coral, DQ395470
clone CSCor-02Eub, Mediterranean Lophelia pertusa, AJ876959
Nitrospira
A01_CR02, red Lophelia pertusa, AM911346, 13
C04_CW03, white Lophelia pertusa, AM911407, 4
F07_CR01, red Lophelia pertusa, AM911383, 18
clone ctg_CGOCA75, Bamboo Coral, DQ395537
E04_CR02, red Lophelia pertusa, AM911374, 13
clone IndB1-5, inactive deep-sea hydrothermal vent chimney, AB099995
A05_CW03, white Lophelia pertusa, AM911403, 4
E07_CW02, white Lophelia pertusa, AM911416, 2
clone ctg_CGOCA60, Bamboo Coral, DQ395513
Verrucomicrobia
C10_CR01, red Lophelia pertusa, AM911362, 2
clone Therm30-E08, hydrocarbon sediment, AY534070
F05_CR02, red Lophelia pertusa, AM911380, 3
clone JdFBGBact_75, East Pacific basalt glass, DQ070834
H05_CW02, white Lophelia pertusa, AM911423, 4
clone pIR3BE02, Rainbow hydrothermal vent sediment, AY354172
Planctomycetes
Aquifex aeolicus, AE000709
0.10

Fig. 11: Maximum likelihood tree sub-divided into proteobacterial (a) and other bacterial (b) relevant OTUs from white and red Norwegian *L. pertusa* (grey and red), Mediterranean *L. pertusa* (orange), other corals (blue), and from reference organisms (black). For each sequence its name, source (if available), EMBL accession number, and the number of similar clones with 97% identity cut-off (sequences from this study) are given. Bootstrap proportions ≥50% from 100 re-samples are shown next to the clusters they support. The sequence of *Aquifex aeolicus* (AE000709) was used to root the tree. The shaded box in (b) marks a group of coral-inhabiting *Mycoplasmataceae*. The scale bar (a) and b), bottom left) denotes 0.10 nucleotide substitutions per alignment position.

The ***α-Proteobacteria*** contained most of the coral-derived OTUs from this study. Within this class sequences of the family *Rhodobacteraceae* constituted the largest sub-cluster, dominated by clones from white *L. pertusa*. In particular, 65 identical sequences from white *L. pertusa* (37% of all white *L. pertusa*-hosted sequences; reference: D05_CW03_full) showed high similarity to two bacterial strains DIII4* (AF254106; 98%) and EI1* (AF254105; 98%) (asterisks are part of the clone names) isolated from North Atlantic continental slope sediments at 1500 m depth (Teske et al. 2000). These strains were capable of thiosulphate ($S_2O_3^{2-}$) oxidation. A sequence of presumably the same bacterial species (DQ395503, 98%) had also been found on deep-sea octocorals of the family Isididae, so-called "Bamboo Corals" (Octocorallia, Gorgonacea, Isididae; scientific species names not provided) growing on seamounts in the Gulf of Alaska (Penn et al. 2006). 3 sequences from white (reference: D10_CW02) and sequence H11_CR02 from red corals (both *Rhodobacteraceae*) were closely related to a clone (AY922245, 97% and 98%, respectively) associated with the remains of a deep-sea "whale fall" off the West Antarctic Peninsula Shelf (Tringe et al. 2005).

Several bacterial sequences from red *L. pertusa* within the *a-Proteobacteria* affiliated with sequences from other animal-associated bacteria: A group of 6 sequences (reference: A04_CW03) in the above-mentioned *Rhodobacteraceae* cluster were identical with the 16S rDNA of a cultivated bacterium (AJ344506) from the North Sea bryozoan *Flustra foliacea* (Pukall et al. 2001). D08_CW03 (also *Rhodobacteraceae*) was similar to a sequence (AY700622; 97%) associated with the tropical scleractinian coral *Pocillopora damicornis* (Astrocoeniina, Pocilloporidae) (Bourne and Munn 2005). Several sequences from *L. pertusa* associated with sequences form Isididae (accession numbers DQ395xxx): E06_CR01 (*Afipia* sp.) with DQ395711 (98%); a cluster of 19 sequences from red and 7 sequences from white *L. pertusa* (references: A04_CR02_full and A10_CW03_full) and B05_CR01 from red *L. pertusa* (all *Brevundimonas* sp.) with DQ395857 (97%, 98%, and 100%,

respectively); 2 sequences (reference: D11_CR01; *Rhizobiales*) with DQ395424 (99%); 3 sequences (reference: B02_CR01; unclassified *a-Proteobacteria*) with DQ395443 (99%). E07_CR01 (*Rhodospirillaceae*) associated with a sequence (AY654769; 97%) obtained from the mucus of the shallow-water scleractinian *Oculina patagonica* (Faviina, Oculinidae) (Koren and Rosenberg, unpubl.). Other *a-proteobacterial* sequences from both white and red *L. pertusa* (F09_CW03 and H07_CR01) were virtually identical with that of *Methylobacterium radiotolerans* (AB175637; 100% in both cases) (Kato et al. 2005); a larger sister-cluster of 7 sequences from white and 2 from red corals (references: B05_CW03 and H11_CR01) also belonged to the genus *Methylobacterium*.

The ***γ-Proteobacteria*** cluster was dominated by bacterial sequences from red *L. pertusa*. The largest group of them comprised 17 sequences with reference E12_CR02_full (unclassified *γ-Proteobacteria*). This cluster showed closest relatedness to endosymbionts of the two deep-sea mussels *Calyptogena phaseoliformis* (AF035724; 94%) (Peek et al. 1998) and *Bathymodiolus* aff. *brevior* (DQ077891; 93%) (McKiness and Cavanaugh 2005). 2 other sequences (reference: G02_CR02_full) belonged to the same cluster but were more distantly related to the above-mentioned database sequences (88% and 87%, respectively). Out of each 100 hits for BLAST searches with references E12_CR02_full and G02_CR02_full, respectively, about 60 sequences originated from sulphur oxidising symbiotic bacteria hosted by the above-mentioned and other species of deep-sea mussels. Even sequences of free-living bacteria with lowest similarity values were clearly related to thiotrophy or hydrothermal activity, respectively. Sequences C02_CR01 from red and H03_CW02 (both *Shigella* sp.) from white corals were almost identical with a clone sequence (DQ170293; 100% in both cases) obtained from a human wound (Frank et al., unpubl.). Sequence C08_CR01 (*Vibrio* sp.) from red *L. pertusa* was identical with that of another bacterium from the tropical scleractinian *P. damicornis* (AY700625; 100%). A clone of probably the same species has also been identified on mucus of the scleractinian coral *Pocillopora meandrina* (Astrocoeniina, Pocilloporidae) (EU249970; 99% to both *L. pertusa*-derived sequences) (Speck et al., unpubl.).

The ***Bacteroidetes*** cluster exclusively consisted of sequences associated with red *L. pertusa*. 3 sequences (reference: A03_CR02; *Flavobacteriaceae*) were closely related to sequence DQ070805 (98%) acquired from basalt glass of the East Pacific Rise (Di Meo-Savoie et al., unpubl.). 2 other sequences of *Flavobacteriaceae* (reference: D01_CR02) were identical to sequence AY534034 (100%) obtained from Mediterranean sediments rich in petroleum hydrocarbons and n-alkanes

(Polymenakou et al. 2005). 2 sequences (reference: E03_CR02; *Bacteroidetes*) were remotely related to a clone sequence (AY672513; 91%) associated with distinct mineralogical layers of a white smoker spire from a deep-sea hydrothermal vent site (Kormas et al. 2006). Sequence C07_CR01 (*Chryseobacterium* sp.) was phylogenetically related to sequence DQ188008 obtained from the shallow-water scleractinian *Porites* sp. (Fungiina, Poritidae) from the Arabian Sea (Kapley et al. 2007). There was no overlap between C07_CR01 and DQ188008, but DQ188008 was 96% similar to *Chryseobacterium hispanicum* AM159183, which in turn showed 100% similarity to C07_CR01.

The ***Firmicutes*** cluster comprised mostly sequences from white *L. pertusa* that were closely related to bacteria form other corals: D12_CW02 (*Staphylococcus* sp.) affiliated with a sequence from *P. damicornis* (AY700659; no overlap, 99% to *Staphylococcus caprae* AB009935), and 2 sequences (reference: F11_CR01, *Clostridiaceae*) were highly similar to an isolate from an enriched anaerobic microbial community (AB059480; 100%) (Ueno et al. 2001).

A cluster of 9 sequences (reference: D11_CW02_full, *Mycoplasmataceae*) were only distantly related to the next cultivated relative *Mycoplasma sphenisci* (AY756171; 89%) (Frasca et al. 2005). They formed a separate cluster with bacteria associated with Isididae (DQ395509; 91%) and the Caribbean coral *Muricea elongata* (Octocorallia, Gorgonacea, Plexauridae) (DQ917898; 90%) (Ranzer et al., unpublished), which is marked by a shaded box in Fig. 11 b. An additional maximum likelihood tree (Fig. 12) was constructed with closest cultivated and uncultivated relatives of *L. pertusa*-hosted *Mycoplasmataceae* to determine the exact position of this coral-related sub-cluster. The model of nucleotide substitution was again GTR+I+G. Several sequences of the *Mycoplasma pneumoniae* group, *Spiroplasma* group, and "*Candidatus* Hepatoplasma crinochetorum" (Wang et al. 2004) were used as outgroup. (Note that taxonomy is not always congruent with phylogeny in *Mycoplasmataceae*). The bootstrap proportion of 55% (marked with an asterisk in Fig. 12) for the overall group of coral-related *Mycoplasmataceae* (shaded box in Fig. 12) was deteriorated as compared to 100% in the complete phylogeny (Fig. 11 b). This was most likely due to the inclusion of partial sequences into the calculations (dotted branches in Fig. 12), which are known to impair bootstrap analysis (cf. Gutiérrez et al. 2002). Yet, these sequences had to be considered because they obviously constituted the next relatives to the coral-inhabiting *Mycoplasmataceae*. Repeated bootstrap analysis without these partial sequences (not shown) resulted in high bootstrap values near 100% for the coral-related sequence cluster. Other sequences of cultivated

Mycoplasma species appeared to be slightly closer to D11_CW02_full than that of *M. sphenisci* (AY756171), but the latter still featured highest similarity to the *L. pertusa*-derived sequence (89%).

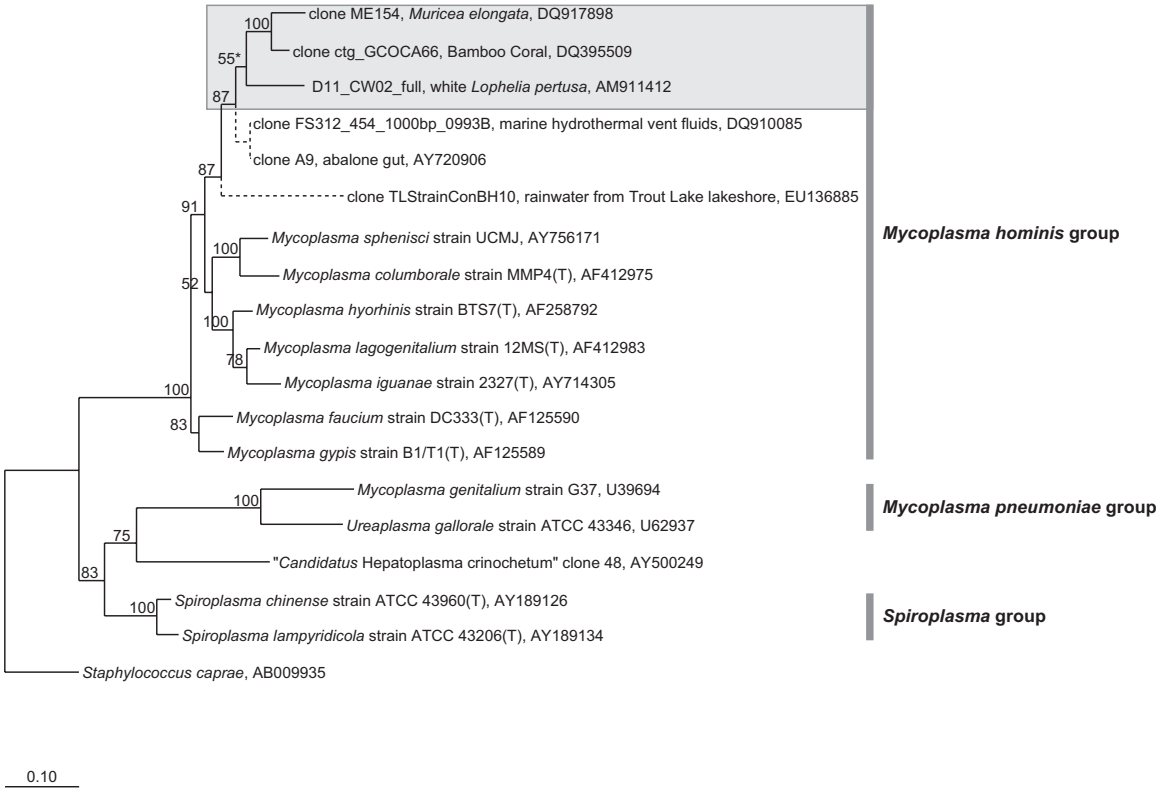

Fig. 12: Maximum likelihood tree of *L. pertusa*-inhabiting *Mycoplasmataceae* with sequences of cultivated and uncultivated relatives within the *Mycoplasma hominis* group. The coral-related sequences are marked by a shaded box. For each sequence its name, source (if clone), and EMBL accession number are given. A '(T)' behind the strain designation denotes a type strain. Bootstrap proportions ≥50% from 100 re-samples are shown next to the clusters they support. The low bootstrap proportion of 55% for the coral-related cluster (marked with an asterisk) is most likely due to incorporation of partial sequences (≤1012 nt, dotted branches). The sequence of *Staphylococcus caprae* (AB009935) was used to root the tree. The scale bar (bottom left) denotes 0.10 nucleotide substitutions per alignment position.

Cyanobacteria were found in both white and red *L. pertusa* (references B10_CW03 and G05_CR01, respectively) and belonged to the genus *Synechococcus*. Bacteria of the same genus are hosted by the tropical reef coral *P. damicornis* (AY700638; 98% to both references).

Candidate division TM7 had 2 representatives from white *L. pertusa* (reference: F05_CW03) that were 98% similar to the partial 16S rDNA sequence X84546 obtained from activated sludge (Bond et al. 1995).

The ***Actinobacteria*** cluster comprised sequences from both white and red *L. pertusa*. 5 sequences (reference: D07_CR02_full; unclassified *Actinobacteria*) were closely related to DQ070822 (98%) acquired from basalt glass of Cobb Seamount at the Juan de Fuca Ridge (Di Meo-Savoie et al., unpubl.). Sequence G01_CR02 (unclassified *Actinobacteria*) affiliated with a sequence from Isididae (DQ395502; 97%). A large sub-cluster consisting of 9 sequences from red *L. pertusa* (reference: A02_CR02_full) and 32 sequences from white *L. pertusa* (reference: H04_CW03_full; *Propionibacterium acnes*) were identical with sequence AJ309523 (100%) obtained from the brine-seawater interface of Kebrit Deep in the Red Sea (Eder et al. 2001).

In the ***Verrucomicrobia*** a large proportion of sequences affiliated with sequences from Isididae (accession numbers DQ3955xx): 18 sequences (reference: F07_CR01; *Rubritalea* sp.) were identical with DQ395537 (100%); a large sister cluster of 13 sequences from red and 4 sequences from white *L. pertusa* (references: A01_CR02 and C04_CW03) belonged to the same genus *Rubritalea* (92% similarity to DQ395537); 2 sequences (reference: E07_CW02, *Verrucomicrobiales*) were identical with DQ395513 (100%). Another sub-cluster consisted of 13 sequences from red *L. pertusa* (reference: E04_CR02) and 4 sequences from white *L. pertusa* (reference: A05_CW03) (both *Rubritalea* sp.) that showed high similarity to sequence AB099995 (98% and 97%, respectively) of an uncultured bacterium from inactive deep-sea hydrothermal vent chimneys (Suzuki et al. 2004).

The ***Planctomycetes*** cluster comprised coral-associated sequences of both white and red *L. pertusa*, too. 2 sequences of *Planctomycetaceae* from red corals (reference: C10_CR01) were almost identical to sequence AY534070 (99%) acquired from petroleum- and n-alkane-rich sediment in the Eastern Mediterranean Sea (Polymenakou et al. 2005). 3 other sequences from red corals (reference: F05_CR02; *Planctomycetaceae*) were closely related to sequence DQ070834 (97%) from basalt glass of Cobb Seamount at the Juan de Fuca Ridge (Di Meo-Savoie et al., unpubl.). 4 sequences from white *L. pertusa* (reference: H05_CW02; *Planctomyces* sp.) showed closest relatedness to sequence AY354172 (98%) of an uncultured bacterium from sediment of Rainbow vent field on the Mid-Atlantic Ridge (Nercessian et al. 2005).

Bacteria from Mediterranean *L. pertusa* (accession numbers AJ8769xx) (Yakimov et al. 2006) did not show direct affiliation with Norwegian *L. pertusa*-hosted bacteria. Because the authors sequenced their bacterial clones partially from the 3' end, while 5' partial sequencing was used for most clones in the present study, straight comparison was impeded by missing sequence overlap. Still, Mediterranean and Norwegian sequences did not even have common relatives from the online database in most cases except for two instances: AJ876951 and 2 sequences from red *L. pertusa* (reference: C05_CR02; *γ-Proteobacteria*) both clustered with a clone obtained from deep-sea sediment (AJ567535; 97% and 90%, respectively), and sequences AJ876956 and F09_CR01 (*γ-Proteobacteria*) from red *L. pertusa* showed 96% and 99% similarity to an uncultured soil bacterium (AY850300). However, F09_CR01 was the one sequence closely related to a sequence from Trondheimsfjord sediment (C08_S02A; 99%) and the corresponding bacterium was thus not exclusively confined to *L. pertusa* in its Norwegian habitat. AJ876953 from Mediterranean *L. pertusa* was in a sister clade of E07_CR01 (*a-Proteobacteria*, *Rhodospirillaceae*) associated with a sequence originating form *O. patagonica* (see above). A very conspicuous feature of several sequences from Mediterranean *L. pertusa* was their affiliation with clones from hydrocarbon seep or hydrothermal sediments.

The clusters ***Gemmatimonadetes***, ***Acidobacteria***, and ***Nitrospira*** exclusively consisted of sequences from Mediterranean *L. pertusa*. Sequence AJ876950 had been classified as member of *Actinobacteria* in the original study and was re-classified as member of *Gemmatimonadetes* in this study. Within the *Nitrospira* cluster sequence AJ876959 (*Nitrospira* sp.) showed moderate relatedness to another sequence from an isidid coral (DQ395470; 95%). The above-mentioned affiliation with deep-sea and seep-related bacteria was most distinct within the *Gemmatimonadetes* and *Acidobacteria*.

3.2.2 Comparison of T-RFLP Data and 16S rDNA Sequences

From the sequences of 16S rDNA clones the lengths of their theoretical terminal restriction fragments (T-RFs) can be calculated assuming that the molecules had been digested by a respective restriction enzyme. Such 'in-silico' digestion enables comparison between 16S rDNA sequences of a certain sample type and the actual T-RF profiles of that sample type. In this way it can be determined in retrospect which bacterial phylotype gave rise to a distinct peak in the T-RFLP electropherograms. This comparison can also be used to consider the resolution of T-RFLP, i.e.,

whether certain peaks comprise more than one bacterial group. Taking the abundances of clones and the area (or height) of electropherogram peaks into account one can also assess the degree of congruence between the two methods: If both methods ideally depicted the bacterial communities in the same manner, it could be expected that every clone matches a peak (and vice versa) and abundant clones coincide with dominant peaks. Since most clones of this study were sequenced partially from the 5' end, only 5' clone T-RFs were compared to T-RFLP electropherograms based on the forward primer (27f).

T-RFs of clone sequences as determined by TRF-CUT were grouped into three abundance categories: T-RF positions occupied by (1) one clone ('rare'), (2) two to five clones ('intermediate frequency'), and (3) more than five clones ('frequent'). In most cases clone T-RF lengths and frequencies correlated with peak positions and intensities in the electropherograms (Fig. 4), although with a slight displacement between peak positions and clone T-RF lengths. Very often clones of two or more different phyla or classes shared the same T-RF length. For example, with the enzyme / primer combination Alu I / 27f, T-RF length 74 nt comprised sequences of *Bacteroidetes*, *Firmicutes*, *Planctomycetes*, *a-Proteobacteria*, and *γ-Proteobacteria*. Furthermore, several OTUs had T-RFs longer than 500 nt and thus showed no corresponding peak in the respective electropherogram (e.g., in *Verrucomicrobia* and *Bacteroidetes*).

3.3 Fluorescence In-Situ Hybridisation

3.3.1 Bacteria Associated with Coral Ectoderm

For testing of the CARD-FISH method freshly harvested polyps of aquarium-reared *L. pertusa* were hybridised with a mixture of probes EUB338 I-III. This probe combination targets the majority of all known bacteria (Daims et al. 1999). Bright fluorescence signals were obtained from remains of mucus attached to the thin-sectioned coral tissue (Fig. 13) indicating that the coral mucus was densely inhabited by microbes.

Thin sections of coral samples from the Trondheimsfjord hybridised with probes EUB338 I-III did not feature mucus-colonising bacteria like those in aquarium-reared *L. pertusa*, obviously because the mucus had been washed off the polyps. Instead, fluorescence signals in the peripheral ectoderm of the tentacles were observed (Fig. 14 a) that were not as abundant and dense as compared to the signals in Fig. 13. Brightest fluorescence was caused by aggregates of bacterial cells situated on the distal ends of nematocysts of the spirocyst type (cf. Rifkin 1991) arranged in nematocyst batteries (Fig. 14 c, e). The fluorescing bacterial cells had a flask-like shape (about 1.6 μm long and 0.5 μm wide) with a tip at one end (Fig. 14 f). DAPI counterstaining confirmed that the bacterial cells highlighted by CARD-FISH contained DNA and were thus no artefacts (Fig. 14 b, d). Documentation of DAPI signals was hampered though by coral tissue autofluorescence and the much brighter signals of the coral cell nuclei underneath or in direct vicinity of the prokaryote aggregates. Beside bacterial cells some other structures were marked by the fluorescent dyes, in particular stylets of nematocysts belonging to the stenotele type (Fig. 14 c, e) and other nematocyst parts. However, from their size, shape, and lack of a DAPI signal, these structures could be clearly distinguished from bacterial cells. No unspecific marking of bacterial cells was observed after hybridisation with control probe NON338 (not shown). The flask-like bacteria described above prevailed on the nematocyst batteries. Sporadic cells of the same morphotype were only observed on the coral coenosarc (not shown) but not on the endoderm.

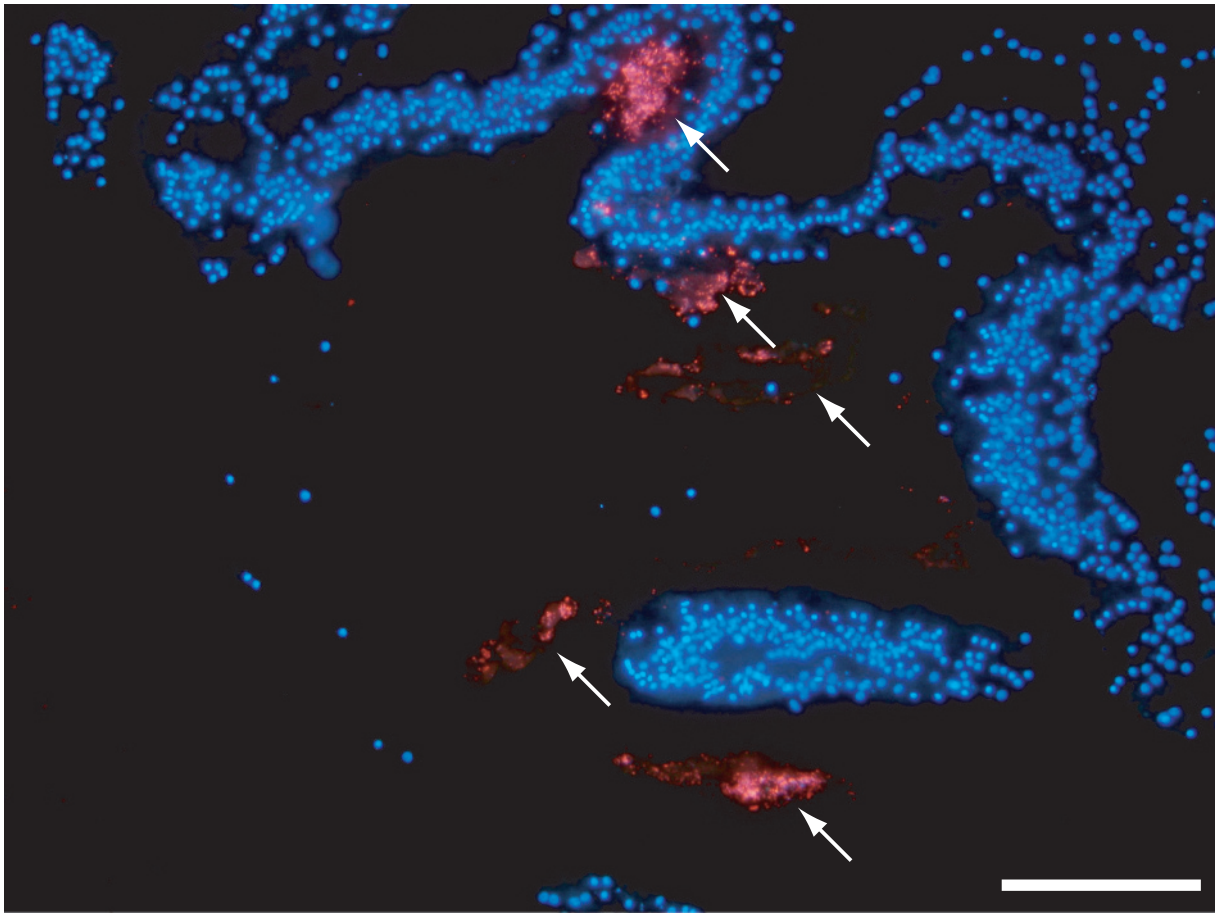

Fig. 13: Epifluorescence micrographs of bacteria in the mucus of an aquarium-reared *L. pertusa* polyp. The image is an overlay of DAPI signals (blue) targeting DNA of coral cell nuclei and bacteria, and hybridisation signals of probes EUB338 I-III with Cy3 TSA (red). Arrows mark mucus secretions with considerably large amounts of bacteria. Scale bar, 100 µm.

To identify the prokaryotes on a sub-domain level probes targeting all abundant *L. pertusa*-associated bacterial groups in the sequence library (Table 1) were employed. In all cases hybridisation under stringent conditions failed to mark the majority of ectoderm-associated bacteria. Cells hybridised with *α-* and *γ-Proteobacteria*-specific probes were observed only few and far between on the ectoderm (not shown). Additional application of achromopeptidase to support cell wall permeabilisation had no effect. Subsequently, hybridisation was repeated with only 20% formamide in the hybridisation buffer allowing the probes also to bind to not strictly complementary target sites. This procedure proved successful in case of the *Firmicutes*-specific probe LGC0355. Comparison with the sequence library revealed two clusters with a single-nucleotide deviation from the probe's target sequence (5'-CAGCAGTAGGGAATCTTCC-3'): the *Mycoplasmataceae* cluster with reference sequence D11_CW02_full (target site, 5'-CAGCAGTAGGGAAT**A**TTCC-3') and the

TM7 cluster with reference sequence F05_CW03 (target site, 5'-CAGCAGTAGGGAATT**T**T-TCC-3'). No mismatches were observed for the other (16S rRNA-targeting) FISH probes with their respective binding sites in sequences originating from Norwegian *L. pertusa*.

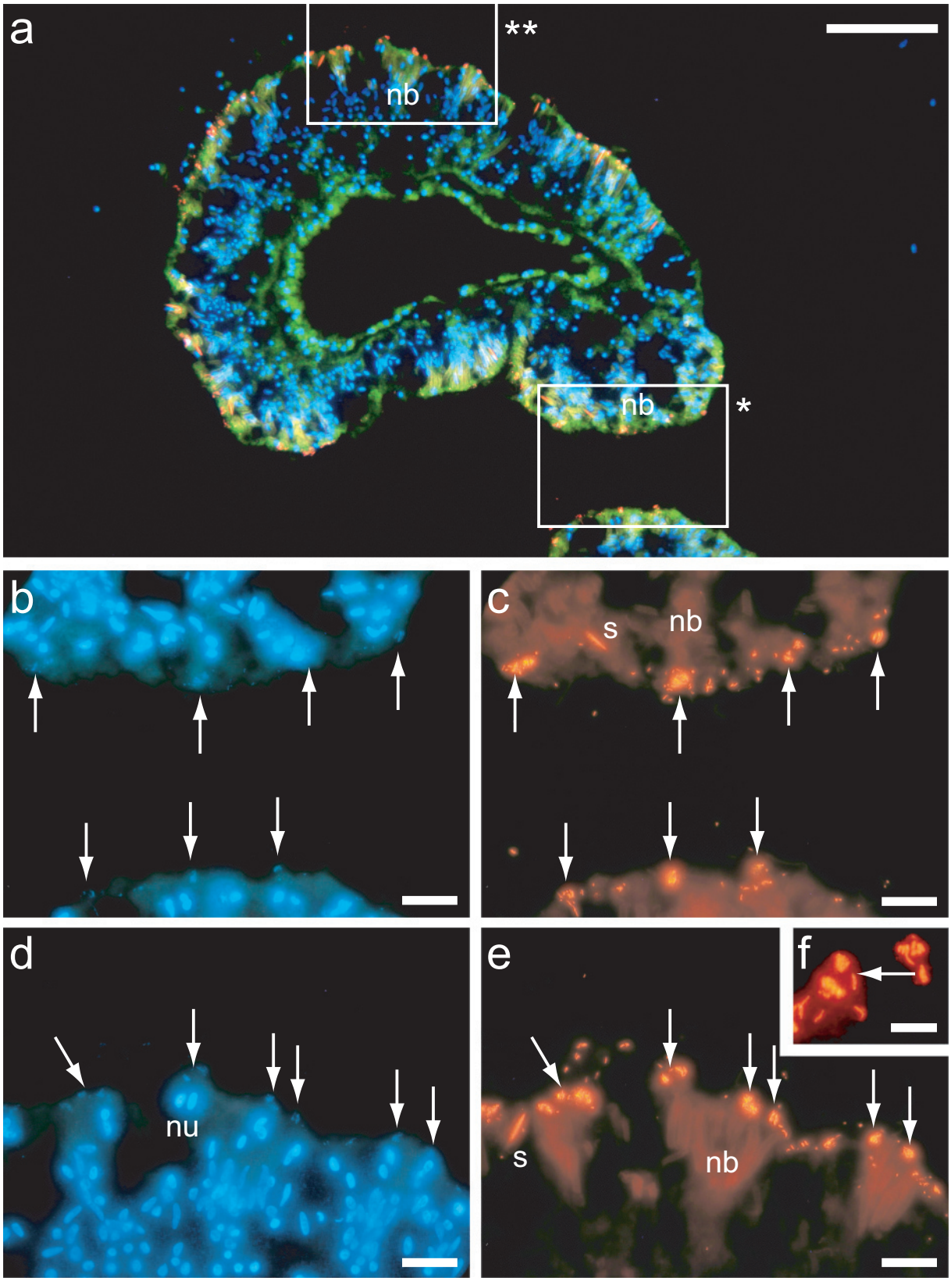

Fig. 14: Epifluorescence micrographs of bacteria on a thin section in the tentacle region of a *L. pertusa* polyp (red coral colour variety, station 3). a) Overview of a cross-sectioned tentacle. The image is an overlay of coral tissue autofluorescence (green), DAPI signals of coral cell nuclei (blue), and hybridisation signals of probes EUB338 I-III with Cy3 TSA (red). b-e) Micrograph details 1 (b, c) and 2 (d, e) showing DAPI (b, d) and Cy3 (c, e) signals of bacterial aggregates on the nematocyst batteries of the tentacle ectoderm. f) Single flask-shaped bacterial cells. Annotations: *, frame of micrograph detail 1; **, frame of micrograph detail 2; nb, nematocyst battery; nu, coral cell nuclei; s, nematocyst stylet; arrows in b-e), corresponding DAPI and Cy3 signals of selected bacterial aggregates; arrow in f), tip at one end of a bacterial cell. Scale bars, 100 μm (a), 20 μm (b-e), 5 μm (f).

For the larger *Mycoplasmataceae* cluster a modified probe LGC0355b (Table 1) was designed that compensated the sequence deviation in the target site of the original probe LGC0355. If the bacteria on the coral ectoderm had the same target site as the *Mycoplasmataceae* sequences in the library, binding efficiency of the modified probe would be higher than that of the original probe. Accordingly, there should be a stringency condition (formamide concentration) in hybridisation that allowed for specific binding of probe LGC0355b but not of probe LGC0355. In addition, probe MYC850 (Table 1) was designed following the recommendations of Hugenholtz et al. (2002). While both probes LGC0355b and MYC850 were designed to hybridise *Mycoplasmataceae* sequences, the target site of probe MYC850 was highly specific only to the coral-borne *Mycoplasmataceae* and thus suitable for direct identification of corresponding microbes.

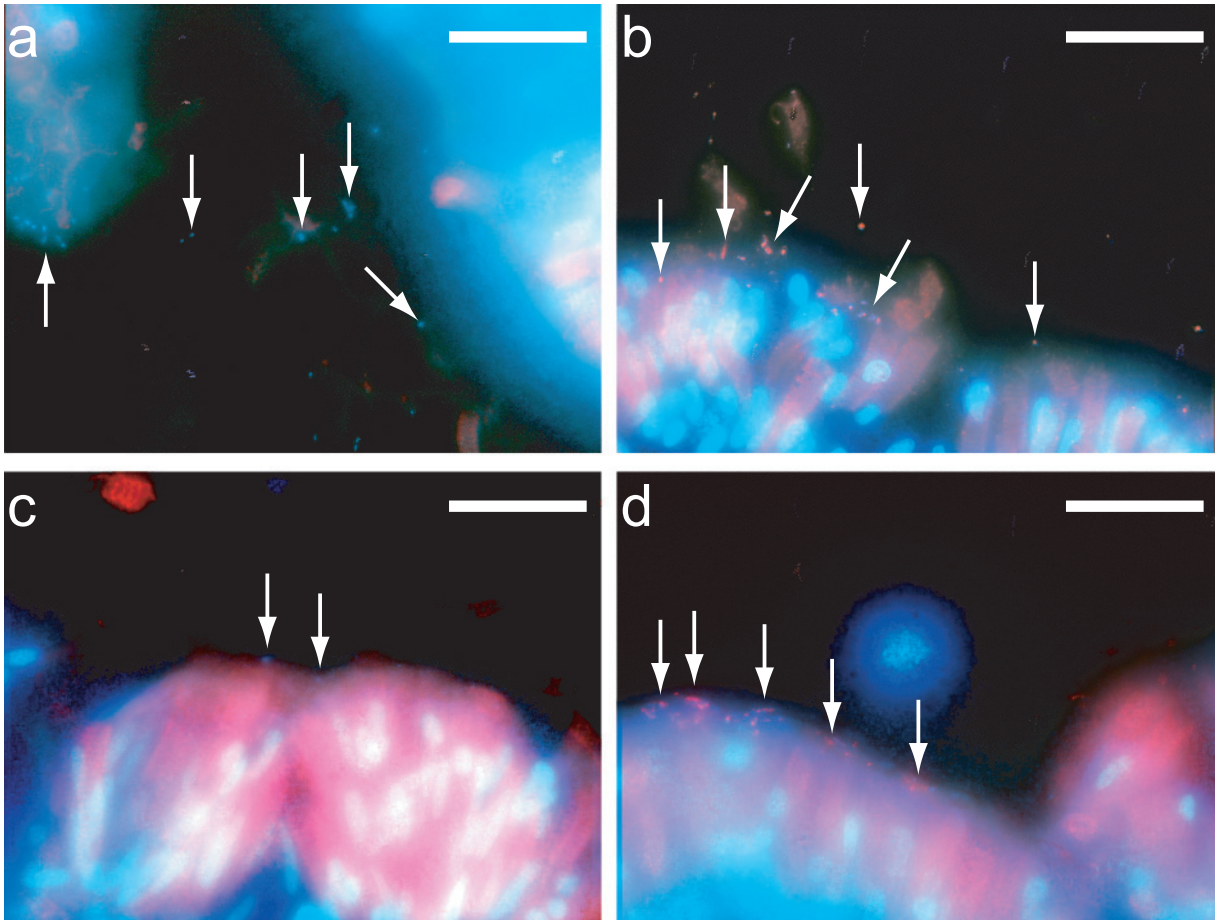

Fig. 15: Epifluorescence micrographs of bacteria on thin sections in the tentacle region of *L. pertusa* polyps. The images are overlays of DAPI (blue) and Cy3 signals (red). a, b) Red coral colour variety, station 1. c, d) White coral colour variety, station 3. Thin sections were hybridised with probes LGC0355 (a, c) and LGC0355b (c, d), respectively, under the same conditions (35% formamide in hybridisation buffer). Arrows mark DAPI and Cy3 signals of selected bacterial cells. Scale bars, 20 µm (a-d).

Hybridisation with 35% formamide gave a negative result for the original probe LGC0355 (Fig. 15 a, c) but yielded conspicuous specific signals for the modified probe LGC0355b (Fig. 15 c, d). Test hybridisations of probe MYC850 with 20% formamide were negative. Results of the specificity cross check for probes LGC0355 and LGC0355b are shown in Fig. 16. For hybridisation of *Bacillus subtilis* (with the binding site of probe LGC0355) the main fluorescence peak of the newly designed probe LGC0355b is less pronounced and shifted towards lower brightness values as compared to the original probe LGC0355. In addition, probe LGC0355b exhibits more pixels with low brightness values than probe LGC0355. These results indicate a lower binding efficiency of probe LGC0355b with *B. subtilis* as compared to that of probe LGC0355.

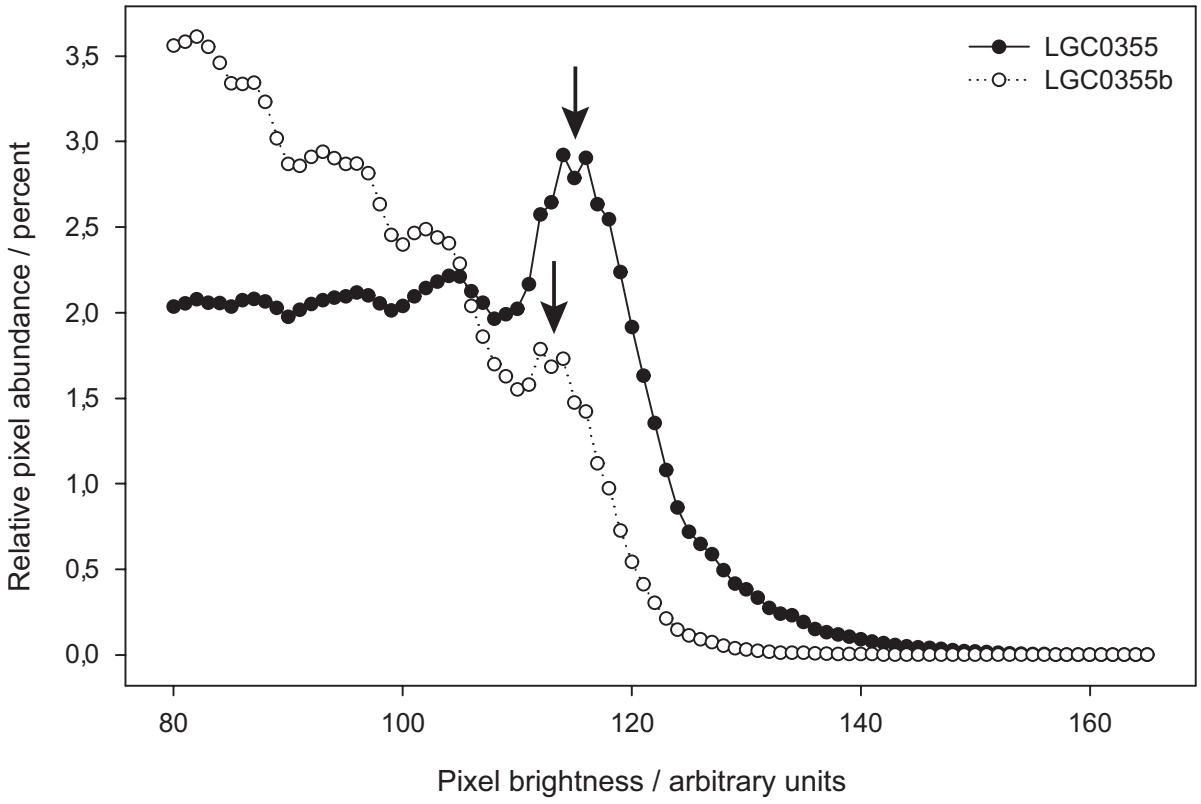

Fig. 16: Specificity cross check for probes LGC0355 and LGC0355b. Histograms of signal brightness (expressed as pixel brightness values of digital images) for hybridisation of the firmicute *Bacillus subtilis* with probes LGC0355 and LGC0355b under the same conditions (35% formamide in hybridisation buffer). Arrows denote the main fluorescence signals of both probes.

An additional assay was conducted to test whether cell wall permeabilisation was crucial for hybridisation with HRP-coupled oligonucleotide probes (Fig. 17). Permeabilisation by lysozyme was necessary for both gram-negative (Fig. 17 a-d) and gram-positive bacteria (Fig. 17 e, f) having thin and thick peptidoglycan cell walls, respectively. For the bacteria on *L. pertusa* tentacles, however, omission of lysozyme treatment resulted in no apparent loss in abundance and brightness of hybridisation signals (Fig. 17 g-k).

Double hybridisation with probes LGC0355b and EUB338 I demonstrated that virtually all detectable bacteria on *L. pertusa* thin sections could also be hybridised with the *Mycoplasmataceae*-specific probe (Fig. 18 a, c, e). Lack of signals from control probe NON338 confirmed specificity of the double hybridisation (Fig. 18 b, d, f). No evident discrepancies in bacterial abundances were observed between coral samples from different stations or of different colour.

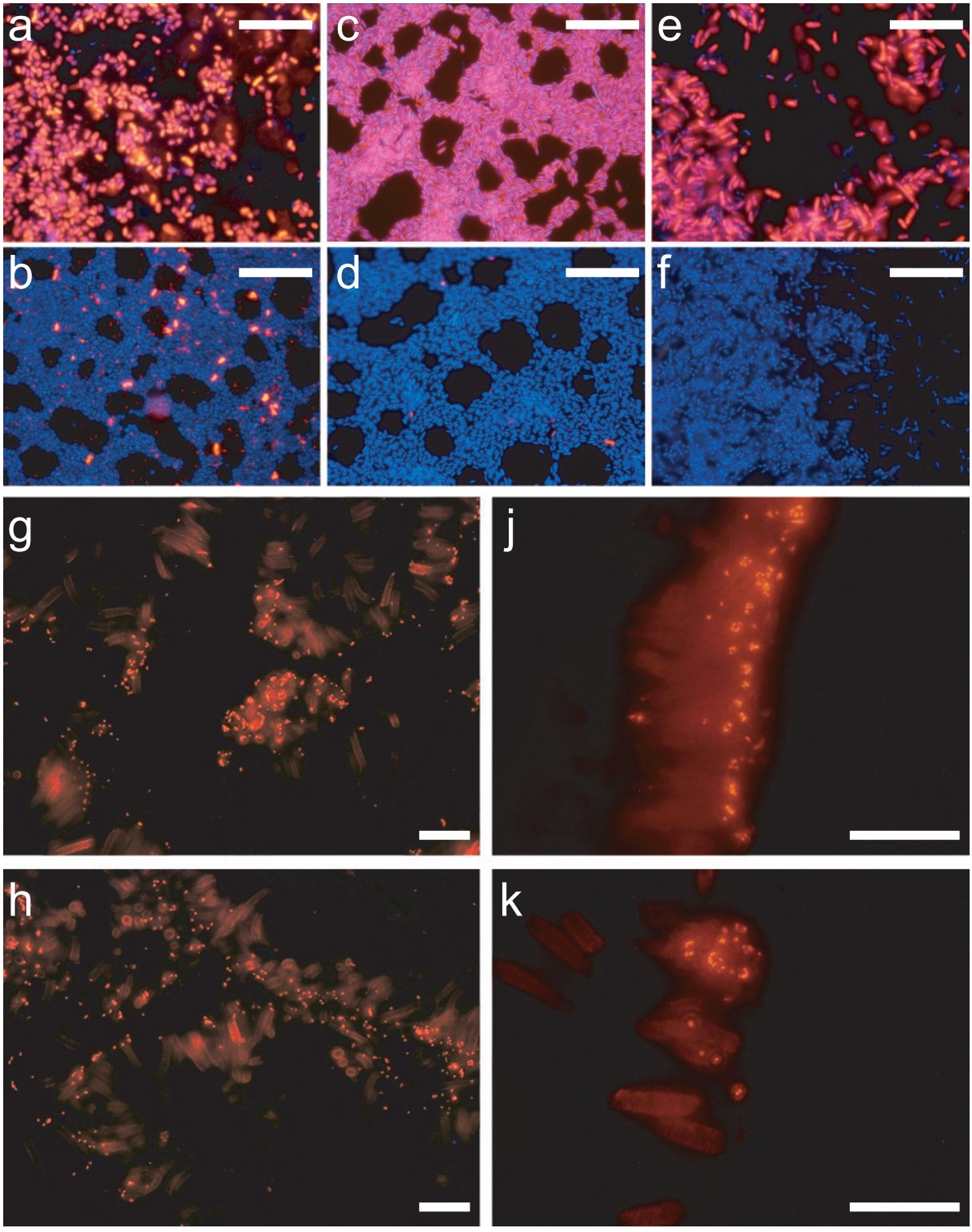

Fig. 17: Epifluorescence micrographs of bacteria hybridised with probe EUB338 I. a-f) Overlay images of DAPI (blue) and Cy3 signals (red). a, b) *a-Proteobacteria*, environmental isolate. c, d) *γ-Proteobacteria*, *Escherichia coli*. e, f) *Firmicutes*, *Bacillus subtilis*. g-k) Thin sections in the tentacle region of *L. pertusa* polyps. g, h) Red coral colour variety, station 1. j, k) Red coral colour variety, station 2. Bacteria had been permeabilised with lysozyme (a, c, e, g, j) or not permeabilised (b, d, f, h, k) prior to hybridisation. Scale bars, 20 μm (a-k).

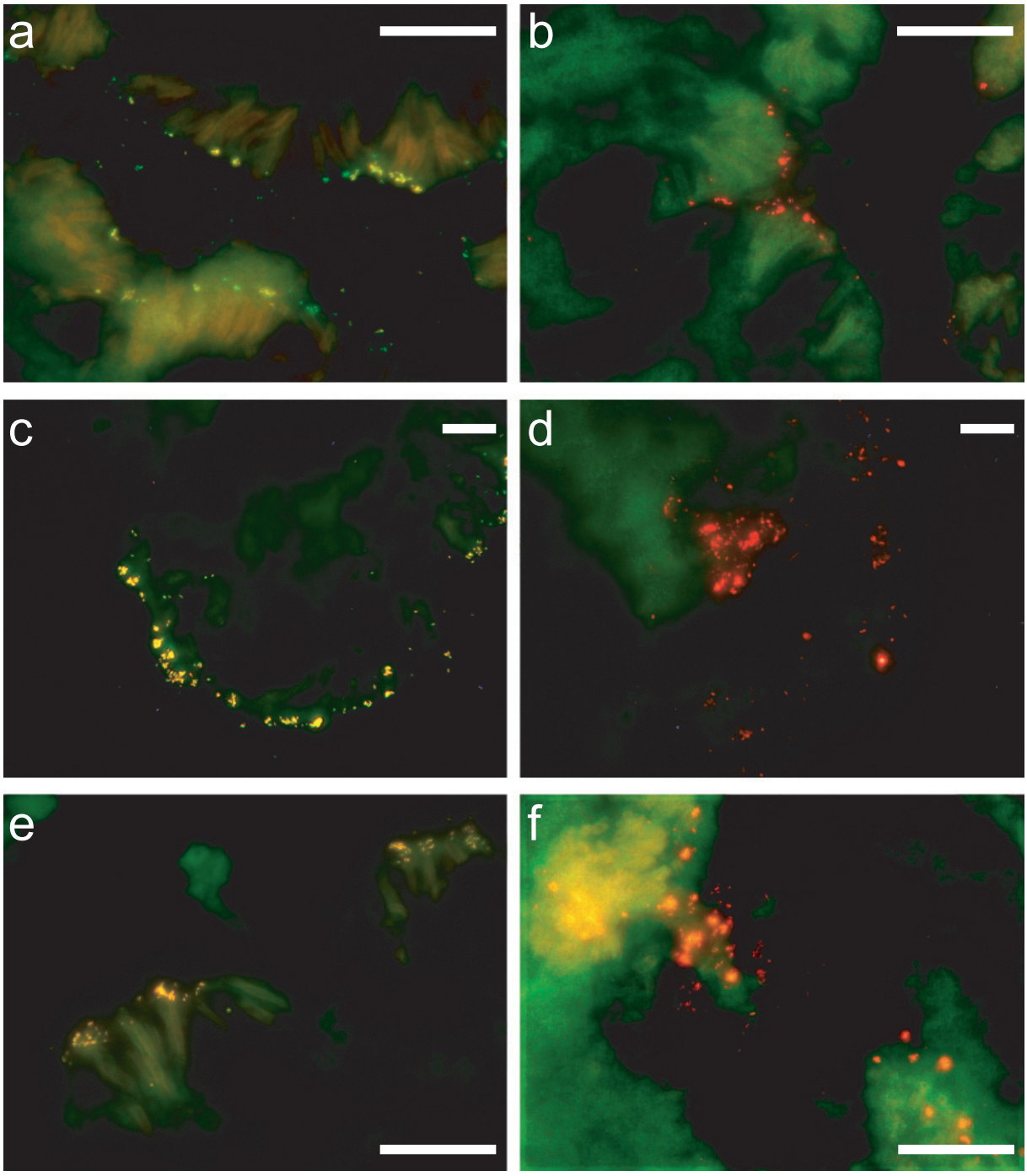

Fig. 18: Epifluorescence micrographs of bacteria on thin sections in the tentacle region of *L. pertusa* polyps. a, b) Red coral colour variety, station 1. c, d) Red coral colour variety, station 2. e, f) White coral colour variety, station 3. The images are overlays of Cy3 (red) and fluorescein signals (green). Double hybridisation with probes LGC0355b (+ Cy3) and EUB338 I (+ fluorescein) resulted in a yellowish overlay signal (a, c, e). Double hybridisation with probes LGC0355b (+ Cy3) and NON338 (+ fluorescein) resulted in a red overlay signal since no hybridisation signal was obtained with control probe NON338 (b, d, f). Scale bars, 20 µm (a-f).

3.3.2 Bacteria Associated with Coral Endoderm

Corals from all stations and both colour varieties harboured filamentous structures in their endoderm (Fig. 19). These structures were thin (0.6 μm) twisted chains about 20 μm long consisting of short rod-shaped cells about 1 μm in length (Fig. 19 a, b). Filaments were scattered within the septal tissue of the gastral cavity. Despite the lack of conspicuous DAPI signals the structures exhibited bright fluorescence upon hybridisation with probe EUB338 I (Fig. 19 c, d). Negative results with control probe NON338 on parallel thin sections (not shown) confirmed the specificity of this hybridisation.

Identification on the sub-domain level was approached as described above (→ 3.3.1). As with the tentacle-associated microbes, only hybridisation with the *Firmicutes*-specific probe LGC0355 under low-stringency conditions (20% formamide in the hybridisation buffer) resulted in positive FISH signals (Fig. 19 a, b). The filaments did not hybridise with probe LGC0355b under stringent conditions (not shown). Omitting the cell wall permeabilisation step in the CARD-FISH protocol resulted in a visible weakening, though not complete loss of the hybridisation signal (Fig. 19 d) as compared to permeabilised cells (Fig. 19 a-c). As in the case of ectoderm-associated bacteria, abundances of filamental structures did not diverge conspicuously between coral samples from different stations or of different colour.

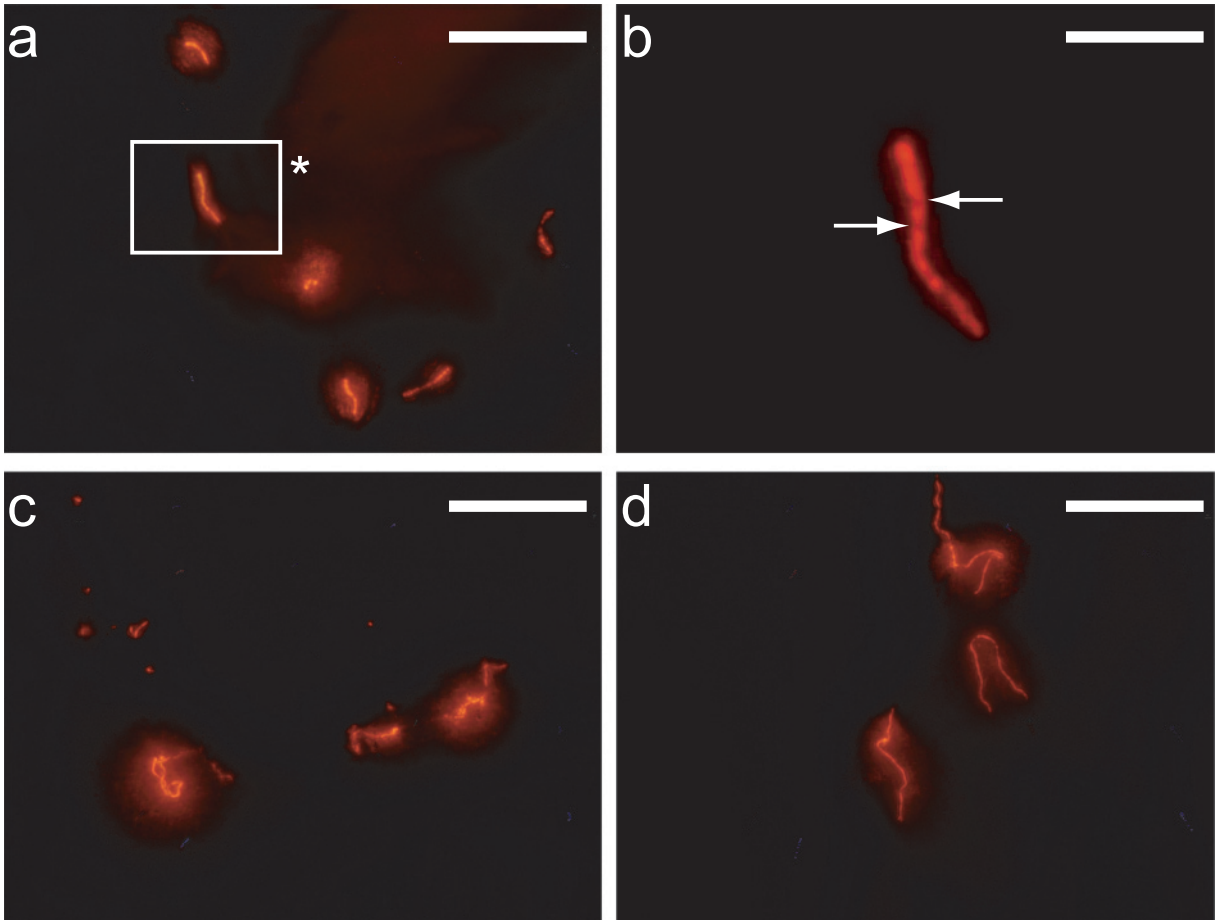

Fig. 19: Epifluorescence micrographs of bacteria on thin sections of the gastral cavity of *L. pertusa* polyps. a, b) White coral colour variety, station 3. b) Micrograph detail of (a) showing a filament that consists of nine cells. c, d) Red coral colour variety, station 1. Thin sections were hybridised with probe LGC0355 under low stringency conditions (20% formamide in hybridisation buffer) (a, b) and probe EUB338 I (c, d), respectively, with Cy3 TSA. Bacteria had been permeabilised with Lysozyme (a-c) or not permeabilised (d) prior to hybridisation. Annotations: *, frame of micrograph detail (b). Arrows in b) mark the gaps between a single cell and adjacent cells in the filament. Scale bars, 20 µm (a, c, d) and 5 µm (b).

4 Discussion

4.1 Differences in Bacterial Assemblages of *L. pertusa*

4.1.1 Comparison of Coral and Environmental Samples

In this study first evidence of special bacterial associations in Norwegian *L. pertusa* from the Trondheimsfjord is presented. Bacterial associations clearly differed from microbial communities of the environment, which was in accordance with results of other studies (Großkurth 2007; Schöttner et al. 2008).

T-RFLP fingerprinting was used to compare microbial communities in *L. pertusa* to those of the coral's environment. The method was demonstrated to be robust in identifying similarities and differences in the composition of complex microbial communities (Dunbar et al. 2000). The main advantages of T-RFLP over the commonly used Denaturing Gradient Gel Electrophoresis (DGGE) lie in higher resolution (Moeseneder et al. 1999) and direct availability of electropherograms in digital form providing high precision and easy downstream data processing. Average peak numbers found in the respective sample types mirrored the complexity (richness) of their microbial assemblages: While the sediment is commonly expected to house the most species-rich microflora, seawater bacteria were found to be less diverse than the sediment but richer than the coral samples, which present a rather special environment for bacteria. This was corroborated by non-parametric Kruskal-Wallis-ANOVA. The microflora hosted by red *L. pertusa* appeared to be richer than that of white *L. pertusa*, but this difference was insignificant for the given dataset.

MDS-aided comparison of T-RFLP profiles demonstrated clear differences between coral, water, and sediment samples (Fig. 5). Since stress values of all ordinations were mostly below 0.10 and never exceeded 0.15, results form dimensional downscaling could be safely used to infer relations between the samples (cf. Clarke 1993). Differences between sample types were again substantiated by both parametric (MANOVA and Duncan's test) and non-parametric (Kruskal-Wallis-ANOVA and Mann-Whitney U test) statistics. Separation of the three sample types was no mere bias caused by different concentrations of the respective PCR products, or only due to water- or sediment-specific T-RFs. It could also be ascribed to a great number of peaks occurring exclusively in the corals (Table 3) denoting a special bacterial community on *L. pertusa*. Consequently,

MDS ordination based only on binary (presence – absence) peak data (Fig. 5 b) led to the same conclusion regarding sample clustering as ordination based on normalised peak areas (Fig. 5 a).

Two more remote water and sediment sample points were observed in the MDS plot based on binary peak data (Fig. 5 b). This scattering mirrors a certain lack of reproducibility in DNA extraction with the UltraClean™ Soil DNA Kit that was only recently documented by Carrigg et al. (2007). The kit extracted bacterial DNA from different samples with varying efficiency (i.e., the amount of DNA per unit of sample material). This in turn affected amplification of 16S rRNA genes from different bacterial groups in subsequent PCR. DNA extraction efficiency was apparently above average with the water and sediment sample in question resulting in more PCR products. This was also seen in the analysis of binary peak data because all peaks were weighted equally regardless of their mostly very low signal intensities. However, the aberrant data points showed greater distance to the coral data than did the other water and sediment samples. This indicated that their additional peaks even enhanced the differences to coral-hosted bacterial communities. Thus, performance issues of the extraction kit did not affect the study in an unacceptable way. In addition, DNA extracts had been pooled prior to phylogenetic analyses: Mixing of parallel extracts of the same sample type levelled differences in their DNA composition. As a result, cloning and sequencing characterised the "average" bacterial community to be covered by DNA extraction from a respective sample type.

4.1.2 Differences between Coral Samples

Associations between *L. pertusa* and bacteria varied within the Trondheimsfjord: For both rare and consistent T-RF data post hoc tests revealed differences between stations 1 ('Tautra') and 2 ('Stokkbergneset') 32.5 km apart from each other. For rare T-RFs (i.e., organisms of more variable occurrence within *L. pertusa*) differences also manifested between stations 2 and 3 ('Røberg') that lay only 3.9 km apart but on opposite sides of the bottleneck connecting the seaward fjord basin with the open sea (Fig. 3). In contrast, variations between stations 1 and 3 remained insignificant in all analyses, though their distance of 28.7 km was almost as large as between stations 1 and 2. Accordingly, divergence in bacterial community composition was not related to distances between sampling sites. Results from binary T-RF data suggested that these differences were not only caused by shifts in relative bacterial abundances: Though there was no indication that

presence of dominant groups varied between stations, changes in presence of rare species or groups were significant.

Also Großkurth (2007) observed spatial variation of *L. pertusa*-associated bacterial communities from adjacent locations by analysis of DGGE patterns and suggested influence of the local environment as an explanation for these inconstancies. Salinity measurements of the present study (→ 2.1.2; 30.1-31.9 PSU) deviated considerably from values (34-34.7 PSU) reported by other authors for comparable locations in the Trondheimsfjord (Jacobson 1983; Børsheim et al. 1999). Since the possibility of exceptional environmental conditions during the sampling time appears rather remote, a systematic measurement error was assumed to be responsible for the aberrant salinity values of the present study. Nevertheless, relative differences in salinity could still be considered in a meaningful way. Relative differences in the temperature and salinity revealed the presence of slightly warmer and more brackish sub-surface water at station 1, while no conspicuous divergences of water masses were observed between stations 2 and 3. However, this does not explain the differences between bacterial associations of coral samples from the three stations (see above). Other physicochemical environmental factors might vary in the sampling region (e.g., current velocity, oxygen saturation, light, non-conservative ions, trace gases, dissolved and particulate organic matter). In addition, site-specific macrofaunal associations or differences in the developmental stage of the corals could account for the observed variations (Großkurth 2007).

In contrast, the finding that the two colour varieties of *L. pertusa* diverged in their bacterial composition (Fig. 7 b, Fig. 8) was unexpected and constituted one of the most intriguing results of this study. Although not as striking as the discrepancies between coral and environmental samples this divergence was statistically significant for relative abundances of consistent peaks, which comprise the most dominant T-RFs (Fig. 6). Contrary to the site-dependent variations, these colour-dependent differences in microbial communities are not explicable ad hoc. This was the reason to lay focus on the latter aspect. Details and implications of this finding are discussed in the following chapters.

4.1.3 Comparison of T-RFLP Data and 16S rDNA Sequences

T-RFLP data were based on PCR products from single-sample DNA extractions, whereas 16S rDNA sequences were obtained from amplified pooled DNA. Also, PCR protocols differed between the two methods. Nevertheless, there were conspicuous congruities between peak positions and intensities of T-RFLP data on the one hand, and T-RF lengths and frequencies of clones on the other (Fig. 4). In particular, most dominant electropherogram peaks were mirrored by frequent clone T-RFs. The slight displacement between peak positions and clone T-RF lengths can be explained by a systematic error introduced by the GeneScan® software during size calling. Given the necessity to limit the number of analysed clones one must not expect to find a matching clone T-RF for every electropherogram peak. Peaks without corresponding clone T-RFs might also constitute artefacts, so-called pseudo-T-RFs. These are caused either by intra-strand reannealing of PCR products, which is strongly dependent on the number of PCR cycles (Egert and Friedrich 2003), or by incomplete restriction enzyme digestion (Osborn et al. 2000). Pseudo-T-RFs may lead to an overestimation of microbial diversity. However, since all samples had been treated in the same way (i.e., equal number of PCR cycles and digestion time), they were also equally prone to this kind of error, so that statistical analysis was not expected to be biased.

Fingerprints generated by T-RFLP reproducibly reflect the composition of the dominant PCR-targeted members of the community, while rare members are likely to be overlooked due to detection threshold effects (Lukow et al. 2000; Osborn et al. 2000). Factoring peak intensity (T-RF abundance) into the analysis must be treated with caution keeping in mind ubiquitous biases in PCR-aided analyses (von Wintzingerode et al. 1997). However, final PCR product concentrations are generally biased toward a 1:1 ratio regardless of the initial template concentrations (Suzuki and Giovannoni 1996). This means that infrequent ribotypes tend to become more abundant with increasing cycle number, while frequent ribotypes remain frequent throughout the PCR. It is thus still safe to assume that dominating phylotypes depicted by both PCR-based methods were also most abundant in situ. This is of importance when it comes to considering bacterial richness: Due to the great variety of bacterial ribotypes (OTUs) in red *L. pertusa*, to reach a theoretical coverage as high as that of white *L. pertusa* (Fig. 9, Table 4) more than 770 clones would have had to be analysed in red *L. pertusa* according to Thiel, Neulinger et al. (2007b). Since this would have been far too cost-intensive and time-consuming, infrequent ribotypes remained

elusive to detailed phylogenetic analysis. For these reasons, conclusions on the ecology of *L. pertusa*-associated microbes (chapter 4.2) were chiefly limited to abundant phylotypes.

Comparison of the two methods also solves seemingly contradictory results: (1) While over one third (37%) of the T-RFs occurred both in corals and environmental samples (water and / or sediment; Table 3), the sequence library shows virtually no common overlap of bacterial consortia for corals and environmental samples except for three proteobacterial OTUs. (2) T-RFLP only detected differences in relative bacterial abundances between coral colour varieties, whereas phylogenetic analysis revealed far more striking disparities between bacterial communities of both coral phenotypes. (3) Phylogenetic analysis supported predictions of bacterial richness by T-RFLP (average peak numbers per sample) with respect to the relations between sediment and water, between sediment and corals, and among coral colour varieties. Yet, contrary to T-RFLP bacterial richness assigned to red corals by phylogenetic analysis was unequivocally higher than that of white corals, even higher than bacterial richness of the surrounding seawater (Fig. 9, Fig. 10, Table 4). The solution for all three issues lies in the fact that different bacterial species, even if they were of different phyla, could produce the same T-RFs with a given restriction enzyme digestion, which reduced resolution of T-RFLP. This was especially the case with dominant peaks. As a consequence thereof, fingerprinting did not resolve the minor differences between corals and environment or differences among coral colour varieties as accurately as the phylogenetic approach. Interestingly, data of Schöttner et al (2008) even suggested highest bacterial diversity to exist in *L. pertusa*, not in the sediment. Whether this is a matter of methodology, or inherent to different properties of sediment or corals sampled in both studies, remains speculative for the time being.

4.2 Dominant Bacterial Groups of *L. pertusa* and their Ecological Potential

4.2.1 Phylogenetic and Ecological Inference

Molecular phylogenetic inference involves comparison of nucleotide sequences – in this case, of the 16S rDNA – according to mathematical algorithms. All such comparisons base on an alignment that defines homologous sequence positions. There are regions of the 16S rDNA with base

counts strongly varying between taxa, wherein assignment of homologous sequence positions is extremely ambiguous. It is therefore impossible to align sequences from diverse bacterial groups (as present in this study) consistently over their whole length. Errors likely to be made here would severely affect downstream analyses (cf. Swofford et al. 1996). The positional mask employed in ARB (→ 2.4) ensured dependable phylogenetic analyses because it admitted only unambiguously alignable sequence positions into phylogenetic analyses. A similar strategy was also used by other authors (e.g., Lanoil et al. 2001). The resulting phylogenies (Fig. 11, Fig. 12) were consistent with high-level bacterial taxonomy and reliably assorted sequences within their respective clusters as confirmed by bootstrapping.

Naturally, the ecology of bacteria is not directly evident from their molecular phylogeny, since 16S rDNA, as a structural gene, does not contain information on the physiological capabilities of the respective organisms. However, evidence of their ecological potential can be deduced from comparison with closely related organisms, whose biochemistry is well known, or by evaluation of common features innate to the whole phylogenetic group they affiliate with.

Bacteria of *L. pertusa* from the Trondheimsfjord mostly affiliated with organisms or groups featuring the following aspects: (1) Cycling of sulphur compounds, (2) methylotrophy, or (3) symbiotic or parasitic relationships with other organisms, especially other corals. It therefore appeared reasonable to examine the potential ecological role of *L. pertusa*-related microbial biodiversity from these angles. In several cases the mentioned aspects were interconnected, as shown in the following.

4.2.2 Sulphur Cycling

Sequences of coral-hosted bacteria with potential thiotrophic abilities (i.e., hydrogen sulphide (H_2S) /thiosulphate ($S_2O_3^{2-}$) oxidation) were confined to the phylum *Proteobacteria*. The class *a-Proteobacteria* was dominated by sequences of the family *Rhodobacteraceae* from white *L. pertusa* (over one third of all sequences obtained from white corals), which plays an important role in the marine sulphur cycle (Gonzalez et al. 1999). Like purple sulphur bacteria, this family of non-obligately aerobic purple bacteria often features red pigments. Many (but not all) representatives perform aerobic anoxygenic phototrophy, but mostly with organic carbon sources (Buchan et al. 2005). Despite their trivial name "non-sulphur" purple bacteria, several groups of *Rhodobacteraceae*

are also able to transform inorganic forms of sulphur, including elemental sulphur, sulphide, sulphite, and thiosulphate. These pathways facilitate sulphur-based litho*hetero*trophy (Buchan et al. 2005), which represents a special type of mixotrophy. It makes their metabolism more flexible as compared to that of obligately chemotrophic species (Sorokin et al. 2005): By drawing energy from sulphur oxidation the bacteria can exploit even small amounts of organic material as carbon sources. Reference strains DIII4* and EI1* showed greatly increased $S_2O_3^{2-}$ oxidation after pyruvate supplementation (Teske et al. 2000). This indicates that these organisms are lithoheterotrophic as well. *Rhodobacteraceae* can use a variety of organic substances as carbon sources, among which are organic and amino acids, sugars, and alcohols (Madigan et al. 2003). Besides, members of the clade are able to degrade N-acetyl-D-glucosamine (chitin) (Cottrell et al. 2000). Some *L. pertusa*-affiliated *Rhodobacteraceae* were related to microorganisms found on whale bones. These bacteria profit from H_2S that is produced through coupling between decomposition of bone lipids and seawater sulphate reduction (Goffredi et al. 2004). Moreover, almost all representatives of the *a-Proteobacteria* (*Rhodobacteraceae*, *Rhodospirillaceae*, *Methylobacterium*, and *Afipia*) are able or likely to exploit dimethylsulphoniopropionate (DMSP), or its derivatives such as dimethylsulphide (DMS), methanesulphonate, and dimethylsulphone as a source of energy (González et al. 1999; González et al. 2000; Zubkov et al. 2001; Yoch 2002; Moosvi et al. 2005). This property links them to methylotrophy (→ 4.2.3).

Two OTUs within the *y-Proteobacteria* comprising 19 sequences exclusively from red *L. pertusa* showed closest relation to endosymbionts of two deep-sea mussels, *Calyptogena phaseoliformis* and *Bathymodiolus* aff. *brevior*. These mussels are part of the fauna colonising hydrothermal vents at the ocean floor spreading centres, an environment rich in H_2S. With their foot tucked in fissures in the seafloor they take up H_2S from hydrothermal fluid seeping from beneath. Since H_2S is toxic for the mussels, it is detoxified either by binding to high molecular binding factors in the hemolymph (*Calyptogena*) (Arp et al. 1984; Powell and Somero 1986) or by transformation into other compounds (*Bathymodiolus*) (Pruski et al. 2002). The transformed reduced sulphur is transported to the bacteria in the gills. They oxidise the reduced sulphur species with oxygen from the surrounding seawater to obtain energy and electrons for CO_2 fixation. These endosymbionts are thus litho*auto*trophic, more precisely, thioautotrophic organisms as opposed to the lithoheterotrophic *a-Proteobacteria* discussed above. Coral-hosted sequences from the present study form an unambiguously monophyletic cluster with the group of these thiotrophs. Taking also the results

from additional BLAST searches into account, these organisms represented by reference sequences E12_CR02_full and G02_CR02_full obviously constitute novel thiotrophs associated with the red colour variety of *L. pertusa*.

Representatives of four other bacterial phyla, *Bacteroidetes*, *Actinobacteria*, *Verrucomicrobia*, and *Planctomycetes*, once more point to the importance of sulphur metabolism in *L. pertusa*-associated bacteria: Closest relatives of these groups were found at active and inactive deep-sea hydrothermal vent sites (Suzuki et al. 2004; Nercessian et al. 2005), basalt glass from an ocean spreading zone (Di Meo-Savoie et al., unpubl.), and in hydrocarbon-rich sediments (Polymenakou et al. 2005). Even at sites without active fluid venting, chemolithotrophy can still occur via metal sulphide oxidation, e.g. by *Archaea* (Edwards et al. 2000); the outer glassy part of submarine erupted basalt contains high amounts of reduced sulphur (Moore and Fabbi 1971); and presence of hydrocarbons in the sediment always implies the release of H_2S through anaerobic methane oxidation: $CH_4 + SO_4^{2-} + 2\,H^+ \rightarrow CO_2 + H_2S + 2\,H_2O$ (e.g., Hansen et al. 1998). Admittedly, a direct involvement in the cycling of sulphur cannot be assumed for all members of the groups in question: A recently described novel member of *Flavobacteriaceae* (*Bacteroidetes*), *Flaviramulus basaltis*, was also found at basalt glass, but with a chemoorganotrophic metabolism and no reported utilisation of sulphur compounds (Einen and Øvreås 2006). The same holds for the representatives of *Verrucomicrobia*, which belong to the genus *Rubritalea* (→ 4.2.4) from inactive deep-sea hydrothermal vent chimneys (Suzuki et al. 2004). These organisms might rather profit from metabolites of sulphur-oxidising bacteria. In contrast, *Actinobacteria* are known to possess highly variable physiological and metabolic properties. Their direct physical association with marine gas hydrates as reported by Lanoil et al. (2001) suggests straight participation in sulphur cycling. This is also conceivable for *Planctomycetes*, as for instance representatives of this phylum isolated from sulphidic sediments were shown to reduce elemental sulphur to sulphide under strictly anaerobic conditions (Elshahed et al. 2007).

4.2.3 Methylotrophy

Methylotrophs have the capacity to aerobically exploit organic single-carbon (C_1) compounds as a sole source of carbon and energy. If the C_1 compound is methane the organism is termed a *methano*troph. The presence of apparent thiotrophs in *L. pertusa*, related to endosymbionts in

Bathymodiolus, raises the question whether there could be a bimodal symbiosis in *L. pertusa* combining thiotrophy and methanotrophy, as was observed in other *Bathymodiolus* species (Duperron et al. 2005; Duperron et al. 2006). From both white and red *L. pertusa* bacterial sequences identified as those of *Methylobacterium radiotolerans* and other members of *Methylobacterium* were obtained. *M. radiotolerans* is a facultative methylotroph. Like all members of the genus it is aerobic and features pink pigmentation. However, this species does not exploit methane (Kato et al. 2005), which rules out a direct link to methanotrophy. Methane utilisation of other members of the genus has been suggested (Van Aken et al. 2004), but is still discussed controversially (Dedysh et al. 2004). While methanotrophic bacteria are confined to exploiting organic C_1 substances (i.e., carbon compounds without C-C bonds), methane-non-utilising methylotrophs such as *Methylobacterium* can also degrade, for instance, organic acids, ethanol, or sugars (Madigan et al. 2003) just like "non-sulphur" purple bacteria (→ 4.2.2).

Another organism abundant in both white and red corals was identified as *Propionibacterium acnes*. Though this actinobacterium is predominantly known as a parasite of the human skin, it is found in the environment as well (e.g., Salvador Pedro et al. 2001): *Propionibacterium* was observed in methanogenic reactors (Fernández et al. 1999; Tsurumi et al. 2000) and in direct association with gas hydrates (Lanoil et al. 2001). Most notably, a sequence identical to those of the present study was obtained from the brine-seawater interface of Kebrit Deep (Arab. *kebrit*, sulphur), a site with considerable concentrations of CH_4 (22 ml l^{-1}) and H_2S (sulphur content 12 to 14 mg l^{-1}). For this location archaeal methanogenesis in sedimentary organic matter as well as biotic methane oxidation at the brine-seawater interface were suggested (Eder et al. 2001). These examples demonstrate a correlation of *Propionibacterium* with methane- and / or sulphide-rich habitats linking it indirectly to thiotrophs (→ 4.2.2). A main characteristic of this genus is the production of large amounts of organic acids, especially propionic and acetic acid, by fermentation of more complex organic substrates such as lactate, carbohydrates, and polyhydroxyl alcohols (Madigan et al. 2003).

Relatives of the *Clostridiaceae* obtained from red *L. pertusa* live strictly anaerobic and occur ubiquitously in nature, particularly in the digestive tract of mammals (Madigan et al. 2003). Like the microbes discussed above they degrade high molecular substances such as sugars, amino acids, and cellulose to low molecular carbon and sulphur compounds including H_2S (Madigan et al. 2003). *Clostridiaceae* are also able to degrade chitin (Schwarz 2001).

4.2.4 Parallels to Other Symbiotic and Parasitic Associations

Almost every bacterial phylum detected in *L. pertusa* from the Trondheimsfjord comprised OTUs that were closely related to sequences obtained from other coral species. Relatives of bacteria associated with several other scleractinians from different suborders and families were found: *Pocillopora damicornis* (4 OTUs), *Porites* sp., (1 OTU), *Oculina patagonica* (1 OTU), and *Pocillopora meandrina* (1 OTU). They are all hermatypic warm-water species.

By far the most similarities (9 OTUs from Norwegian and 1 OTU from Mediterranean *L. pertusa*) were however observed with bacterial lineages from deep-sea gorgonians, so-called "Bamboo Corals" (Isididae), named after their likeness to bamboo plants (Noé and Dullo 2006). Source specimens of bacterial sequence data were sampled from three seamounts in the Gulf of Alaska at depths between 634 m and 3,300 m (Penn et al. 2006). The family's range of distribution exhibits remarkable parallels to that of *L. pertusa* (→ 1.1): It lives from less than 100 m to more than 4,000 m depth along the Indo-Pacific and Atlantic margins and in the Mediterranean (Roark et al. 2005) in areas of high hydrodynamic energy and sufficient advection of zooplankton and particulate organic matter as food sources (Heikoop et al. 2002). In addition, another gorgonian *Muricea elongata*, was found to host bacteria similar to that from Isididae and *L. pertusa* (1 OTU).

Representatives of the *Roseobacter* clade (*a-Proteobacteria*) form symbiotic relationships with various marine organisms (Buchan et al. 2005), as was demonstrated for some *Rhodobacteraceae* species from *L. pertusa* that equally live on the bryozoan *Flustra foliacea* (Pukall et al. 2001). Notably, bacteria of the genus *Sulfitobacter* within this clade are associated with the tubeworm *Lamellibrachia* sp. from cold seeps (Kimura et al. 2003). *a-Proteobacteria* involved in sulphur cycling and methylotrophy (→ 4.2.2, 4.2.3) were also regularly found on other corals: *Roseobacter* strains are known as coral pathogens, e.g., as agents of Black Band Disease in scleractinians (Buchan et al. 2005). They are obviously an integral part of the coral holobiont in both warm- and cold-water habitats as demonstrated by bacterial sequences from Isididae, *P. damicornis*, and *L. pertusa* from this study. Sequences of *Rhodospirillaceae*, another lineage of "non-sulphur" purple bacteria were equally found in *O. patagonica*, Norwegian *L. pertusa*, and – even if not in the same OTU – in Mediterranean *L. pertusa*. Also members of the *Rhizobiales* were found in both Isididae and Norwegian *L. pertusa*, among which is *Afipia* sp. Members of this genus have been shown to

exploit methanesulphonate and dimethylsulphone (Moosvi et al. 2005) and may be both significant sulphur cyclers and methylotrophs in natural environments.

Also *γ-Proteobacteria* in *L. pertusa* can be assigned to other symbiotic bacteria: Relatedness of a distinct group of *γ-Proteobacteria* in red *L. pertusa* to thiotrophic symbionts of deep-sea mussels was already discussed (→ 4.2.2). Similar sulphur-oxidisers were again present on *O. patagonica* (Koren and Rosenberg 2006). Contrary to the thiotrophs of the present study these bacteria belonged to another clade of symbionts predominantly associated with vestimentiferan tubeworms and were not as abundant as in *L. pertusa*. One OTU of the genus *Shigella* was found on both red and white corals. *Shigella* is a facultatively anaerobic pathogen commonly inhabiting the intestinal tract of humans and other primates (Zaika et al. 1998). A closely related organism has also been identified on the scleractinian coral *P. meandrina* (Speck et al., unpubl.) and another scleractinian, *Acropora palmata*, shows antibiotic activity against this germ (Ritchie 2006). It can thus not be ruled out that *Shigella* sp. also affects stony corals as a potential pathogen. One γ-proteobacterial OTU comprising a sequence from *P. damicornis* belonged to the genus *Vibrio* (Bourne and Munn 2005). *Vibrio* appears to be a common part of both hard and soft coral microflora (e.g., Ducklow and Mitchell 1979; Koren and Rosenberg 2006). Members are non-obligate anaerobes (Madigan et al. 2003) and able to degrade chitin (Hunt et al. 2007). But the genus also holds many pathogenic species, some of which are agents of coral diseases: *V. shiloi* (isolated from *O. patagonica*) (Banin et al. 2000b), *V. coralliilyticus* and *V. harveyi* (both isolated from *P. damicornis*) (Ben-Haim et al. 2003; Luna et al. 2007), and *V. tasmaniensis* (isolated from a diseased gorgonian coral) (Vattakaven et al. 2006). Yet, all specimens of *L. pertusa* analysed in the present study were apparently healthy, as were the specimens of *P. damicornis* in the study of Bourne and Munn (2005). Consequently, *Vibrio* sp. found in both coral species may be an opportunistic pathogen constituting a normal component of the healthy coral microbiota until environmental or physiological factors trigger a pathogenic response (Bourne and Munn 2005). The same might hold for *Chryseobacterium* sp. (*Bacteroidetes*) and *Staphylococcus* sp. (*Firmicutes*) that were also found in corals: Clone HKT72 (DQ188008) from *Porites* sp. (Kapley et al. 2007) was identified as uncultured *Chryseobacterium* reported in diseased aquatic animals (Bernardet et al. 2005). The genus *Staphylococcus*, also observed on *P. damicornis* (Bourne and Munn 2005), is likewise associated with diseases of marine crustaceans (Costa et al. 1998; Becker et al. 2004). The role of *Staphylococcus* as potential coral pathogen was very recently discussed by Dinsdale et al. (2008).

The occurrence of the photoautotrophic cyanobacterium *Synechococcus* sp. in both coral colour varieties seems surprising at first glance, since sampling was performed well below the euphotic zone of the Trondheimsfjord, which is not likely to exceed a depth of 20 m (Sakshaug and Myklestad 1973). The possibility that these organisms are mere planktonic bycatch exported from surface waters seems remote in view of the absence of cyanobacterial sequences in the water column. A great variety of hermatypic scleractinians produce secondary metabolites *against* this very cyanobacterial genus (Koh 1997): According to this author *Synechococcus* sp. could be repressed because it features the same cell wall characteristics as *Phormidium corallyticum*, one of the members of a pathogenic microbial consortium causing Black Band Disease (Richardson and Kuta 2003). *Synechococcus* sp. could also be antagonised by hermatypic corals because it might compete with the symbiotic zooxanthellae for photosynthetic resources. Both these arguments are untenable in the case of *L. pertusa*, since the species neither suffers from Black Band Disease nor hosts zooxanthellae. The genus *Synechococcus* frequently forms symbiotic relationships with sponges, which was recently shown for *Tethya aurantium* by Thiel, Neulinger et al. (2007b). Diazotrophic symbiosis was also described for other cyanobacteria-scleractinian associations (Williams et al. 1987; Lesser et al. 2004) with cyanobacteria residing intracellularly in the host tissue. As the latter was not observed in this study, *Synechococcus* sp. appears to live extracellularly on or in *L. pertusa* polyps. Thermophilic *Synechococcus* spp. in microbial mats perform photosynthesis by day and seem to ferment stored carbohydrates to generate reduction equivalents for nitrogen fixation in the dark (Steunou et al. 2006). Cyanobacteria – specifically symbiotic species – can completely resort to chemoheterotrophy in the absence of light while maintaining their capability of nitrogen fixation (Tredici et al. 1988). Under the assumption that such light-independent chemoheterotrophic nitrogen fixation also occurs in *Synechococcus* sp. from the present study a diazotrophic relationship with *L. pertusa* is conceivable.

Most members of the *Verrucomicrobia* found in *L. pertusa* (predominantly in the red colour variety) belonged to the genus *Rubritalea*. This genus owes its name to the production of carotenoids of orange or reddish colour (L. *ruber*, red and *talea*, rod). All four species described to date were isolated from marine sponges: *R. marina* (Scheuermayer et al. 2006), *R. squalenifaciens* (Kasai et al. 2007), and *R. spongiae* and *R. tangerina* (Yoon et al. 2007). All but *R. marina* produced squalene, a triterpenic hydrocarbon that acts as an antioxidant (Ko et al. 2002), as is the case with the carotenoids (Shindo et al. 2007). *R. squalenifaciens* was reported to catabolise chitin (Kasai et al. 2007).

Sequences affiliating with the family *Mycoplasmataceae* (*Firmicutes*, *Mollicutes*) found in this study were phylogenetically remote from their next characterised relative *Mycoplasma sphenisci*, which is a parasite isolated from a Jackass Penguin (*Spheniscus demersus*) (Frasca et al. 2005). Phylogenetic analysis (Fig. 12) suggested that the *Mycoplasmataceae* from *L. pertusa* formed a monophyletic and well-defined cluster within the *Mycoplasma hominis* group together with above-mentioned sequences from Isididae and *M. elongata*. Most mollicutes live as commensals but are also widespread in nature as parasites of a variety of animal groups (including humans) and plants (Razin et al. 1998). (Note that the trivial terms "mycoplasmas" or "mollicutes" are often used synonymously to refer to any species of the class *Mollicutes*.) Though members of the class *Mollicutes* have evolved from cell wall-possessing bacteria and are classified into the phylum *Firmicutes* (L. *firmus*, strong and *cutis*, skin), they are distinguished phenotypically from all other bacteria by their total lack of a cell wall (Razin et al. 1998). This circumstance also led to their name (L. *mollis*, soft). Since the cell membrane is their only barrier, the mycoplasmas are osmotically much more sensitive than other bacteria; however, the constant milieu of their host offers protection (Razin et al. 1998). Due to this deformable membrane the dominating shape of mycoplasmas is a sphere, but cytoskeletal elements in various groups facilitate other appearances, too: Many pathogenic mycoplasmas have a flask- or club-like cell shape with a protruding tip, which serves as an organelle for cytadhesion to epithelial linings of their host (Razin et al. 1998). Mycoplasmas usually exhibit a rather strict host and tissue specificity probably reflecting their nutritionally exacting nature and obligate parasitic mode of life (Razin et al. 1998). They underwent a distinct reductive way of evolution characterised by 'genetic economisation'. Surveys have shown a particular scarcity of genes in mycoplasmas coding for energy and intermediary metabolism (Razin et al. 1998). Because of the absence of cytochromes the major route for ATP synthesis in mycoplasmas is probably substrate-level phosphorylation (Dybvig and Voelker 1996). Lacking the ability of de-novo synthesis of amino and fatty acids makes them totally reliant on external sources of these vital compounds (Razin et al. 1998).

Candidate division TM7 is one of several newly described bacterial divisions exclusively characterised by environmental sequence data (Hugenholtz et al. 1998; Hugenholtz et al. 2001). TM7 sequences have been detected in a range of chemically and geographically diverse habitats (Hugenholtz et al. 2001). These include activated sludges (Bond et al. 1995) as well as hydrothermal sediment at Rainbow vent site (López-García et al. 2003). The latter constitutes yet another

link towards sulphur cycling (→ 4.2.2). TM7 were even found in the human oral cavity, where it is believed to be a pathogen connected to the development of periodontitis (Brinig et al. 2003; Ouverney et al. 2003). Yet, the recent discovery of TM7 as part of the natural microflora of the marine sponge *Chondrilla nucula* (Thiel et al. 2007a) represents further analogy between coral- and sponge-associated bacteria. This indicates a symbiotic potential of this candidate division.

4.3 In-Situ Location of *L. pertusa*-Associated Microbes

4.3.1 Bacteria Associated with Coral Ectoderm

Autofluorescence of the coral tissue could be successfully surmounted by CARD-FISH. By far the most bacteria were detected on the nematocyst batteries of *L. pertusa* (Fig. 14). The bacteria could be successfully hybridised with a modified *Firmicutes*-specific oligonucleotide sequence, probe LGC0355b (Table 1), targeting the 16S rRNA of *Mycoplasmataceae* present in the sequence library. Results of hybridisations at stringent conditions (Fig. 15) and specificity cross check (Fig. 16) showed that the modified probe LGC0355b specifically detects the single-nucleotide deviation from the target sequence of the original probe LGC0355.

Like most oligonucleotide probes LGC0355b is not exclusively specific to *Mycoplasmataceae* but also targets other taxa, predominantly of the class *Bacilli* in the common phylum *Firmicutes*. Morphology of the latter is quite similar to that of the observed microbes. For that reason, probe MYC850 was designed to confirm that the tentacle-associated bacteria on *L. pertusa* belonged to the family *Mycoplasmataceae*. Unfortunately, probe MYC850 did not yield a specific hybridisation signal. Since such a failure is quite common with untested FISH probes (Amann et al. 1995), this negative result was not rated as counterevidence for the identity of *Mycoplasmataceae* in this study. Re-evaluation of probe MYC850 according to the approach of Yilmaz and Noguera (2004) revealed that its overall binding efficiency was too low to perform well under CARD-FISH conditions. Hence, alternative evidence had to be furnished to corroborate that the microbes discovered on *L. pertusa* tentacles were indeed mycoplasmas. The lack of a cell wall is an exclusive property of representatives of the *Mollicutes* (Razin et al. 1998). It could be demonstrated that with the CARD-FISH protocol used in the present study, cell wall permeabilisation was crucial to obtain brightest fluorescence after TSA. The fact that an equally strong hybridisation signal was

obtained from the ectoderm-associated bacteria even without lysozyme treatment confirmed that these prokaryotes lacked a cell wall.

In summary, the results of phylogenetic analysis and CARD-FISH led to the conclusion that the microbes colonising the nematocyst batteries of *L. pertusa* are representatives of a thus far unknown *Mycoplasmataceae* species. Their cell morphology (Fig. 14 f) resembled the flask-shaped and elongate forms with unipolar tip structures of *M. sphenisci* (Frasca et al. 2005), which was the closest characterised relative to the *Mycoplasmataceae* sequences from this study.

Double hybridisation with probes LGC0355b and EUB338 I (Fig. 18) was used to determine the abundance of the new *Mycoplasmataceae* species relative to other bacterial groups on *L. pertusa* thin sections. It could be shown for all coral samples, regardless of their provenience or colour variety, that the bacterial clusters situated on their nematocyst batteries consisted almost entirely of mycoplasmas.

4.3.2 Bacteria Associated with Coral Endoderm

Long and twisted filamentous structures were found in the gastral cavity of red and white coral phenotypes from all stations. Due to the lack of a visible DAPI signal, these structures were first considered artefacts. However, similar filaments had been observed with FISH in *L. pertusa* samples from other Norwegian locations (S Schöttner, pers. comm.) and specificity of the hybridisation was proven by means of the control probe NON338. Poor DNA staining with DAPI was previously reported for other microbes (Boetius et al. 2000).

The phylum *Actinobacteria* abundantly represented in the corals by 16S rDNA sequences is rich in filamentous morphotypes. In contrast, like all sub-phylum level probes used in this survey, also the *Actinobacteria*-specific probe HGC236 failed to hybridise the filaments under stringent conditions. The filamentous bacteria could only hybridise with the *Firmicutes*-specific probe LGC0355 with low stringency, just like the ectoderm-associated mycoplasmas. The only *L. pertusa*-associated sequences, except for those of *Mycoplasmataceae*, which permitted such unspecific probe binding, were that of candidate division TM7 (reference: F05_CW03). The sequence of probe LGC0355 is 5'-GGAA**G**ATTCCCTACTGCTG-3'), its original target site on the bacterial ribosome is 5'-CAGCAGUAGGGAAU**C**UUCC-3' (the reverse complement of the probe

sequence). TM7 sequences show only one mismatch as compared to this site (5'-CAGCAG-UAGGGAAU**U**UUCC-3'), which is at the same position as with *Mycoplasmataceae* (5'-CAGCAG-UAGGGAAU**A**UUCC-3') but has uridine instead of adenosine. This could also explain why hybridisation of filamentous bacteria with the *Mycoplasmataceae*-specific probe LGC0355b (5'-GGAA**T**ATTCCCTACTGCTG-3') failed under stringent conditions: ΔG (Gibbs free energy) of hybrid formation is less negative for the U-T mismatch between the TM7 target site and probe LGC0355b than it is for the matching pair A-T in *Mycoplasmataceae* under the same hybridisation conditions.

The filaments found in this study also resembled morphotypes of TM7 bacteria from the human oral cavity (Brinig et al. 2003; Ouverney et al. 2003) and from a laboratory scale bioreactor (Hugenholtz et al. 2001). The latter study reported members of candidate division TM7 to be gram-positive. Coral endoderm-associated bacteria showed visible fluorescence attenuation when cell wall permeabilisation was omitted (unlike *Mycoplasmataceae*). This indicates that they have a cell wall. It though appears to be a priori more permeable to the large CARD-FISH probe molecules than the cell walls of other, namely gram-positive bacteria (cf. Fig. 17 a-f). Other filamentous bacteria were described to occur endolithically (i.e., in the skeleton) in the Mediterranean coral *O. patagonica* (Ainsworth et al. 2008), but due to their autofluorescence typical for chlorophyll they were most likely cyanobacteria.

For the time being, identity of the endoderm-associated filaments found in *L. pertusa* cannot be determined with sufficient confidence. Nevertheless, indirect evidence presented here permits addressing of these bacteria as bona fide TM7.

4.3.3 Comparison of Sequence Frequencies and Bacterial in-Situ Abundances

The high microbial diversity of 27 OTUs in white and 54 OTUs in red corals as depicted by the sequence library is in marked contrast to CARD-FISH results: Irrespective some sporadic *a-* and *y-Proteobacteria* only two groups of bacteria (probably two species) were abundant and in direct association with the coral tissue, namely *Mycoplasmataceae* and bona fide TM7. Test hybridisations with aquarium-reared *L. pertusa* polyps (Fig. 13) indicated that the mucus of this coral was densely populated by bacteria, which were apparently far more abundant than bacteria on coral tissue thin

sections. These findings reveal that the major bacterial diversity – and most likely the numerical majority of bacteria – is sited in the mucus and probably also in the gastric fluid of *L. pertusa*.

The reason why bacteria associated with coral mucus and gastric fluid were observed by 16S rDNA analysis but not CARD-FISH is given by the different preparation procedure of the two techniques: For DNA extraction mucus and gastric fluid were never completely removed from coral-specimens. In contrast to that, storage, decalcification, paraffin embedding and de-paraffination, and the multiple washing steps of the thin sections during the CARD-FISH procedure washed away mucus as well as gastric fluid from the polyps. Loose bacteria living therein were thus not preserved on the slides except for very few cells of *a-* and *γ-Proteobacteria*, the apparently largest groups on *L. pertusa*. Even in the aquarium-reared polyps that were immediately decalcified after fixation without additional storage time, only wisps of mucus remained attached to the tissue thin sections. Thus, the starting material was different for both techniques.

Embedding the polyps in artificial resin prior to thin sectioning might have better preserved unbound bacteria. However, resin embedding has a considerable drawback in combination with CARD-FISH, because the dense matrix of the resin obstructs diffusion of the large HRP-labelled probe. Moreover, tissue boundaries stand out much clearer in paraffin-embedded samples than in resin-embedded as observed for test samples in Histocryl acrylic resin. It would neither have been useful to examine the mucus of aquarium-hatched coral samples, because significant compositional changes in *L. pertusa*'s microbial community were reported to occur in the artificial environment (Schöttner et al. 2008). For all these reasons, the present study was confined to investigate the in-situ location of the tissue-associated bacteria of *L. pertusa* (→ 1.3).

Both coral colour varieties hosted *Mycoplasmataceae* and bona fide TM7 without discernible differences in abundance. This finding conflicted with phylogenetic analysis, according to which both groups of bacteria should live exclusively on the white *L. pertusa* colour variety (Fig. 10, Fig. 11). This inconsistence can be explained by statistical effects and PCR interference: The probability for a distinct PCR product to become cloned and sequenced is a function of its relative proportion in the overall mixture of amplified gene fragments. This probability is particularly low for rare fragments in a diverse mixture as in the case of red *L. pertusa* (Fig. 9). Since the two epithelium-bound bacterial groups most probably constituted minor fractions of the total bacterial

quantum on the coral polyps (see above), they are less likely to be detected in red corals by cloning and sequencing than in white corals.

Furthermore, obstruction of primer annealing or elongation could have occurred: Primer-template mismatch can never be ruled out with primers targeting a broad range of phylogenetic groups and might occur in both *Mycoplasmataceae* and TM7. In many mycoplasmas, the adenine residues at GATC sites are methylated, while in others the cytosine residues are methylated (Razin et al. 1998). Because this motif is part of the forward primer 27f sequence (5'-AGAGTT-T**GATC**MTGGCTCAG-3') and its reverse complement reads the same, binding of the primer is likely to be restricted in *Mycoplasmataceae* (Herman et al. 1996). Methylation may also inhibit elongation (Rountree and Selker 1997). These factors could also have reduced the yield of respective PCR products in white *L. pertusa* leading to the observed underrepresentation of *Mycoplasmataceae* and TM7 sequences. In red *L. pertusa* the effects of low primer binding probability (see above) and obstruction of primer annealing or elongation would be combined. Consequently, the probability of *Mycoplasmataceae* and TM7 sequences to become retrieved from red *L. pertusa* would be further impaired, which could explain why no sequences of these groups were found in that coral colour variety.

4.4 Relations between *L. pertusa* and its Associated Bacteria

4.4.1 Partitioning and Specificity of the Bacterial Community

The present study confirmed that also *L. pertusa* from the Trondheimsfjord hosted a special and highly diverse bacterial community, as do members of the same coral species from other geographic regions (Yakimov et al. 2006; Großkurth 2007; Schöttner et al. 2008) (→ 4.1.1). Members of this bacterial community are – preponderantly – not present in the coral's environment (→ 4.1.3). Notably, this was also true for samples from station 1 ('Tautra'), one of the shallowest occurrences of *L. pertusa* (Hovland and Risk 2003) and thus likely to show greater variations in environmental conditions than deeper habitats.

Data presented here and by Großkurth (2007) displayed spatial variations of coral associated bacteria within the respective sampling areas. Even more outstanding differences were shown in the present study by comparative analysis of *L. pertusa*-derived DNA sequences from different geo-

graphic regions: Apart from marginal intersections in the *a-* and *γ-Proteobacteria* Mediterranean *L. pertusa* (Yakimov et al. 2006) hosted bacterial phylotypes that were almost completely different from those in Norwegian specimens. Oceanographic data from the Central Mediterranean where these corals had been sampled show that bottom temperature and salinity are generally around 13.6°C and 38.7 PSU (Klein et al. 1999; Seritti et al. 2003). These values are much higher than those reported for the Trondheimsfjord (→ 2.1.1). *L. pertusa* actually lives at the limits of its physiological niche (→ 1.1) in the Mediterranean, which might be the reason why living deep-water coral banks are generally rare there (Delibrias and Taviani 1985; Tursi et al. 2004). A species existing in a suboptimal milieu may unsurprisingly host a bacterial community that is adapted to these specific conditions. This strongly suggests temperature and salinity to be additional physicochemical factors (→ 4.1.2) accounting for the divergence between prokaryotic consortia from Norwegian and Mediterranean *L. pertusa*.

A considerable partitioning of the bacterial community was observed on *L. pertusa* by comparison of 16S rDNA sequence frequencies and bacterial in-situ abundances (→ 4.3.3): Only two groups of bacteria (*Mycoplasmataceae* and bona fide TM7) were bound to the coral tissues, while most bacteria were apparently present in the mucopolysaccharide layer and gastric fluid. Data from other studies obtained with the fingerprinting methods DGGE (Großkurth 2007) and ARISA (Schöttner et al. 2008) indicated a similar partitioning of bacterial groups in *L. pertusa*. The tissue-bound bacteria were equally found on corals from all stations and both colour varieties (→ 4.3.1, 4.3.2). Hence, the observed location- and colour-related differences between coral-associated groups (→ 4.1.2) could only be ascribed to communities in the "liquid" parts of the host, i.e., in the mucus and gastric fluid. These communities fluctuated in their relative abundances and – in the case of spatial variation – even in presence and absence. They appear thus to be sensitive to physicochemical factors (→ 4.1.2) varying from site to site. Association of these "liquid-inhabiting" bacterial groups with the coral can thus not be regarded as constitutive but rather as adaptive to the prevailing environmental conditions.

To call the observed coral-microbial association truly 'specific' it has to be constant over time and space. While *temporal* variations still need to be investigated, results of the present study gave evidence for a *spatially* constant fraction of tissue-associated bacteria in *L. pertusa*. Yet, this was not mirrored on a wider geographic level, since Großkurth (2007) reported spatial variations of both

mucus- and tissue-associated bacteria on *L. pertusa* from offshore locations in the NE Atlantic. This coral is known to form distinct, genetically isolated offshore and fjord populations in the NE Atlantic (Le Goff-Vitry et al. 2004). Thus, it could be speculated that each of these populations hosts a unique bacterial community and that there is no really constitutive coral-bacterial association in *L. pertusa* at all. Also Yakimov et al. (2006) did not find *Mycoplasmataceae* and TM7 on Mediterranean *L. pertusa*. Then again, there is the possibility that these bacterial groups had simply been overlooked in the former studies, since culture-independent techniques had been employed which are susceptible to biases similar to those described in this study (→ 4.3.3). Unpublished FISH data suggested the presence of at least bona fide TM7 on corals from other Norwegian locations (S Schöttner, pers. comm.). There is a good chance that the use of CARD-FISH or other bio imaging techniques in future studies will reveal these tissue-associated microbes on *L. pertusa* from other geographic regions.

The coral's microbiology features numerous similarities to other bacterial symbioses, notably with marine sponges. Similarities to sponge symbionts were also described for Mediterranean *L. pertusa* by Yakimov et al. (2006), who point out that specialised microbiota may be important for protecting the coral from pathogens through the production of secondary antibiotics as demonstrated for some sponges. Parallels between microbial inhabitants of *L. pertusa* and symbionts from other warm- and cold-water corals indicate that microbial populations associated with corals are globally distributed as postulated by Bourne and Munn (2005). Such parallels are particularly frequent in the case of Isididae, cold-water corals whose distribution and habitat requirements are very similar to those of *L. pertusa*.

In summary, the bacterial community of *L. pertusa* from the Trondheimsfjord could not be termed 'specific' *sensu stricto* but had to be divided into two sub-communities differing in their location on the coral: (1) a tissue-bound bacterial fraction on the ecto- and endoderm that was spatially constant at least on a regional scale and (2) a "liquid-associated" bacterial fraction in the mucus and gastric fluid varying with location and colour variety of its host. Parallels to other coral-bacterial associations suggested the existence of certain 'cold-water coral-specific' bacterial groups *sensu lato*.

The "liquid-associated" community comprised bacterial groups with important alimentary characteristics, in particular thio- and methylotrophy (→ 4.2.2, 4.2.3). Their implications on various

aspects of the ecology of *L. pertusa* are discussed in detail in the following chapters 4.4.2 and 4.4.3, while the roles of tissue-associated bacteria are addressed in chapter 4.4.4.

4.4.2 Implications for Nutrition, Health, and Dispersal of *L. pertusa*

L. pertusa is thought to feed primarily on mesozooplankton (Kiriakoulakis et al. 2005). However, in radiocarbon labelling experiments conducted with several species of stony corals Sorokin (1973) showed that the polyps actively incorporate planktonic bacteria. The amount of this bacterial organic carbon assimilated per day was equivalent to 10-20% of the carbon content of the polyp's body. Bacteria could thus provide subsidiary alimentation for *L. pertusa*. In fact, corals have been suggested to harbour microbial communities for beneficial effect (Rohwer and Kelley 2004) which amongst others also includes nutrition: By ingesting their own mucus (Coles and Strathmann 1973), a process that was also observed with *L. pertusa* (Mortensen 2001), corals can harvest contained bacteria after the continuous-flow culture principle. It has been shown that the growth rate of microbes living in the corals' surface mucopolysaccharide layer can be accelerated through elevation of DOC levels by an order of magnitude (Kline et al. 2006). In the Trondheimsfjord large amounts of DOC accumulate in the euphotic zone during the productive season (Børsheim et al. 1999). A considerable proportion of mono- and particularly polysaccharides are exported from the euphotic zone to the deep fjord, probably through the sinking of phytoplankton cells which are degraded in the depth (Børsheim et al. 1999). Though *L. pertusa* is unable to benefit from dissolved substances in the water column, most members of its bacterial consortium can degrade these sugar compounds (→ 4.2.2 f) and incorporate them into their own biomass. This can in turn be utilised by the coral. In a way, that scenario shows similarities to a "host-bound" variant of the water column 'microbial loop' (Azam et al. 1983) without nanoplanktonic heterotrophic flagellates as interlink but the coral as direct terminal consumer.

In this context, also a diazotrophic symbiosis between *Synechococcus* sp. (assuming the ability of light-independent nitrogen fixation) and *L. pertusa* would make sense: Though the coral may not directly suffer nitrogen limitation from feeding on zooplankton, utilisation of organic compounds from the water column by its bacterial inhabitants could require a supplementary source of nitrogen, since exported organic matter is known to be nitrogen-depleted.

Additionally, the associated bacterial groups can catabolise cellulose from phytoplankton that was ingested either through mucus entrapment (Lewis and Price 1975) or as part of the diet of the coral's prey. Even the chitin in the exoskeleton of prey crustaceans can be degraded by *Vibrio*, *Clostridiaceae*, probably *Rubritalea* sp., and most notably, by the dominant *Rhodobacteraceae*. This offers a significant contribution to the carbon and nitrogen budget (McCarthy et al. 1997; Aluwihare et al. 2005) of the coral holobiont.

Almost all *a-Proteobacteria* occurring in Norwegian *L. pertusa* can exploit DMSP or its derivatives (→ 4.2.2). DMSP is an osmoprotectant produced in high concentrations by marine phytoplankton. It was even measured in a variety of tropical coral reef invertebrates as a consequence either of their phytoplankton diet or, in the case of cnidarians, their symbiosis with zooxanthellae (Van Alstyne et al. 2006). Damm et al. (2008) argued that DMSP degradation is responsible for a direct in-situ methane production / consumption cycle in another NE Atlantic fjord environment (Storfjorden, Svalbard Archipelago). The substance and its derivatives should thus also occur in considerable amounts in highly productive coastal regions and fjords such as the Trondheimsfjord, especially during phytoplankton blooms. In addition to providing the coral with energy from DMSP-degradation, the mentioned *a-Proteobacteria* are regarded to play an important role in the cycling of these organic sulphur compounds (Penn et al. 2006) produced in and exported from the euphotic zone.

Several bacterial groups observed in Norwegian *L. pertusa* (*Rhodobacteraceae*, *Rhodospirillaceae*, *Vibrio*, *Propionibacterium*, *Planctomyces*, *Clostridiaceae*) can tolerate or even strictly require anaerobic conditions. Finding sequences from coral-associated *Archaea* closely related to strict and facultative anaerobes on coral surface microlayers led Kellogg (2004) to hypothesise that anaerobic microniches may exist in the mucus of tropical reef corals. Anthozoan polyps and colonies are in fact diffusion-limited in their oxygen consumption even under well-stirred, air-saturated conditions (Shick 1990). This can result in total oxygen depletion within the diffusion boundary layer on the surface of coral polyps (Shashar et al. 1993). This layer is 0.2-4 mm thick depending on the growth form of the colony, polyp size, and current velocity (Shashar et al. 1993; Kühl et al. 1995). Contraction of the polyps even enhances hypoxia, thus favouring anaerobic metabolism in the gastral cavity (Levy et al. 2001). Observations on aquarium-reared *L. pertusa* showed that its polyps can stay retracted for three weeks and longer (Mortensen 2001) and also retract after

feeding for up to several days (A Form, pers. comm.). This strongly implies that hypoxia occurs in *L. pertusa*'s polyps and, as a consequence, fermentation may significantly contribute to the nutrition of this coral. The above-mentioned bacterial groups appear to constitute a specialised community that profits from further degrading end products of the coral's own anaerobic metabolism. Low molecular organic acids produced by *P. acnes* and *Clostridiaceae* can thereby in turn serve as substrates for *Rhodobacteraceae* and *Rhodospirillaceae*, and for *Methylobacterium* under (temporarily) oxic conditions.

Deep-water coral reefs are highly endangered ecosystems (Fosså et al. 2002; Hall-Spencer et al. 2002; Roberts and Hirshfield 2004). The direct consequences of ocean acidification by anthropogenic CO_2 on the calcification process in cold-water corals have already been recognised (Orr et al. 2005). But shifts in both pH and temperature can also threaten these animals *indirectly* through detrimental responses of their bacterial microflora: Coral-pathogenic *Vibrio* (*V. shiloi*, *V. coralliilyticus*) become virulent only at higher water temperatures (Ben-Haim and Rosenberg 2002; Ben-Haim et al. 2003; Vattakaven et al. 2006). One must be apprehensive of the possibility that *Vibrio* sp., but also *Shigella* sp., *Chryseobacterium* sp., and *Staphylococcus* sp. found in *L. pertusa* exhibit a pathogenic potential that is likewise stimulated by temperature rise. Environmental changes can also affect other members of the microbial community. Resulting disruption of the balance between the coral and its associated microbiota (even if they are harmless under natural circumstances) can trigger coral mortality as well (Kline et al. 2006).

To my knowledge, no investigations have been made so far on the nature of the two phenotypes of *L. pertusa*. It is not even known whether they are genetically or environmentally controlled (Mortensen 2001). Both colour varieties of *L. pertusa* were found growing entwined at all stations in the Trondheimsfjord (cf. Fig. 1), so divergence in their bacterial composition cannot be explained by spatial separation. In contrast, personal observations by myself and other researchers imply that *L. pertusa*'s white colour variety occurs more frequently along the NE Atlantic continental margin than the red one. Cold-water reefs along the southern and central parts of this margin comprise exclusively white *L. pertusa* (A Freiwald, pers. comm.). What does the red coral phenotype cause to be rarer than the white one? Their distribution may be limited by some hitherto unknown internal or external factor that affects red *L. pertusa* more than white, consequently allowing common occurrence only in locations where this factor is optimal for both

corals. The dominance of *Rhodobacteraceae* in white corals (or rather, the scarcity of them in red corals) might constitute an *internal* factor: Because of their mixotrophy these bacteria can be highly productive also under conditions of moderate carbon supply. This would enable the white phenotype to exist also in regions that offer less amounts of dissolved and / or particulate organic matter, where the red phenotype could not survive according to this line of thought. An *external* factor that might affect coral dispersal is given by the 'Hydraulic Theory' proposed by Hovland and colleagues (Hovland 1990; Hovland and Thomsen 1997; Hovland et al. 1998; Hovland and Risk 2003). These authors proposed that chemotrophic bacteria might provide the corals with supplementary nutriment at sites where hydrocarbon-rich fluids emanate from the seafloor. Remarkably enough, the vast majority of sequences with relatives from marine environments rich in reduced sulphur compounds are found on red *L. pertusa*. In particular, the red coral colour variety exclusively features a phylogenetic cluster of *γ-Proteobacteria*, whose relatedness to thiotrophic endosymbionts strongly suggests their aptitude to draw energy from the oxidation of reduced sulphur compounds. The latter can be formed by anaerobic methane oxidation occurring along with fluid seepage (→ 4.2.2). If red *L. pertusa*, because of these specialised bacterial consortia, preferred higher concentrations of substrates for chemotrophy in the ambient seawater than white *L. pertusa*, the two colour varieties would only occur together at sites where fluid-seepage is sufficiently high for both phenotypes. From statistical analysis of fingerprinting data, station 2 ('Stokkbergneset') showed the most pronounced dissimilarities to the other stations in terms of relative and absolute composition of *L. pertusa*-related bacterial communities (→ 4.1.2). Acoustic measurements provided evidence for hydrocarbon-enriched pore water seepage in the Agdenes reef complex (Hovland and Risk 2003) fringing the southern side of the sound between seaward fjord and Norwegian Sea. Judging from its position in the Trondheimsfjord (Fig. 3) it is well conceivable that station 2 lies within the reach of this seepage and fluid emanation may constitute another physicochemical factor (→ 4.1.2) controlling the bacterial consortia on *L. pertusa* in the sense of the 'Hydraulic Theory'.

Albeit thiotrophic *γ-Proteobacteria* on red corals could be positively influenced by seepage-coupled anaerobic methane oxidation, this coral phenotype is obviously not completely reliant on hydrocarbon seepage, since it also grows in regions for which such activity can be ruled out (e.g., station 1) (Hovland and Risk 2003). A trophic linkage appears to exist that enables independence of the above-mentioned *γ-Proteobacteria* from exogenous H_2S: The gas can also be produced

through decomposition of sulphur-containing amino acids by *Clostridiaceae*. Strikingly enough, that group, too, appears to occur exclusively on red *L. pertusa*. Of course, this proposition calls for further studies including stocktaking of coral phenotypes and detailed measurements of water chemistry on various sites.

Interestingly, relatedness of bacteria from Mediterranean *L. pertusa* to microbes from hydrocarbon seep or hydrothermal sediments (→ 3.2.1) suggests that they, too, are involved in metabolising reduced sulphur compounds. This in turn implies that, howbeit Mediterranean corals hosts different bacterial groups owing to the special environmental conditions, these groups occupy the same or similar ecological niches connected to sulphur cycling as microbes in Norwegian *L. pertusa* (→ 4.4.2).

4.4.3 Bacterial Community Composition and Colouring of *L. pertusa*

The finding of coral colour-dependent variations in the bacterial consortia of *L. pertusa* imposes two other questions: What is the cause for the observed differences in bacterial community composition of the two coral phenotypes? And: Could bacteria cause the different colouring in *L. pertusa*?

Mucus-mediated selection of bacterial symbionts was shown in the scleractinian coral *Acropora palmata*, suggesting the coral mucus to play a role in the structuring of beneficial coral-associated microbial communities (Ritchie 2006). Selection of certain bacterial groups by antibiotic or growth-stimulating coral metabolites was also demonstrated for *L. pertusa* (Großkurth 2007). The variability of the "liquid-associated" bacterial fraction (→ 4.4.1) observed in the present study could be caused by such metabolites. Colour-related differences in bacterial community composition imply that white and red *L. pertusa* colonies produce different microbiologically active substances that lead to colour-specific selection of certain bacterial groups over others.

Bacterial pigmentation is already well known to play a role in eukaryote-prokaryote symbioses. In particular, bacterially induced colouring applies to the Caribbean scleractinian coral *Montastraea cavernosa* (Lesser et al. 2004): Its bright fluorescent orange colour is not caused by the animal itself but by accessory pigments belonging to symbiotic cyanobacteria inside the coral tissue. It is of course unlikely that staining in *L. pertusa* is caused by photosynthesis-related pigments, as this

species grows in virtually complete darkness. But pigmentation is a common phenomenon in bacteria and does not necessarily coincide with photosynthesis or light protection. Light-independent carotenoid formation, so-called scotochromogenesis, has been suggested to be a protection against oxidative damage involving oxygen radicals (Madigan et al. 2003). Several bacteria found in this study are know to produce reddish pigments: *Rhodobacteraceae*, *Methylobacterium*, and *Rubritalea* sp. All three groups occurred in both white and red *L. pertusa*. The *Roseobacter* clade, though more abundant in white corals, does not necessarily produce red pigments: Closest cultivated relatives from the most abundant *Roseobacter* group in white *L. pertusa*, strains DIII4* and EI1*, were in fact colourless (Teske et al. 2000). *Methylobacterium* was only of minor abundance in the two colour varieties. This leaves *Rubritalea* sp. (*Verrucomicrobia*), the only microbe both obligatory red and prevailing on red *L. pertusa*, as the potential candidate for coral colouration. Since *Verrucomicrobia* were not detected on or in the coral tissue, a direct colouring of the tissue by the bacteria as observed in *M. cavernosa* (Lesser et al. 2004) can be ruled out. Instead, conservation of the carotenoids by the host cells upon digestion of the bacteria is conceivable. They could serve the corals as protective agents against oxidative stress, as is the case for the squalene produced by *Rubritalea* sp.

4.4.4 The Role of Tissue-Associated Bona Fide TM7 and *Mycoplasmataceae*

Two bacterial groups, *Mycoplasmataceae* and bona fide TM7, were found in close association with the tissues of *L. pertusa*. From the interpretation of CARD-FISH data (→ 4.3) a schematic illustration was created (Fig. 20). This scheme is meant to serve as a synoptic impression elucidating positions and proportions of the two groups in relation to their host. Bacteria associated with the coral's mucus and gastric fluid are not shown in Fig. 20.

For the first time, sequences of candidate division TM7 were found in corals. With high probability, those sequences belong to the filamentous bacteria observed in the gastrocoel of *L. pertusa* (Fig. 20). General physiology and ecology of this group remain subject to speculation until additional knowledge from isolation assays becomes available. From what was said above on hypoxia in the coral (→ 4.4.2), the location of these bona fide TM7 filaments indicates an anaerobic metabolism. Their obviously tight attachment to the endodermal tissue suggests an interaction with the gastromuscular cells probably involving the exchange of metabolites with its host.

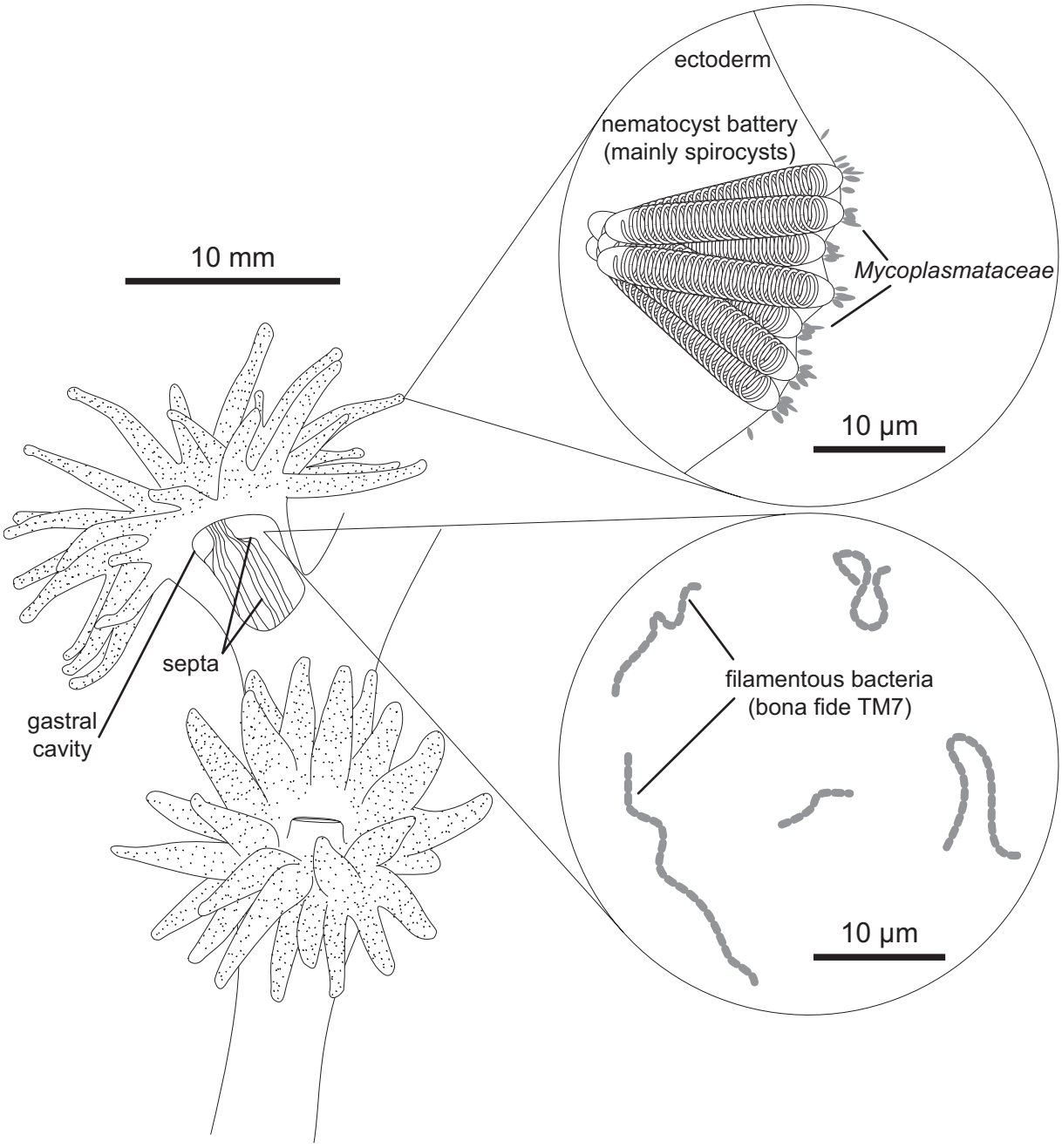

Fig. 20: Schematic illustration of *L. pertusa* polyps and bacteria hosted on their ectoderm and endoderm. Bacteria associated with mucus and gastric fluid of the coral are not shown.

Mycoplasmas commonly live either attached to interior epithelia or inside cells of their hosts. Several species were reported to colonise the external ear canal of goats (Cottew and Yeats 1981; DaMassa et al. 1994). To my knowledge, the present study constitutes the first report on *Mycoplasmataceae* residing on exterior parts of their host, directly facing the environment. Given the osmotic sensivity of this group (→ 4.2.4) their protection at this exposed location could be ascribed to buffer properties of the coral's mucopolysaccharide layer. Conclusions from the

general biology of mycoplasmas (→ 4.2.4) and their distinct boundedness to *L. pertusa*'s spirocysts (Fig. 20) lead to the following theory: Capturing procedure in corals involves discharge of stenoteles and other penetrant cnidocysts that perforate the prey and inject neurotoxins. Spirocyst threads bear hollow tubules that solubilise upon discharge and contact with sea water and adhere to the prey (Mariscal et al. 1977). Thus, the prey is kept affixed to the tentacles while the paralysing effect of the neurotoxins evolves. Penetration of the prey will lead to leakage of hemolymph. This process is comparable to the release of DOC from planktonic algae by 'sloppy feeding' in zooplankton (e.g., Møller 2005). Their location on the distal ends of the spirocysts allows coral-associated *Mycoplasmataceae* to directly assimilate from the leaking hemolymph amino and fatty acids that they cannot synthesise themselves. The bacteria prevent themselves from getting removed during the coral's feeding process by adhesion to the host tissue via their tip structure. The available evidence suggests that these *L. pertusa*-associated mycoplasmas live as commensals in contrast to many of their parasitic relatives. They profit from the prey capture activity but are neither advantageous nor detrimental to their coral host.

Closest relatives of the newly discovered *Mycoplasmataceae* are common on octocorals (Isididae and *M. elongata*) (Fig. 11). Together these sequences form a monophyletic cluster within the *Mycoplasma hominis* group (Fig. 12) (→ 3.2.1, 4.2.4). It is therefore reasoned that these organisms are members of a novel phylogenetic lineage currently consisting of three apparently coral-specific *Mycoplasmataceae* species. Its representative from *L. pertusa* is proposed as a novel candidate species, "*Candidatus* Mycoplasma corallicola", which is formally described in the following chapter.

4.4.5 Proposal of "*Candidatus* Mycoplasma corallicola"

As suggested by Murray and Stackebrandt (1995), the category "*Candidatus*" should be used for a description of prokaryotic entities that is based on more information than just a DNA sequence but which lacks characteristics required according to the International Code of Nomenclature of Bacteria. The *Mycoplasmataceae* described here represent a novel lineage of *Mollicutes*. 16S rDNA sequence similarity is 89% and below to all other described *Mycoplasma* species, which justifies proposition of a new candidate species. The lineage should be designated "*Candidatus* Mycoplasma corallicola" (co.ral.li.co'la. L. n. *corallum*, coral; L. suff. *-cola*, inhabitant dweller; N.L. n.

corallicola, coral-dweller, referring to the host of the microorganism). The phylotype inhabiting the cold-water coral *L. pertusa* is currently the only representative of this candidate species.

Assignment to "*Candidatus* Mycoplasma corallicola" is based on (1) the 16S rRNA gene sequence of the above-mentioned phylotype (D11_CW02_full, EMBL accession number AM911412), (2) a flask-shaped cell morphology of 0.5 × 1.6 μm, (3) the absence of a cell wall, (4) preferential attachment to the spirocysts on the tentacle ectoderm of *L. pertusa*, and (5) positive hybridisation with the oligonucleotide probe LGC0355b (5'-GGAATATTCCCTACTGCTG-3').

4.5 Significance and Outlook

The present study tries to provide comprehensive report on the bacterial microflora associated with the cold-water coral *L. pertusa*. Connections between the microbiology of this and other marine hosts, most notably other corals were discovered. The association with certain types of bacteria gave a number of clues about the ecology of *L. pertusa*. However, this indirect evidence has to remain necessarily speculative in some points. Further studies based on these results will offer new directions for research. In particular, the following aspects might be addressed:

(1) Comparison of *L. pertusa*-associated communities from a range of other locations to broaden the data pool for conclusions on distribution patterns.

(2) Examination of the novel thiotrophic *γ-Proteobacteria*, bona fide TM7, and "*Candidatus* Mycoplasma corallicola" by use of both cultivation and culture-independent methods.

(3) Investigation into the role of sulphur cycling, methylotrophy, and anaerobiosis in the coral, e.g., by microsensor measurements and enzyme assays.

(4) Finding the cause of different colouring of *L. pertusa* by chemical analysis of its pigments and comparing them to bacterial ones.

(5) Examination of the mechanisms used by *L. pertusa* colour varieties to maintain different microbial communities, e.g., by analysis of antimicrobial factors in the coral mucus.

Investigation into these aspects will further elucidate the role of bacteria for the ecology of this important cold-water coral species.

Acknowledgements

- First of all, I would like to express my greatest thanks to Prof. Dr. Karin Lochte (now director of the Alfred Wegener Institute for Polar and Marine Research (AWI), Bremerhaven) for her ingratiating, patient, and encouraging supervision, and for offering me additional financial support through the AWI.

- Equal thanks go to my co-supervisor Prof. Dr. Wolf-Christian Dullo (Leibniz Institute for Marine Sciences (IFM-GEOMAR), Kiel) who offered me the opportunity to work on the fascinating relationship between *L. pertusa* and bacteria. In particular, my research was part of the "Moundforce" project (DU/29/35-1) of the German Research Foundation (DFG) and received considerable co-financing through Prof. Dr. Dullo's Leibniz award (DU/29/33).

- I am deeply indebted to Dr. Johanna Järnegren (now Norwegian Institute for Nature Research, Trondheim) and Martin Ludvigsen (Norwegian University of Science and Technology, Trondheim), Prof. Dr. Egil Sakshaugh, Prof. Dr. Jon-Arne Sneli, the staff of Trondhjem Biological Station, the crew of R/V "Vita", and – not least – Dr. Eike Breitbarth (now University of Göteborg) for their organisational aid.

- Prof. Dr. Ulf Riebesell and Dipl.-Biol. Armin Form (IFM-GEOMAR) not only provided me with aquarium-reared *L. pertusa* specimens but also with loads of valuable information on this species.

- My T-RFLP analyses were enabled by the kind donation of GeneScan® software by Dr. Klaus Heidorn (Institute for Hematopathology, Kiel University Hospital) and the permission of Prof. Dr. Johannes F. Imhoff and his work group (IFM-GEOMAR) to use their facilities.

- High-quality genetic sequencing service was provided by Anita Dietsch and Melanie Friskovec (Institute for Clinical Molecular Biology, Kiel University Hospital).

- Dipl. Biol. Miriam Weber (Max Planck Institute for Marine Microbiology, Bremen) taught me the art of CARD-FISH.

– Dipl.-Biol. Andrea Gärtner (IFM-GEOMAR) provided me with the bacterial test strains for CARD-FISH. I very much appreciate her efforts to culture them several times only for this purpose.

– Prof. Dr. Ulrich Sommer and his work group (IFM-GEOMAR) allowed me to use their epifluorescence microscope.

– Dipl.-Biol. Annegret Stuhr (IFM-GEOMAR) put the digital still camera at my disposal.

– It is thanks to Dipl.-Biol. Sandra Schöttner (Max Planck Institute for Marine Microbiology, Bremen) that I re-examined my coral thin sections and realised the irregular filaments on them were no artefacts.

– Many thanks to Dr. Vera Thiel (IFM-GEOMAR) for her constructive critique on methodology and contents of this thesis.

– Erling Svensen provided me generously with a free top quality underwater photograph of *L. pertusa* (Fig. 1).

– This work would not have been successful without the precious advice and aid of many persons. Some who definitely deserve to be mentioned here are (in alphabetical order): Dr. Martina Blümel, Peter Fritsche, Dr. Michael Hügler, Diana Hümmer, Tania Klüver, B.Sc. Rebecca Langlois, Dr. Frank Lappe, Kerstin Nachtigall, Dr. Andres Rüggeberg, Dr. Jörg Süling, Dipl.-Biol. Marcus Tank, and Dr. Jutta Wiese (all IFM-GEOMAR).

– I am grateful to all people I made friends with during the time of my work.

References

Ainsworth TD, Fine M, Roff G, Hoegh-Guldberg O (2008) Bacteria are Not the Primary Cause of Bleaching in the Mediterranean Coral *Oculina patagonica*. ISME J 2:67-73

Altschul SF, Gish W, Miller W, Myers EW, Lipman DJ (1990) Basic Local Alignment Search Tool. J Mol Biol 215:403-410

Aluwihare LI, Repeta DJ, Pantoja S, Johnson CG (2005) Two Chemically Distinct Pools of Organic Nitrogen Accumulate in the Ocean. Science 308:1007-1010

Amann R, Binder BJ, Olson RJ, Chrisholm SW, Devereux R, Stahl DA (1990) Combination of 16S rRNA-Targeted Oligonucleotide Probes with Flow Cytometry for Analyzing Mixed Microbial Populations. Appl Environ Microbiol 56:1919-1925

Amann R, Ludwig W, Schleifer K-H (1995) Phylogenetic Identification and in Situ Detection of Individual Microbial Cells without Cultivation. Microbiol Rev 59:143-169

Arp AJ, Childress JJ, Fisher CR (1984) Metabolic and Blood-Gas Transport Characteristics of the Hydrothermal Vent Bivalve *Calyptogena magnifica*. Physiol Zool 57:648-662

Azam F, Fenchel T, Field JG, Gray JS, Meyer-Reil LA, Thingstad F (1983) The Ecological Role of Water-Column Microbes in the Sea. Mar Ecol Prog Ser 10:257-263

Banin E, Ben-Haim Y, Israely T, Loya Y, Rosenberg E (2000a) Effect of the Environment on the Bacterial Bleaching of Corals. Water Air Soil Poll 123:337-352

Banin E, Israely T, Kushmaro A, Loya Y, Orr E, Rosenberg E (2000b) Penetration of the Coral-Bleaching Bacterium *Vibrio shiloi* into *Oculina patagonica*. Appl Environ Microbiol 66:3031-3036

Becker P, Smolowitz R, Porter M, Hsu A, Roberts S (2004) Characterization of Bacteria Associated with Lobster Shell Disease. Biol Bull 207:171-171

Ben-Haim Y, Rosenberg E (2002) A Novel *Vibrio* sp. Pathogen of the Coral *Pocillopora Damicornis*. Mar Biol 141:47-55

Ben-Haim Y, Thompson FL, Thompson CC, Cnockaert MC, Hoste B, Swings J, Rosenberg E (2003) *Vibrio coralliilyticus* sp. nov., a Temperature-Dependent Pathogen of the Coral *Pocillopora Damicornis*. Int J Syst Evol Microbiol 53:309-315

Bernardet JF, Vancanneyt M, Matte-Tailliez O, Grisez L, Tailliez P, Bizet C, Nowakowski M, Kerouault B, Swings J (2005) Polyphasic Study of *Chryseobacterium* Strains Isolated from Diseased Aquatic Animals. Syst Appl Microbiol 28:640-660

Beuck L, Freiwald A (2005) Bioerosion Patterns in a Deep-Water *Lophelia pertusa* (Scleractinia) Thicket (Propeller Mound, Northern Porcupine Seabight). In: Freiwald A, Roberts JM (eds) Cold-Water Corals and Ecosystems. Springer, Berlin, Heidelberg, pp 915-936

Boetius A, Ravenschlag K, Schubert CJ, Rickert D, Widdel F, Gieseke A, Amann R, Jørgensen BB, Witte U, Pfannkuche O (2000) A Marine Microbial Consortium Apparently Mediating Anaerobic Oxidation of Methane. Nature 407:623-626

Bond PL, Hugenholtz P, Keller J, Blackall LL (1995) Bacterial Community Structures of Phosphate-Removing and Non-Phosphate-Removing Activated Sludges from Sequencing Batch Reactors. Appl Environ Microbiol 61:1910-1916

Børsheim KY, Myklestad SM, Sneli J-A (1999) Monthly Profiles of DOC, Mono- and Polysaccharides at Two Locations in the Trondheimsfjord (Norway) During Two Years. Mar Chem 63:255-272

Bourne DG, Munn CB (2005) Diversity of Bacteria Associated with the Coral *Pocillopora Damicornis* from the Great Barrier Reef. Environ Microbiol 7:1162-1174

Brinig MM, Lepp PW, Ouverney CC, Armitage GC, Relman DA (2003) Prevalence of Bacteria of Division TM7 in Human Subgingival Plaque and Their Association with Disease. Appl Environ Microbiol 69:1687-1694

Brosius J, Dull TJ, Sleeter DD, Noller HF (1981) Gene Organization and Primary Structure of a Ribosomal Operon from *Escherichia coli*. J Mol Biol 148:107-127

Buchan A, González JM, Moran MA (2005) Overview of the Marine *Roseobacter* Lineage. Appl Environ Microbiol 71:5665-5677

Buddemeier RW, Kienze RA (1976) Coral Growth. Oceanogr Mar Biol Ann Rev 14:183-225

Buhl-Mortensen L, Mortensen PB (2004) Symbiosis in Deep-Water Corals. Symbiosis 37:33-61

Bythell JC, Barer MR, Cooney RP, Guest JR, O'Donnell AG, Pantos O, Le Tissier MDA (2002) Histopathological Methods for the Investigation of Microbial Communities Associated with Disease Lesions in Reef Corals. Lett Appl Microbiol 34:359-364

Carrigg C, Rice O, Kavanagh S, Collins G, O'Flaherty V (2007) DNA Extraction Method Affects Microbial Community Profiles from Soils and Sediment. Appl Microbiol Biot 77:955-964

Casamayor EO, Massana R, Benlloch S, Øvreås L, Diez B, Goddard VJ, Gasol JM, Joint I, Rodriguez-Valera F, Pedrós-Alió C (2002) Changes in Archaeal, Bacterial and Eukaryal Assemblages Along a Salinity Gradient by Comparison of Genetic Fingerprinting Methods in a Multipond Solar Saltern. Environ Microbiol 4:338-348

Clarke KR (1993) Nonparametric Multivariate Analyses of Changes in Community Structure. Aust Ecol 18:117-143

Cole JR, Chai B, Farris RJ, Wang Q, Kulam-Syed-Mohideen AS, McGarrell DM, Bandela AM, Cardenas E, Garrity GM, Tiedje JM (2007) The Ribosomal Database Project (RDP-II): Introducing myRDP Space and Quality Controlled Public Data. Nucleic Acids Res 35:D169-D172

Cole JR, Chai B, Marsh TL, Farris RJ, Wang Q, Kulam SA, Chandra S, McGarrell DM, Schmidt TM, Garrity GM, Tiedje JM (2003) The Ribosomal Database Project (RDP-II): Previewing a New Autoaligner That Allows Regular Updates and the New Prokaryotic Taxonomy. Nucleic Acids Res 31:442-443

Coles SL, Strathmann R (1973) Observations on Coral Mucus 'Flocs' and Their Potential Trophic Significance. Limnol Oceanogr 18:673-678

Cooney RP, Pantos O, Le Tissier MDA, Barer MR, O'Donnell AG, Bythell JC (2002) Characterization of the Bacterial Consortium Associated with Black Band Disease in Coral Using Molecular Microbiological Techniques. Environ Microbiol 4:401-413

Costa R, Mermoud I, Koblavi S, Morlet B, Haffner P, Berthe F, Legroumellec M, Grimont P (1998) Isolation and Characterization of Bacteria Associated with a *Penaeus stylirostris* Disease (Syndrome 93) in New Caledonia. Aquaculture 164:297-309

Cottew GS, Yeats FR (1981) Occurrence of Mycoplasmas in Clinically Normal Goats. Aust Vet J 57:52-53

Cottrell MT, Wood DN, Yu LY, Kirchman DL (2000) Selected Chitinase Genes in Cultured and Uncultured Marine Bacteria in the Alpha- and Gamma-Subclasses of the *Proteobacteria*. Appl Environ Microbiol 66:1195-1201

Daims H, Brühl A, Amann R, Schleifer K-H, Wagner M (1999) The Domain-Specific Probe Eub338 Is Insufficient for the Detection of All Bacteria: Development and Evaluation of a More Comprehensive Probe Set. Syst Appl Microbiol 22:434-444

DaMassa AJ, Tully JG, Rose DL, Pitcher D, Leach RH, Cottew GS (1994) *Mycoplasma auris* sp. nov., *Mycoplasma cottewii* sp. nov., and *Mycoplasma yeatsii* sp. nov., New Sterol-Requiring Mollicutes from the External Ear Canals of Goats. Int J Syst Bacteriol 44:479-484

Damm E, Kiene RP, Schwarz J, Falck E, Dieckmann G (2008) Methane Cycling and Its Relationship with DMSP During a Phytoplankton Bloom. Geophys Res Abs 10:1607-7962/gra/EGU2008-A-03226

Dedysh SN, Dunfield PF, Trotsenko YA (2004) Methane Utilization by *Methylobacterium* Species: New Evidence but Still No Proof for an Old Controversy. Int J Syst Evol Microbiol 54:1919-1920

Delibrias G, Taviani M (1985) Dating the Death of Mediterranean Deep-Sea Scleractinian Corals. Mar Geol 62:175-180

Denner EBM, Smith GW, Busse H-J, Schumann P, Narzt T, Polson SW, Lubitz W, Richardson LL (2003) *Aurantimonas coralicida* gen. nov., sp. nov., the Causative Agent of White Plague Type II on Caribbean Scleractinian Corals. Int J Syst Evol Microbiol 53:1115-1122

Dinsdale EA, Pantos O, Smriga S, Edwards RA, Angly F, Wegley L, Hatay M, Hall D, Brown E, Haynes M, Krause L, Sala E, Sandin SA, Thurber RV, Willis BL, Azam F, Knowlton N, Rohwer F (2008) Microbial Ecology of Four Coral Atolls in the Northern Line Islands. PLoS ONE 3:e1584

DiSalvo LH (1969) Isolation of Bacteria from the Corallum of *Porites lobata* (Vaughn) and Its Possible Significance. Am Zool 9:735-740

DiSalvo LH (1971) Regenerative Functions and Microbial Ecology of Coral Reefs: Labelled Bacteria in a Coral Reef Microcosm. J Exp Mar Biol Ecol 7:123-136

Dons C (1944) Norges Korallrev. Det Kongelige Norske Videnskabers Selskab. Forhandlinger 16:37-82

Ducklow HW, Mitchell R (1979) Bacterial Populations and Adaptations in the Mucus Layers on Living Corals. Limnol Oceanogr 24:715-725

Dunbar JM, Ticknor LO, Kuske CR (2000) Assessment of Microbial Diversity in Four Southwestern United States Soils by 16S rRNA Gene Terminal Restriction Fragment Analysis. Appl Environ Microbiol 66:2943-2950

Duperron S, Bergin C, Zielinski F, Blazejak A, Pernthaler A, McKiness ZP, DeChaine E, Cavanaugh CM, Dubilier N (2006) A Dual Symbiosis Shared by Two Mussel Species, *Bathymodiolus azoricus* and *Bathymodiolus puteoserpentis* (Bivalvia: Mytilidae), from Hydrothermal Vents Along the Northern Mid-Atlantic Ridge. Environ Microbiol 8:1441-1447

Duperron S, Nadalig T, Caprais JC, Sibuet M, Fiala-Medioni A, Amann R, Dubilier N (2005) Dual Symbiosis in a *Bathymodiolus* sp. Mussel from a Methane Seep on the Gabon Continental Margin (Southeast Atlantic): 16S rRNA Phylogeny and Distribution of the Symbionts in Gills. Appl Environ Microbiol 71:1694-1700

Dybvig K, Voelker LL (1996) Molecular Biology of Mycoplasmas. Annu Rev Microbiol 50:25-57

Eder W, Jahnke LL, Schmidt M, Huber R (2001) Microbial Diversity of the Brine-Seawater Interface of the Kebrit Deep, Red Sea, Studied Via 16S rRNA Gene Sequences and Cultivation Methods. Appl Environ Microbiol 67:3077-3085

Edwards KJ, Bond PL, Gihring TM, Banfield JF (2000) An Archaeal Iron-Oxidizing Extreme Acidophile Important in Acid Mine Drainage. Science 287:1796-1799

Egert M, Friedrich MW (2003) Formation of Pseudo-Terminal Restriction Fragments, a PCR-Related Bias Affecting Terminal Restriction Fragment Length Polymorphism Analysis of Microbial Community Structure. Appl Environ Microbiol 69:2555-2562

Einen J, Øvreås L (2006) *Flaviramulus basaltis* gen. nov., sp. nov., a Novel Member of the Family *Flavobacteriaceae* Isolated from Seafloor Basalt. Int J Syst Evol Microbiol 56:2455-2461

Elshahed MS, Youssef NH, Luo Q, Najar FZ, Roe BA, Sisk TM, Buhring SI, Hinrichs K-U, Krumholz LR (2007) Phylogenetic and Metabolic Diversity of *Planctomycetes* from Anaerobic, Sulfide- and Sulfur-Rich Zodletone Spring, Oklahoma. Appl Environ Microbiol 73:4707-4716

Erhart R, Bradford D, Seviour RJ, Amann R, Blackall LL (1997) Development and Use of Fluorescent in Situ Hybridization Probes for the Detection and Identification of "Microthrix Parvicella" in Activated Sludge. Syst Appl Microbiol 20:310-318

Fernández A, Huang S, Seston S, Xing J, Hickey R, Criddle C, Tiedje JM (1999) How Stable Is Stable? Function Versus Community Composition. Appl Environ Microbiol 65:3697-3704

Fisher MM, Triplett EW (1999) Automated Approach for Ribosomal Intergenic Spacer Analysis of Microbial Diversity and Its Application to Freshwater Bacterial Communities. Appl Environ Microbiol 65:4630-4636

Fosså JH, Mortensen PB, Furevik DM (2002) The Deep-Water Coral *Lophelia pertusa* in Norwegian Waters: Distribution and Fishery Impacts. Hydrobiologia 471:1-12

Franzisket L (1970) The Effect of Mucus on Respirometry of Reef Corals. Int Rev Gesamt Hydrobiol 55:409-412

Frasca S, Jr., Weber ES, Urquhart H, Liao XF, Gladd M, Cecchini K, Hudson P, May M, Gast RJ, Gorton TS, Geary SJ (2005) Isolation and Characterization of *Mycoplasma sphenisci* sp. nov. From the Choana of an Aquarium-Reared Jackass Penguin (*Spheniscus demersus*). J Clin Microbiol 43:2976-2979

Freiwald A (1998) Geobiology of *Lophelia pertusa* (Scleractinia) Reefs in the North Atlantic. Habilitation thesis, Universität Bremen, Bremen

Freiwald A (2002) Reef-Forming Cold-Water Corals. In: Wefer G, Billett D, Hebbeln D, Jørgensen BB, Schlüter M, van Weering TCE (eds) Ocean Margin Systems. Springer, Berlin, Heidelberg, pp 365-385

Freiwald A, Henrich R, Paetzold J (1997) Anatomy of a Deep-Water Coral Reef Mound from Stjernsund, West Finnmark, Northern Norway. In: James NP, Clarke Jonathan AD (eds) Cool-Water Carbonates. SEPM (Society for Sedimentary Geology), Tulsa, pp 141-162

Freiwald A, Wilson JB, Henrich R (1999) Grounding Pleistocene Icebergs Shape Recent Deep-Water Coral Reefs. Sed Geol 125:1-8

Frias-Lopez J, Zerkle AL, Bonheyo GT, Fouke BW (2002) Partitioning of Bacterial Communities between Seawater and Healthy, Black Band Diseased, and Dead Coral Surfaces. Appl. Environ. Microbiol. 68:2214-2228

Gärtner A, Wiese J, Imhoff JF (2008) *Amphritea atlantica* gen. nov., sp. nov., a Gammaproteobacterium from the Logatchev Hydrothermal Vent Field. Int J Syst Evol Microbiol 58:34-39

Goffredi SK, Paull CK, Fulton-Bennett K, Hurtado LA, Vrijenhoek RC (2004) Unusual Benthic Fauna Associated with a Whale Fall in Monterey Canyon, California. Deep Sea Res I 51:1295-1306

Gonzalez JM, Kiene RP, Moran MA (1999) Transformation of Sulfur Compounds by an Abundant Lineage of Marine Bacteria in the Alpha -Subclass of the Class Proteobacteria. Appl. Environ. Microbiol. 65:3810-3819

González JM, Kiene RP, Moran MA (1999) Transformation of Sulfur Compounds by an Abundant Lineage of Marine Bacteria in the Alpha-Subclass of the Class *Proteobacteria*. Appl Environ Microbiol 65:3810-3819

González JM, Simó R, Massana R, Covert JS, Casamayor EO, Pedrós-Alió C, Moran MA (2000) Bacterial Community Structure Associated with a Dimethylsulfoniopropionate-Producing North Atlantic Algal Bloom. Appl Environ Microbiol 66:4237-4246

Großkurth AK (2007) Analysis of Bacterial Community Composition on the Cold-Water Coral *Lophelia pertusa* and Antibacterial Effects of Coral Extracts. Diploma thesis, Carl von Ossietzky Universität, Oldenburg, 105 pages

Guindon S, Gascuel O (2003) A Simple, Fast, and Accurate Algorithm to Estimate Large Phylogenies by Maximum Likelihood. Syst Biol 52:696-704

Gutiérrez G, Sánchez D, Marín A (2002) A Reanalysis of the Ancient Mitochondrial DNA Sequences Recovered from Neandertal Bones. Mol Biol Evol 19:1359-1366

Hallberg KB, Coupland K, Kimura S, Johnson DB (2006) Macroscopic Streamer Growths in Acidic, Metal-Rich Mine Waters in North Wales Consist of Novel and Remarkably Simple Bacterial Communities. Appl Environ Microbiol 72:2022-2030

Hall-Spencer J, Allain V, Fosså JH (2002) Trawling Damage to Northeast Atlantic Ancient Coral Reefs. P Roy Soc Lond B Bio 269:507-511

Hansen LB, Finster K, Fossing H, Iversen N (1998) Anaerobic Methane Oxidation in Sulfate Depleted Sediments: Effects of Sulfate and Molybdate Additions. Aquat Microb Ecol 14:195-204

Heikoop JM, Hickmott DD, Risk MJ, Shearer CK, Atudorei V (2002) Potential Climate Signals from the Deep-Sea Gorgonian Coral *Primnoa resedaeformis*. Hydrobiologia 471:117-124

Herman JG, Graff JR, Myohanen S, Nelkin BD, Baylin SB (1996) Methylation-Specific PCR: A Novel PCR Assay for Methylation Status of CpG Islands. P Natl Acad Sci USA 93:9821-9826

Hovland M (1990) Do Carbonate Reefs Form Due to Fluid Seepage? Terra Nova 2:8-18

Hovland M, Mortensen PB, Brattegard T, Strass P, Rokoengen K (1998) Ahermatypic Coral Banks Off Mid-Norway: Evidence for a Link with Seepage of Light Hydrocarbons. Palaios 13:189-200

Hovland M, Risk MJ (2003) Do Norwegian Deep-Water Coral Reefs Rely on Seeping Fluids? Mar Geol 198:83-96

Hovland M, Thomsen E (1997) Cold-Water Corals - Are They Hydrocarbon Seep Related? Mar Geol 137:159-164

Huber T, Faulkner G, Hugenholtz P (2004) Bellerophon: A Program to Detect Chimeric Sequences in Multiple Sequence Alignments. Bioinformatics 20:2317-2319

Hugenholtz P, Goebel BM, Pace NR (1998) Impact of Culture-Independent Studies on the Emerging Phylogenetic View of Bacterial Diversity. J Bacteriol 180:6793-

Hugenholtz P, Tyson GW, Blackall LL (2002) Design and Evaluation of 16S rRNA-Targeted Oligonucleotide Probes for Fluorescence in Situ Hybridization. Methods Mol Biol 179:29-42

Hugenholtz P, Tyson GW, Webb RI, Wagner AM, Blackall LL (2001) Investigation of Candidate Division TM7, a Recently Recognized Major Lineage of the Domain Bacteria with No Known Pure-Culture Representatives. Appl Environ Microbiol 67:411-419

Hunt DE, Gevers D, Vahora NM, Polz MF (2007) Conservation of the Chitin Utilization Pathway in the *Vibrionaceae*. Appl Environ Microbiol DOI: 10.1128/AEM.01412-07

Hurlbert S (1971) The Nonconcept of Species Diversity: A Critique and Alternative Parameters. Ecology 52:577–586

Jacobson P (1983) Physical Oceanography of the Trondheimsfjord. Geophys Astro Fluid 26:3-26

Kapley A, Siddiqui S, Misra K, Ahmad S, Purohit H (2007) Preliminary Analysis of Bacterial Diversity Associated with the *Porites* Coral from the Arabian Sea. World J Microbiol Biotechnol 23:923-930

Kasai H, Katsuta A, Sekiguchi H, Matsuda S, Adachi K, Shindo K, Yoon J, Yokota A, Shizuri Y (2007) *Rubritalea squalenifaciens* sp. nov., a Squalene-Producing Marine Bacterium Belonging to Subdivision 1 of the Phylum '*Verrucomicrobia*'. Int J Syst Evol Microbiol 57:1630-1634

Kato Y, Asahara M, Arai D, Goto K, Yokota A (2005) Reclassification of *Methylobacterium chloromethanicum* and *Methylobacterium dichloromethanicum* as Later Subjective Synonyms of *Methylobacterium extorquens* and of *Methylobacterium lusitanum* as a Later Subjective Synonym of *Methylobacterium rhodesianum*. J Gen Appl Microbiol 51:287-299

Keane TM, Creevey CJ, Pentony MM, Naughton TJ, McInerney JO (2006) Assessment of Methods for Amino Acid Matrix Selection and Their Use on Empirical Data Shows That Ad Hoc Assumptions for Choice of Matrix are Not Justified. BMC Evol Biol 6

Kellogg CA (2006) Microbial Ecology of the Deep-Sea Coral *Lophelia pertusa* [Abstract Only]. EOS Trans AGU 87.

Kellogg CA (2004) Tropical *Archaea*: Diversity Associated with the Surface Microlayer of Corals. Mar Ecol Prog Ser 273:81-88

Kellogg CA, Stone RP (2004) A Pilot Study of Deep Water Coral Microbial Ecology [Abstract Only]. ASLO/TOS Ocean Research Conference.

Kelman D, Kashman Y, Rosenberg E, Kushmaro A, Loya Y (2006) Antimicrobial Activity of Red Sea Corals. Mar Biol 149:357-363

Kelman D, Kushmaro A, Kashman Y, Loya Y, Benayahu Y (1998) Antimicrobial Activity of a Red Sea Soft Coral, *Parerythropodium fulvum fulvum*: Reproductive and Developmental Considerations. Mar Ecol Prog Ser 169:87-95

Kimura H, Higashide Y, Naganuma T (2003) Endosymbiotic Microflora of the Vestimentiferan Tubeworm (*Lamellibrachia* sp.) from a Bathyal Cold Seep. Mar Biotechnol 5:593-603

Kiriakoulakis K, Fisher E, Wolff GA, Freiwald A, Grehan A, Roberts JM (2005) Lipids and Nitrogen Isotopes of Two Deep-Water Corals from the North-East Atlantic: Initial Results and Implications for Their Nutrition. In: Freiwald A, Roberts JM (eds) Cold-Water Corals and Ecosystems. Springer, Berlin, Heidelberg, pp 715-729

Klein B, Roether W, Manca BB, Bregant D, Beitzel V, Kovacevic V, Luchetta A (1999) The Large Deep Water Transient in the Eastern Mediterranean. Deep Sea Res I 46:371-414

Kline DI, Kuntz NM, Breitbart M, Knowlton N, Rohwer F (2006) Role of Elevated Organic Carbon Levels and Microbial Activity in Coral Mortality. Mar Ecol Prog Ser 314:119-125

Knowlton N, Rohwer F (2003) Multispecies Microbial Mutualisms on Coral Reefs: The Host as a Habitat. Am Nat 162:S51-S62

Ko T-F, Weng Y-M, Chiou RY-Y (2002) Squalene Content and Antioxidant Activity of *Terminalia catappa* Leaves and Seeds. J Agric Food Chem 50:5343-5348

Koh EGL (1997) Do Scleractinian Corals Engage in Chemical Warfare against Microbes? J Chem Ecol 23:379-398

Koren O, Rosenberg E (2006) Bacteria Associated with Mucus and Tissues of the Coral *Oculina patagonica* in Summer and Winter. Appl Environ Microbiol 72:5254-5259

Kormas KA, Tivey MK, Von Damm K, Teske A (2006) Bacterial and Archaeal Phylotypes Associated with Distinct Mineralogical Layers of a White Smoker Spire from a Deep-Sea Hydrothermal Vent Site (9°N, East Pacific Rise). Environ Microbiol 8:909-920

Kühl M, Cohen Y, Dalsgaard T, Jørgensen BB, Revsbech NP (1995) Microenvironment and Photosynthesis of Zooxanthellae in Scleractinian Corals Studied with Microsensors for O_2, pH and Light. Mar Ecol Prog Ser 117:159-172

Kulikova T, Aldebert P, Althorpe N, Baker W, Bates K, Browne P, van den Broek A, Cochrane G, Duggan K, Eberhardt R, Faruque N, Garcia-Pastor M, Harte N, Kanz C, Leinonen R, Lin Q, Lombard V, Lopez R, Mancuso R, McHale M, Nardone F, Silventoinen V, Stoehr P, Stoesser G, Tuli MA, Tzouvara K, Vaughan R, Wu D, Zhu W, Apweiler R (2004) The Embl Nucleotide Sequence Database. Nucleic Acids Res 32:D27-30

Lanoil BD, Sassen R, La Duc MT, Sweet ST, Nealson KH (2001) *Bacteria* and *Archaea* Physically Associated with Gulf of Mexico Gas Hydrates. Appl Environ Microbiol 67:5143-5153

Le Campion-Alsumard T, Golubic S, Hutchings P (1995) Microbial Endoliths in Skeletons of Live and Dead Corals: *Porites lobata* (Moorea, French Polynesia). Mar Ecol Prog Ser 117

Le Goff-Vitry MC, Pybus OG, Rogers AD (2004) Genetic Structure of the Deep-Sea Coral *Lophelia pertusa* in the Northeast Atlantic Revealed by Microsatellites and Internal Transcribed Spacer Sequences. Mol Ecol 13:537-549

Lesser MP, Mazel CH, Gorbunov MY, Falkowski PG (2004) Discovery of Symbiotic Nitrogen-Fixing Cyanobacteria in Corals. Science 305:997-1000

Levy O, Mizrahi L, Chadwick-Furman NE, Achituv Y (2001) Factors Controlling the Expansion Behavior of *Favia favus* (Cnidaria: Scleractinia): Effects of Light, Flow, and Planktonic Prey. Biol Bull 200:118-126

Lewis JB, Price WS (1975) Feeding Mechanisms and Feeding Strategies of Atlantic Reef Corals. J Zool 176:527-544

Lindberg B, Mienert J (2005) Postglacial Carbonate Production by Cold-Water Corals on the Norwegian Shelf and Their Role in the Global Carbonate Budget. Geology 33:537-540

Linnaeus C (1758) Systema Naturae Per Regna Tria Naturae, Secundum Classes, Ordines, Genera, Species, Cum Characteribus, Differentiis, Synonymis, Locis. 10th edition, Stockholm

Liu WT, Marsh TL, Cheng H, Forney L (1997) Characterization of Microbial Diversity by Determining Terminal Restriction Fragment Length Polymorphisms of Genes Encoding 16S rRNA. Appl Environ Microbiol 63:4516-4522

López-García P, Duperron S, Philippot P, Foriel J, Susini J, Moreira D (2003) Bacterial Diversity in Hydrothermal Sediment and Epsilon Proteobacterial Dominance in Experimental Microcolonizers at the Mid-Atlantic Ridge. Environ Microbiol 5:961-976

Ludwig W, Strunk O, Westram R, Richter L, Meier H, Yadhukumar, Buchner A, Lai T, Steppi S, Jobb G, Forster W, Brettske I, Gerber S, Ginhart AW, Gross O, Grumann S, Hermann S, Jost R, Konig A, Liss T, Lussmann R, May M, Nonhoff B, Reichel B, Strehlow R, Stamatakis A, Stuckmann N, Vilbig A, Lenke M, Ludwig T, Bode A, Schleifer K-H (2004) ARB: A Software Environment for Sequence Data. Nucleic Acids Res 32:1363-1371

Lukas KJ (1974) Two Species of the Chlorophyte Genus *Ostreobium* from Skeletons of Atlantic and Caribbean Reef Corals. J Phycol 10:331-335

Lukow T, Dunfield PF, Liesack W (2000) Use of the T-RFLP Technique to Assess Spatial and Temporal Changes in the Bacterial Community Structure within an Agricultural Soil Planted with Transgenic and Non-Transgenic Potato Plants. FEMS Microbiol Ecol 32:241-247

Luna GM, Biavasco F, Danovaro R (2007) Bacteria Associated with the Rapid Tissue Necrosis of Stony Corals. Environ Microbiol 9:1851-1857

Madigan MT, Martinko JM, Parker J (2003) Brock. Mikrobiologie. 9th Edition (in German). Spektrum Akademischer Verlag, Heidelberg, Berlin

Manz W, Amann R, Ludwig W, Wagner M, Schleifer K-H (1992) Phylogenetic Oligodeoxynucleotide Probes for the Major Subclasses of Proteobacteria - Problems and Solutions. Syst Appl Microbiol 15:593-600

Mariscal RN, McLean RB, Hand C (1977) The Form and Function of Cnidarian Spirocysts. Cell Tissue Res 178:427-433

McCarthy M, Pratum T, Hedges J, Benner R (1997) Chemical Composition of Dissolved Organic Nitrogen in the Ocean. Nature 390:150-154

McKiness ZP, Cavanaugh CM (2005) The Ubiquitous Mussel: *Bathymodiolus* aff. *brevior* Symbiosis at the Central Indian Ridge Hydrothermal Vents. Mar Ecol Prog Ser 295:183-190

Moeseneder MM, Arrieta JM, Muyzer G, Winter C, Herndl GJ (1999) Optimization of Terminal-Restriction Fragment Length Polymorphism Analysis for Complex Marine Bacterioplankton Communities and Comparison with Denaturing Gradient Gel Electrophoresis. Appl Environ Microbiol 65:3518-3525

Møller EF (2005) Sloppy Feeding in Marine Copepods: Prey-Size-Dependent Production of Dissolved Organic Carbon. J Plankton Res 27:27-35

Moore JG, Fabbi BP (1971) An Estimate of the Juvenile Sulfur Content of Basalt. Contrib Mineral Petrol 33:118-127

Moosvi SA, Pacheco CC, McDonald IR, De Marco P, Pearce DA, Kelly DP, Wood AP (2005) Isolation and Properties of Methanesulfonate-Degrading *Afipia felis* from Antarctica and Comparison with Other Strains of *A. felis*. Environ Microbiol 7:22-33

Mortensen PB (2001) Aquarium Observations on the Deep-Water Coral *Lophelia pertusa* (L., 1758) (Scleractinia) and Selected Associated Invertebrates. Ophelia 54:83-104

Mortensen PB, Hovland M, Brattegard T, Farestveit R (1995) Deep Water Bioherms of the Scleractinian Coral *Lophelia pertusa* (L.) at 64°N on the Norwegian Shelf: Structure and Associated Megafauna. Sarsia 80:145-158

Mortensen PB, Rapp HT (1998) Oxygen and Carbon Isotope Ratios Related to Growth Line Patterns in Skeletons of Lophelia pertusa (L) (Anthozoa, Scleractinia): Implications for Determination of Linear Extension Rates. Sarsia 83:433-446

Murray RGE, Stackebrandt E (1995) Taxonomic Note - Implementation of the Provisional Status *Candidatus* for Incompletely Described Prokaryotes. Int J Syst Bacteriol 45:186-187

Neef A (1997) Anwendung der in Situ Einzelzell-Identifizierung von Bakterien zur Populationsanalyse in komplexen mikrobiellen Biozönosen. PhD thesis, Technische Universität, Munich

Nercessian O, Fouquet Y, Pierre C, Prieur D, Jeanthon C (2005) Diversity of Bacteria and Archaea Associated with a Carbonate-Rich Metalliferous Sediment Sample from the Rainbow Vent Field on the Mid-Atlantic Ridge. Environ Microbiol 7:698-714

Noé SU, Dullo W-C (2006) Skeletal Morphogenesis and Growth Mode of Modern and Fossil Deep-Water Isidid Gorgonians (Octocorallia) in the West Pacific (New Zealand and Sea of Okhotsk). Coral Reefs 25:303-320

Noé SU, Titschack J, Freiwald A, Dullo W-C (2005) From Sediment to Rock: Diagenetic Processes of Hardground Formation in Deep-Water Carbonate Mounds of the NE Atlantic. Facies DOI: 10.1007/s10347-005-0037-x

Orr JC, Fabry VJ, Aumont O, Bopp L, Doney SC, Feely RA, Gnanadesikan A, Gruber N, Ishida A, Joos F, Key RM, Lindsay K, Maier-Reimer E, Matear R, Monfray P, Mouchet A, Najjar

RG, Plattner G-K, Rodgers KB, Sabine CL, Sarmiento JL, Schlitzer R, Slater RD, Totterdell IJ, Weirig M-F, Yamanaka Y, Yool A (2005) Anthropogenic Ocean Acidification over the Twenty-First Century and Its Impact on Calcifying Organisms. Nature 437:681-686

Osborn AM, Moore ERB, Timmis KN (2000) An Evaluation of Terminal-Restriction Fragment Length Polymorphism (T-RFLP) Analysis for the Study of Microbial Community Structure and Dynamics. Environ Microbiol 2:39-50

Ouverney CC, Armitage GC, Relman DA (2003) Single-Cell Enumeration of an Uncultivated TM7 Subgroup in the Human Subgingival Crevice. Appl Environ Microbiol 69:6294-6298

Peek AS, Feldman RA, Lutz RA, Vrijenhoek RC (1998) Cospeciation of Chemoautotrophic Bacteria and Deep Sea Clams. P Natl Acad Sci USA 95:9962-9966

Penn K, Wu D, Eisen JA, Ward NL (2006) Characterization of Bacterial Communities Associated with Deep-Sea Corals on Gulf of Alaska Seamounts. Appl Environ Microbiol 72:1680-1683

Pernthaler A, Pernthaler J, Amann R (2002) Fluorescence in Situ Hybridization and Catalyzed Reporter Deposition for the Identification of Marine Bacteria. Appl Environ Microbiol 68:3094-3101

Polymenakou PN, Bertilsson S, Tselepides A, Stephanou EG (2005) Bacterial Community Composition in Different Sediments from the Eastern Mediterranean Sea: A Comparison of Four 16S Ribosomal DNA Clone Libraries. Microb Ecol 50:447-462

Powell MA, Somero GN (1986) Adaptations to Sulfide by Hydrothermal Vent Animals: Sites and Mechanisms of Detoxification and Metabolism. Biol Bull 171:274-290

Pruski AM, Rousse N, Fiala-Medioni A, Boulegue J (2002) Sulphur Signature in the Hydrothermal Vent Mussel *Bathymodiolus azoricus* from the Mid-Atlantic Ridge. J Mar Biol Assoc UK 82:463-468

Pukall R, Kramer I, Rohde M, Stackebrandt E (2001) Microbial Diversity of Cultivatable Bacteria Associated with the North Sea Bryozoan *Flustra foliacea*. Syst Appl Microbiol 24:623-633

Rasband W (1997-2007) ImageJ. National Institutes of Health, Bethesda, Maryland, USA

Razin S, Yogev D, Naot Y (1998) Molecular Biology and Pathogenicity of Mycoplasmas. Microbiol Mol Biol R 62:1094-1156

Reitner J (1993) Modern Cryptic Microbialite/Metazoan Facies from Lizard Island (Great Barrier Reef, Australia); Formation and Concepts. Facies 29:3-40

Richardson LL, Kuta KG (2003) Ecological Physiology of the Black Band Disease Cyanobacterium *Phormidium corallyticum*. FEMS Microbiol Ecol 43:287-298

Ricke P, Kolb S, Braker G (2005) Application of a Newly Developed ARB Software-Integrated Tool for in Silico Terminal Restriction Fragment Length Polymorphism Analysis Reveals the Dominance of a Novel pmoA Cluster in a Forest Soil. Appl Environ Microbiol 71:1671-1673

Rifkin JF (1991) A Study of the Spirocytes from the Ceriantharia and Actiniaria (Cnidaria, Anthozoa). Cell Tissue Res 266:365-373

Ritchie KB (2006) Regulation of Microbial Populations by Coral Surface Mucus and Mucus-Associated Bacteria. Mar Ecol Prog Ser 322:1-14

Ritchie KB, Smith GW (1997) Physiological Comparison of Bacterial Communities from Various Species of Scleractinian Corals. Proceedings of the 8th International Coral Reef Symposium 1:521-526.

Roark EB, Guilderson TP, Flood-Page S, Dunbar RB, Ingram BL, Fallon SJ, McCulloch M (2005) Radiocarbon-Based Ages and Growth Rates of Bamboo Corals from the Gulf of Alaska. Geophys Res Lett 32:L04606

Roberts S, Hirshfield M (2004) Deep-Sea Corals: Out of Sight, but No Longer out of Mind. Front Ecol Environ 2:123-130

Rogers AD (1999) The Biology of *Lophelia pertusa* (Linnaeus 1758) and Other Deep-Water Reef-Forming Corals and Impacts from Human Activities. Int Rev Hydrobiol 84:315-406

Rohwer F, Breitbart M, Jara J, Azam F, Knowlton N (2001) Diversity of Bacteria Associated with the Caribbean Coral *Montastraea franksi*. Coral Reefs 20:85-91

Rohwer F, Kelley S (2004) Culture Independent Analyses of Coral-Associated Microbes. In: Rosenberg E, Loya Y (eds) Coral Health and Disease. Springer, New York, Berlin, pp 265–277

Rohwer F, Seguritan V, Azam F, Knowlton N (2002) Diversity and Distribution of Coral-Associated Bacteria. Mar Ecol Prog Ser 243:1-10

Rountree MR, Selker EU (1997) DNA Methylation Inhibits Elongation but Not Initiation of Transcription in *Neurospora crassa*. Genes Dev 11:2383-2395

Sakshaug E, Myklestad SM (1973) Studies on the Phytoplankton Ecology of the Trondheimsfjord. III. Dynamics of Phytoplankton Blooms in Relation to Environmental Factors, Bioassay Experiments and Parameters for the Physiological State of the Populations. J Exp Mar Biol Ecol 11:157-188

Salvador Pedro M, Haruta S, Hazaka M, Shimada R, Yoshida C, Hiura K, Ishii M, Igarashi Y (2001) Denaturing Gradient Gel Electrophoresis Analyses of Microbial Community from Field-Scale Composter. J Biosci Bioeng 91:159-165

Santavy DL (1995) The Diversity of Microorganisms Associated with Marine Invertebrates and Their Roles in the Maintenance of Ecosystems. In: Allsopp D, Colwell RR, Hawksworth DL (eds) Microbial Diversity and Ecosystem Funktion. CAB International, Wallingford, pp 211-229

Scheuermayer M, Gulder TAM, Bringmann G, Hentschel U (2006) *Rubritalea marina* gen. nov., sp. nov., a Marine Representative of the Phylum '*Verrucomicrobia*', Isolated from a Sponge (Porifera). Int J Syst Evol Microbiol 56:2119-2124

Schönhuber W, Fuchs BM, Juretschko S, Amann R (1997) Improved Sensitivity of Whole-Cell Hybridization by the Combination of Horseradish Peroxidase-Labeled Oligonucleotides and Tyramide Signal Amplification. Appl Environ Microbiol 63:3268-3273

Schöttner S, Wild C, Ramette A, Hoffmann F, Boetius A (2008) Habitat Differentiation by the Cold-Water Coral *Lophelia pertusa* (Scleractinia) Governs Bacterial Diversity. Geophys Res Abs 10, DOI: 1607-7962/gra/EGU2008-A-10666

Schwarz WH (2001) The Cellulosome and Cellulose Degradation by Anaerobic Bacteria. Appl Microbiol Biot 56:634-649

Seritti A, Manca BB, Santinelli C, Murru E, Boldrin A, Nannicini L (2003) Relationships between Dissolved Organic Carbon (DOC) and Water Mass Structures in the Ionian Sea (Winter 1999). J Gephys Res 108, C9, 8112, DOI: 10.1029/2002JC001345

Shashar N, Cohen Y, Loya Y (1993) Extreme Diel Fluctuations of Oxygen in Diffusive Boundary Layers Surrounding Stony Corals. Biol Bull 185:455-461

Shashar N, Cohen Y, Loya Y, Sar N (1994) Nitrogen Fixation (Acetylene Reduction) in Stony Corals: Evidence for Coral-Bacteria Interactions. Mar Ecol Prog Ser 111:259-264

Shick JM (1990) Diffusion Limitation and Hyperoxic Enhancement of Oxygen Consumption in Zooxanthellate Sea Anemones, Zoanthids, and Corals. Biol Bull 179:148-158

Shindo K, Mikami K, Tamesada E, Takaichi S, Adachi K, Misawa N, Maoka T (2007) Diapolycopenedioic Acid Xylosyl Ester, a Novel Glyco-C_{30}-Carotenoic Acid Produced by a New Marine Bacterium *Rubritalea squalenifaciens*. Tetrahedron Lett 48:2725-2727

Sieburth JM (1975) Microbial Seascapes: A Pictorial Essay on Marine Microorganisms and Their Environments. University Park Press, Baltimore

Slattery M, McClintock JB, Heine JN (1995) Chemical Defenses in Antarctic Soft Corals: Evidence for Antifouling Compounds. J Exp Mar Biol Ecol 190:61-77

Sorokin DY, Tourova TP, Muyzer G (2005) *Citreicella thiooxidans* gen. nov., sp. nov., a Novel Lithoheterotrophic Sulfur-Oxidizing Bacterium from the Black Sea. Syst Appl Microbiol 28:679-687

Sorokin YI (1973) On the Feeding of Some Scleractinian Corals with Bacteria and Dissolved Organic Matter. Limnol Oceanogr 18:380-385

Squires DF (1959) Deep Sea Corals Collected by the Lamont Geological Observatory. 1. Atlantic Corals. Am Mus Nov 1965:1-42

Stackebrandt E, Goebel BM (1994) A Place for DNA-DNA Reassociation and 16S Ribosomal-RNA Sequence-Analysis in the Present Species Definition in Bacteriology. Int J Syst Bacteriol 44:846-849

Steunou AS, Bhaya D, Bateson MM, Melendrez MC, Ward DM, Brecht E, Peters JW, Kuhl M, Grossman AR (2006) In Situ Analysis of Nitrogen Fixation and Metabolic Switching in Unicellular Thermophilic Cyanobacteria Inhabiting Hot Spring Microbial Mats. P Natl Acad Sci USA 103:2398-2403

Strømgren T (1971) Vertical and Horizontal Distribution of *Lophelia pertusa* (Linnaeus) in Trondheimsfjorden on the West Coast of Norway. Det Kongelige Norske Videnskabers Selskab. Forhandlinger 6:1-9

Suzuki MT, Giovannoni SJ (1996) Bias Caused by Template Annealing in the Amplification of Mixtures of 16S rRNA Genes by PCR. Appl Environ Microbiol 62:625-630

Suzuki Y, Inagaki F, Takai K, Nealson KH, Horikoshi K (2004) Microbial Diversity in Inactive Chimney Structures from Deep-Sea Hydrothermal Systems. Microb Ecol 47:186-196

Swofford DL, Olsen GJ, Waddell PJ, Hillis DM (1996) Phylogenetic Inference. In: Hillis DM, Moritz C, Mable BK (eds) Molecular Systematics. Sinauer, Sunderland, pp 407-514

Teske A, Brinkhoff T, Muyzer G, Moser DP, Rethmeier J, Jannasch HW (2000) Diversity of Thiosulfate-Oxidizing Bacteria from Marine Sediments and Hydrothermal Vents. Appl Environ Microbiol 66:3125-3133

Thiel V, Leininger S, Schmaljohann R, Brümmer F, Imhoff JF (2007a) Sponge-Specific Bacterial Associations of the Mediterranean Sponge *Chondrilla nucula* (Demospongiae, Tetractinomorpha). Microb Ecol 54:101-111

Thiel V, Neulinger SC, Staufenberger T, Schmaljohann R, Imhoff JF (2007b) Spatial Distribution of Sponge-Associated Bacteria in the Mediterranean Sponge *Tethya aurantium*. FEMS Microbiol Ecol 59:47–63

Tredici M, Margheri M, Giovannetti L, Philippis R, Vincenzini M (1988) Heterotrophic Metabolism and Diazotrophic Growth of *Nostoc* sp. From *Cycas circinalis*. Plant Soil 110:199-206

Tringe SG, von Mering C, Kobayashi A, Salamov AA, Chen K, Chang HW, Podar M, Short JM, Mathur EJ, Detter JC, Bork P, Hugenholtz P, Rubin EM (2005) Comparative Metagenomics of Microbial Communities. Science 308:554-557

Tsurumi R, Takeda K, Tonouchi A (2000) Characteristics and Propionate Production of *Propionibacterium* Isolated from a Methane Fermentation Digester. Microb Environ 15:151-159

Tursi A, Mastrototaro F, Matarrese A, Maiorano P, D'onghia G (2004) Biodiversity of the White Coral Reefs in the Ionian Sea (Central Mediterranean). Chem Ecol 20:107-116

Ueno Y, Haruta S, Ishii M, Igarashi Y (2001) Microbial Community in Anaerobic Hydrogen-Producing Microflora Enriched from Sludge Compost. Appl Microbiol Biot 57:555-562

Van Aken B, Peres CM, Doty SL, Yoon JM, Schnoor JL (2004) *Methylobacterium populi* sp. nov., a Novel Aerobic, Pink-Pigmented, Facultatively Methylotrophic, Methane-Utilizing Bacterium Isolated from Poplar Trees (*Populus deltoides* x *nigra* DN34). Int J Syst Evol Microbiol 54:1191-1196

Van Alstyne K, Schupp P, Slattery M (2006) The Distribution of Dimethylsulfoniopropionate in Tropical Pacific Coral Reef Invertebrates. Coral Reefs 25:321-327

Vattakaven T, Bond P, Bradley G, Munn CB (2006) Differential Effects of Temperature and Starvation on Induction of the Viable-but-Nonculturable State in the Coral Pathogens *Vibrio shiloi* and *Vibrio tasmaniensis*. Appl Environ Microbiol 72:6508-6513

Wafar M, Wafar S, David JJ (1990) Nitrification in Reef Corals. Limnol Oceanogr 35:725-730

Wallner G, Amann R, Beisker W (1993) Optimizing Fluorescent in Situ Hybridization with rRNA-Targeted Oligonucleotide Probes for Flow Cytometric Identification of Microorganisms. Cytometry 14:136–143

Wang YJ, Stingl U, Anton-Erxleben F, Geisler S, Brune A, Zimmer M (2004) "*Candidatus* Hepatoplasma crinochetorum", a New, Stalk-Forming Lineage of *Mollicutes* Colonizing the Midgut Glands of a Terrestrial Isopod. Appl Environ Microbiol 70:6166-6172

Wells JW (1956) Scleractinia. In: Moore RC (ed) Treatise on Invertebrate Paleontology, Coelenterata, Part F. Geological Society of America and University of Kansas Press, Lawrence, pp 328-440

Wessel P, Smith WHF (1995) New Version of the Generic Mapping Tools Released. EOS Trans AGU 76:329

Williams WM, Viner AB, Broughton WJ (1987) Nitrogen Fixation (Acetylene Reduction) Associated with the Living Coral *Acropora variabilis*. Mar Biol 94:531-535

Wilsanand V, Wagh AB, Bapuji M (1999) Antibacterial Activities of Anthozoan Corals on Some Marine Microfoulers. Microbios 99:137-145

Wilson JB (1979) Patch Development of the Deep-Water Coral *Lophelia pertusa* (L) on Rockall Bank. J Mar Biol Assoc UK 59:165-177

von Wintzingerode F, Gobel UB, Stackebrandt E (1997) Determination of Microbial Diversity in Environmental Samples: Pitfalls of PCR-Based rRNA Analysis. FEMS Microbiol Rev 21:213-229

Yakimov MM, Cappello S, Crisafi E, Tursi A, Savini A, Corselli C, Scarfi S, Giuliano L (2006) Phylogenetic Survey of Metabolically Active Microbial Communities Associated with the Deep-Sea Coral *Lophelia pertusa* from the Apulian Plateau, Central Mediterranean Sea. Deep Sea Res I 53:62-75

Yilmaz LS, Noguera DR (2004) Mechanistic Approach to the Problem of Hybridization Efficiency in Fluorescent in Situ Hybridization. Appl Environ Microbiol 70:7126-7139

Yoch DC (2002) Dimethylsulfoniopropionate: Its Sources, Role in the Marine Food Web, and Biological Degradation to Dimethylsulfide. Appl Environ Microbiol 68:5804-5815

Yonge CM (1937) Studies on the Biology of Tortugas Corals. III. The Effect of Mucus on Oxygen Consumption. Pap Tortugas Lab Carnegie Inst Wash 31:207-214

Yoon J, Matsuo Y, Matsuda S, Adachi K, Kasai H, Yokota A (2007) *Rubritalea spongiae* sp. nov. And *Rubritalea tangerina* sp. nov., Two Carotenoid- and Squalene-Producing Marine Bacteria of the Family *Verrucomicrobiaceae* within the Phylum '*Verrucomicrobia*', Isolated from Marine Animals. Int J Syst Evol Microbiol 57:2337-2343

Zaika LL, Phillips JG, Fanelli JS, Scullen OJ (1998) Revised Model for Aerobic Growth of *Shigella flexneri* to Extend the Validity of Predictions at Temperatures between 10 and 19°C. Int J Food Microbiol 41:9-19

Zubkov MV, Fuchs BM, Archer SD, Kiene RP, Amann R, Burkill PH (2001) Linking the Composition of Bacterioplankton to Rapid Turnover of Dissolved Dimethylsulphoniopropionate in an Algal Bloom in the North Sea. Environ Microbiol 3:304-311

Appendix

Spatial distribution of sponge-associated bacteria in the Mediterranean sponge *Tethya aurantium*

Vera Thiel, Sven C. Neulinger, Tim Staufenberger, Rolf Schmaljohann & Johannes F. Imhoff

Leibniz-Institut für Meereswissenschaften, IFM-GEOMAR, Kiel, Germany

Correspondence: Johannes F. Imhoff, Leibniz-Institut für Meereswissenschaften, IFM-GEOMAR, Düsternbrooker Weg 20, D-24105 Kiel, Germany. Tel.: +49 (0) 431 6004450; fax: +49 (0) 431 6004452; e-mail: jimhoff@ifm-geomar.de

Received 19 April 2006; revised 12 August 2006; accepted 15 August 2006.

DOI:10.1111/j.1574-6941.2006.00217.x

Editor: Patricia Sobecky

Keywords
16S rRNA gene; DGGE; rarefaction analysis; sponge–bacteria association; local distribution; sponge-specific.

Abstract

The local distribution of the bacterial community associated with the marine sponge *Tethya aurantium* Pallas 1766 was studied. Distinct bacterial communities were found to inhabit the endosome and cortex. Clear differences in the associated bacterial populations were demonstrated by denaturing gradient gel electrophoresis (DGGE) and analysis of 16S rRNA gene clone libraries. Specifically associated phylotypes were identified for both regions: a new phylotype of *Flexibacteria* was recovered only from the sponge cortex, while *Synechococcus* species were present mainly in the sponge endosome. Light conduction via radiate spicule bundles conceivably facilitates the unusual association of *Cyanobacteria* with the sponge endosome. Furthermore, a new monophyletic cluster of sponge-derived 16S rRNA gene sequences related to the *Betaproteobacteria* was identified using analysis of 16S rRNA gene clone libraries. Members of this cluster were specifically associated with both cortex and endosome of *T. aurantium*.

Introduction

The phylum *Porifera* contains an estimated 15 000 species in three taxonomic classes: Calcarea (calcareous sponges), Hexactinellida (glass sponges) and Demospongiae (demosponges) (Hooper & van Soest, 2002). As sessile filter-feeding organisms sponges pump large amounts of water through their aquiferous channel system. They take up bacteria, single-celled algae and other food particles from the filtered water by phagocytosis within the choanocyte chambers, which are located within the inner part of the sponge, the endosome (= choanosome). The endosome is protected against strong currents and high light intensities by an outer region, the cortex (or ectosome) (Sará, 1987); this has also been used as a basis for taxonomic classification. As a protective device (Burton, 1928), the cortex is found to be particularly thick and well structured in species living in shallow waters subject to strong currents and high light intensities. By contrast, species living in more protected habitats have a thin, almost indistinct cortex (Sará, 1987).

Tethya aurantium (Fig. 1a) is characterized by a globular shape and a thick and well-developed cortex, clearly differentiated from the endosome by texture and colour of the tissue (Fig. 1b). In the Mediterranean Sea *T. aurantium* cooccurs with the very similar species of *Tethya citrina*, but inhabits different niches and can be distinguished by the development of its cortex. *Tethya aurantium* generally inhabits areas that are more exposed to light and current in depths of 1–40 m, while *T. citrina* prefers more sheltered places and possesses a thinner cortex than *T. aurantium* (Sará, 1987).

Associations between microorganisms and sponges have been systematically studied using microscopy and isolation methods since the 1970s (Vacelet, 1970, 1971, 1975; Vacelet & Donadey, 1977; Manz *et al*., 2000; Webster & Hill, 2001; Lafi *et al*., 2005). These studies have shown that bacteria are abundant within the mesohyl of sponges and can form up to 40% of the sponge volume (Wilkinson, 1978). More recent studies on sponge–microbe associations were based mainly on culture-independent molecular methods (Hinde *et al*., 1994; Althoff *et al*., 1998; Burja *et al*., 1999; Burja & Hill, 2001; Webster & Hill, 2001; Webster *et al*., 2001). Comparison of 16S rRNA gene clone libraries obtained from several sponges of different geographical origin have revealed unexpected conformity between the different sponge species, and a uniform sponge-associated bacterial community was proposed (Hentschel *et al*., 2002).

The aim of this study was to characterize the microbial community associated with *T. aurantium*. We demonstrate specific differences between bacteria associated with the cortex and endosome. Furthermore, we report on a new phylogenetic cluster of sponge-associated *Betaproteobacteria*

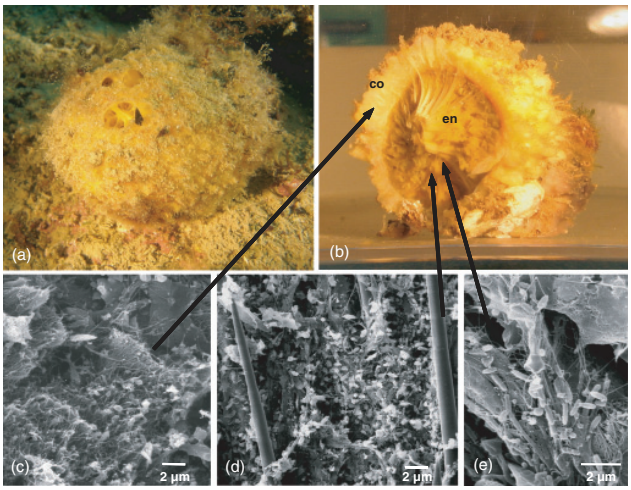

Fig. 1. (a) Photograph of the Mediterranean sponge *Tethya aurantium* Pallas *in situ*. A cross section (b) shows the morphologically different regions endosome (en) and cortex (co). Electron microscopic photography shows no apparent accumulation of bacteria in the cortex (c) and a moderate number of different bacterial morphotypes within the endosome (d and e).

and a possible association of *T. aurantium* with *Cyanobacteria*.

Materials and methods

Sampling sites

The Limski kanal is a semiclosed fjord-like bay in the Adriatic Sea near Rovinj (Istrian Peninsula, Croatia) (45°7, 972′N; 13°43, 734′E). It extends along an east–west axis, with an *c.* length of 11 km, a maximum width of about 650 m and a depth of up to 32 m. The bottom is generally muddy, with insular sites consisting of stones and shallow rocky slopes along the sides. It is characterized by a very high sedimentation rate and rapid water exchange (Kuzmanovic, 1985). In a recent study, 42 sponge species were found in the Limski kanal including three species of the genus *Tethya*: *T. aurantium* Pallas 1766, *Tethya limski* Müller & Zahn 1969 and *T. citrina* Sará & Melone 1965 (Brümmer *et al.*, 2004).

Sponge sampling

Specimens of *T. aurantium* were collected by SCUBA diving from a depth of 5–15 m in April 2003, June 2004 and May 2005. The sponges were placed into sterile plastic bags, cooled in an isolation box, immediately transported to the laboratory and processed within 3 h. In the laboratory the sponges were washed carefully three times in filter-sterilized seawater (0.2 µm) prior to cutting. The sponges were separated into cortex and endosome sections and washed again separately in sterile seawater. Tissues were cut into small pieces of *c.* 20–30 mg each, frozen in liquid nitrogen and kept frozen (− 80 °C) until further investigation.

Ambient seawater was collected into sterile glass bottles (Duran; 1 L) prior to sponge sampling. The water was cooled on the way back to the laboratory and immediately filtered through a cellulose-acetate filter (0.2 µm pore size; Sartorius). The filters were placed in a cryovial, frozen in liquid nitrogen and stored at − 80 °C until further investigation.

Electron microscopy

Sponge samples were prepared for scanning electron microscopy by fixation with 1% glutaraldehyde in seawater, replacement of water with an ethanol series and subsequent critical-point drying. After mounting, samples were sputtered with Au/Pd and observed with a Zeiss DSM 940 scanning electron microscope.

DNA extraction

Genomic DNA was extracted and purified using the QIAGEN DNeasy® Tissue Kit following the manufacturer's protocol for Gram-positive bacteria and animal tissue.

PCR and cloning procedure

Amplification of ribosomal DNA was performed using puReTaq™ Ready-To-Go™ PCR Beads (Amersham Biosciences). For amplification of the nearly complete 16S rRNA gene the eubacterial primers 27f and 1492r (Lane, 1991) were used. The conditions for this PCR were: initial

denaturation (2 min at 94 °C) followed by 30 cycles of primer annealing (40 s at 50 °C), primer extension (90 s at 72 °C) and denaturation (40 s at 94 °C), a final primer annealing (1 min at 42 °C) and a final extension phase (5 min at 72 °C). PCR products were checked for correct length on a 1% Tris-borate-EDTA (TBE) agarose gel (1% agarose, 8.9 mM Tris, 8.9 mM borate, 0.2 mM EDTA), stained with ethidium bromide and visualized under UV illumination.

DNA was purified using the High Pure PCR Product Purification Kit (Roche) prior to ligation into pCR®4-TOPO® vector and transformation into One Shot® Competent *Escherichia coli* cells using the TOPO TA® Cloning Kit (Invitrogen). Inserts were amplified as described above using the M13f/M13r primer set (M13f: 5′-GTAAAACGACGGCCAG-3′; M13r: 5′-CAGGAAACAGCTATGAC-3′) (0.1 μM each). Correct insert size was verified using agarose gel electrophoresis.

PCR for denaturing gradient gel electrophoresis (DGGE) was performed using the primers 342-GCf and 534r (Muyzer *et al*., 1993). The temperature profile was as follows: initial denaturation (2 min at 94 °C) followed by 15 cycles of touchdown primer annealing (40 s at 65–50 °C), primer extension (1 min at 72 °C) and denaturation (40 s at 94 °C), an additional 20 cycles of primer annealing (40 s at 50 °C), primer extension (1 min at 72 °C) and denaturation (40 s at 94 °C), and a final primer annealing (1 min at 42 °C) with a final extension phase (5 min at 72 °C). PCR products were checked for correct length on a 2% TBE-agarose gel. Excised DGGE bands (see below) were reamplified using primers GC/M (5′-GGGGGCAGGGGGGC-3′) and 534r (Muyzer *et al*., 1993) as described above with an annealing temperature of 50 °C and for 30 cycles.

Double gradient DGGE

DGGE was conducted in a double gradient gel (Petri & Imhoff, 2001), containing a linear 6–8% polyacrylamide (acrylamide : bisacrylamide ratio 37.5 : 1) and a 50–80% denaturing gradient (100% corresponds to 7 M urea/40% deionised formamide). The gel was run in a Tris-EDTA-acetic acid (TAE) buffer (10 mM Tris, 5 mM acetic acid, 5 mM EDTA, titrated to pH 7.5) at a voltage of 80 V for 15 h. The gel was stained in 1 × SYBR Gold (Invitrogen) (Tuma *et al*., 1999) in TAE and documented digitally.

Bands exclusively present in sponge samples were cut out and DNA was extracted for sequencing. Excised bands were transferred into 50 μL of molecular grade water, crushed with sterile pistils and incubated overnight at 4 °C. The supernatant (1 μL) was used as template for reamplification with primers GC/M and 534r as described above and sequenced.

Cluster analysis

For statistical comparison of the DGGE banding patterns, similarity cluster analysis (Clarke & Warwick, 1994) and analysis of similarity (ANOSIM) (Clarke, 1993) were performed using the program PRIMER 5 v5.2.2 (PRIMER–E Ltd). Similarity was calculated using the Bray–Curtis index and cluster analysis was conducted with complete linkage. Subsequently, one-way ANOSIM with all possible permutations was performed. In accordance with the PRIMER manual (Clarke & Gorley, 2001) ANOSIM R-values of > 0.75 were interpreted as well separated, $R > 0.5$ as overlapping, but clearly different, and $R < 0.25$ as barely separable at all. Replicate samples were grouped according to source (e.g. endosome, cortex, seawater) as factors for the analyses.

Sequencing and phylogenetic analysis

After verification of correct insert size, clones (for each sample 29–41) were sequenced using the ABI PRISM® BigDye™ Terminator Ready Reaction Kit (Applied Biosystems) and an ABI PRISM® 310 Genetic Analyser (Perkin Elmer Applied Biosystems). Sequence primers used were: plasmid primers M13f and M13r as well as the 16S rRNA gene-specific primers 342f (Muyzer *et al*., 1993), 534r (Muyzer *et al*., 1993), 790f (5′-GATACCCTGGTAGTCC-3′), 907f (5′-GGCAAACTCAAAGGAATTGAC-3′), 1093f (5′-TCCCGCAACGAGCGCAACCC-3′) and 1093r (5′-GGGTTGCGCTCGTTGCGGGA-3′). Sequence data were edited with Lasergene Software SeqMan (DNAStar Inc.) and checked for possible chimeric origin using the program CHECK_CHIMERA (http://35.8.164.52/html/index.html) of the Ribosomal Database Project (http://rdp.cme.msu.edu/index.jsp) (Maidak *et al*., 1999). Putative chimeric sequences were removed from phylogenetic analyses. Next relatives were determined by comparison to 16S rRNA genes in the NCBI GenBank database using BLAST (Basic Local Alignment Search Tool) searches (Altschul *et al*., 1990) and the RDPII Sequence Match Program (http://rdp.cme.msu.edu/seqmatch/seqmatch_intro.jsp). Sequences were aligned using the FastAlign function of the alignment editor implemented in the ARB software package (http://www.arb-home.de) (Ludwig *et al*., 2004) and refined manually employing secondary structure information. For phylogenetic calculations the PhyML software (Guindon & Gascuel, 2003) as well as the online version of PhyML (Guindon *et al*., 2005) were used. Trees were calculated by the maximum-likelihood (ML) method (Felsenstein, 1981) using the GTR model and estimated proportion of invariable sites as well as the Gamma distribution parameter with near full-length sequences ($\geq$1200 and $\geq$1000 bp for trees in Fig. 4b and c, respectively). Calculated trees were imported into ARB and short sequences were subsequently added by use of the ARB parsimony method without

changing the tree topologies. Phylogenetic positions of short sequences (< 1200 bp/ < 1000 bp) were additionally verified by phylogenetic analysis (ML, 100 bootstraps) of full and partial sequences.

Nucleotide sequence accession numbers

The 16S rRNA gene sequences obtained in this study have been deposited in the EMBL database. They have been assigned accession numbers AM259730–AM259769, AM259770–AM259831 and AM259832–AM259898 for the sequences obtained from seawater, endosome and cortex, respectively.

Diversity estimation

Sequences with similarities $> 99.0\%$ were defined as one phylotype, i.e. one operational taxonomic unit (OTU). The proportion of prokaryotic diversity represented by the clone libraries was estimated by rarefaction analysis combined with nonlinear regression, and by calculation of the chao1 estimator as proposed by Kemp & Aller (2004). Rarefaction analysis calculations were performed applying the algorithm described by Hurlbert (1971) with the program aRarefactWin (http://www.uga.edu/strata/software.html). Rarefaction curves were plotted and regressions performed using two different regression equations:

$$y_1 = a_1(1 - e^{-b}1^x) \quad (1)$$

$$y_2 = a_2(1 - e^{-b}2^{\hat{x}c}) \quad (2)$$

where x is the sample size, y the observed number of OTUs and a the number of OTUs to be expected with infinite sample size (i.e. total diversity) (Koellner *et al.*, 2004). Equation (1) is the most common regression approach for rarefaction analysis and has been used by many authors (e.g. Webster *et al.*, 2004; Yakimov *et al.*, 2006). However, curves derived from regression (1) exhibited an apparent misfit to the data points of the rarefaction analysis. The increase in the regression curves was too steep at small OTU numbers and curves flattened visually too early at large sample sizes. The expected underestimation of the maximum species number proposed a modification of regression (1), namely Equation (2). To prove this, we developed an algorithm to simulate sampling of specimens for rarefaction analysis that has the potential to produce datasets ranging from highly diverse (each OTU occurring only once or twice) to almost uniform (one or two abundant OTUs): a cohort of random integer numbers k_i ($i \in N$; $1 \leq i \leq 50$) were created with the equation $k_i = 5 \cdot \Gamma_{\alpha i}(z_i)$, where Γ is the standard Gamma function of z_i (randomized; $0 \leq z < 1$) with shape parameter α_i (randomized; $0.1 \leq \alpha_i < 0.6$). Of this cohort, n numbers k were taken so that $\sum_{i=1}^{n} k_i \leq s$ (randomized; $30 \leq s < 70$). This procedure is tantamount to sampling up to s specimens (i.e. clones) representing n OTUs of abundance k_i. The randomized Gamma function causes the distribution of k_i to be skewed more or less to the right, resembling abundance proportions in most natural communities. The simulated datasets were subjected to rarefaction analysis, and the resulting rarefaction curves were fitted by regressions (1) and (2), respectively. From both equations, the asymptote a and the PRESS (Predicted Residual Error Sum of Squares) statistic were obtained. PRESS is a gauge of how well a regression predicts new data. The smaller the PRESS statistic, the better is the predictive ability of the regression. To test whether the two equations differed statistically from each other, we calculated the ratios $A = a_2/a_1$ and $P = \mathrm{PRESS}_1/\mathrm{PRESS}_2$. If there is one highly abundant OTU ($k_i \geq 20$) beside many OTUs of low abundance ($k_i < 3$) in the sampling datasets, the rarefaction curve tends to converge to a line without apparent limit. This occurred three times with our simulated datasets with $a_2 \gg a_1$ ($10^4 < a_2 < 10^7$; $6 < a_1 < 40$). For these cases, ratio A was not calculated. Transformed ratios $A' = \ln(\ln(A + 1/100))$ and $P' = \ln(P + 1/100)$ did not show significant deviations from the normal distribution (Shapiro–Wilk W-test). A' and P' were tested against the null hypotheses $\overline{A'} = -4.61$ ($\overline{A} = 1$)and $\overline{P'} = 0.01$($\overline{P} = 1$), respectively.

SigmaPlot v6.0 (SPSS) was used for plotting and regression analysis. Statistical tests were performed with Statistica v6.1 (StatSoft).

Results

Electron microscopy

Tethya aurantium cortex and endosome (Fig. 1) samples were studied separately and sponge samples from consecutive years were compared. Electron micrographs revealed large differences between cortex and endosome. Only low numbers of bacteria were associated with the sponge cortex region while bacteria were fairly abundant in the endosome (Fig. 1c–e). Different morphotypes, especially a high abundance of rod-shaped bacteria, were found associated with the sponge endosome.

Cortex- and endosome-specific bacteria

DGGE banding patterns clearly showed the presence of different bacterial communities in endosome and cortex of *T. aurantium* (Fig. 2). Additionally, both parts of the sponge differed in their DGGE banding patterns from surrounding seawater samples. Bacterial phylotypes specifically associated with distinct sponge regions were represented by DGGE bands that were exclusively present in all endosome or cortex samples, respectively, but not found in seawater (Fig. 2a). Other bands were found in all sponge samples (Fig. 2a). Whereas the patterns in subsamples of endosome

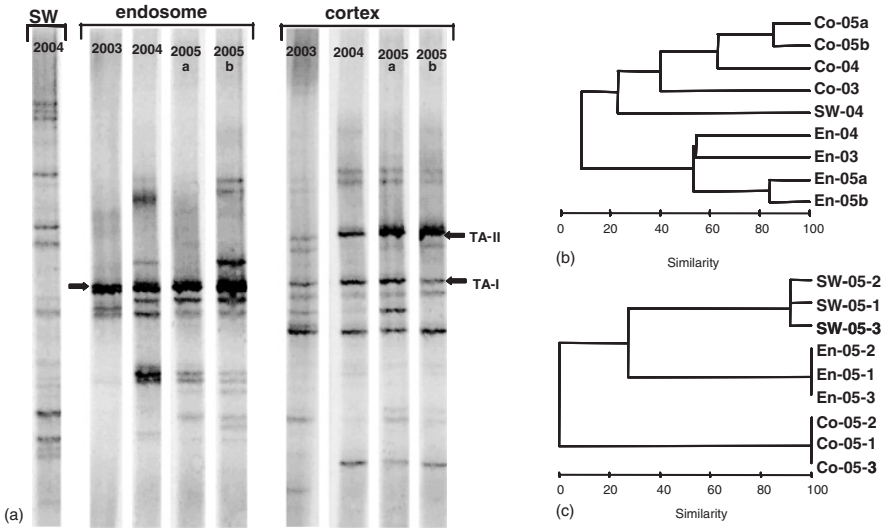

Fig. 2. (a) DGGE banding patterns of amplified bacterial DNA extracted from *Tethya aurantium* Pallas cortex region (2003, 2004 and 2005-a/b), endosomal region (2003, 2004 and 2005-a/b) and surrounding seawater (SW). Specialised bands, which are not present in seawater, occur in all sponge samples (TA-I) and in the cortex only (TA-II). (b and c) Dendograms of similarity cluster analysis with DGGE banding patterns of amplified bacterial DNA extracted from *T. aurantium* cortex (co) and endosomal (en) samples. Comparison of sponge individuals from 2003, 2004 and 2005 and surrounding seawater (b) show that, although not identical, a clear clustering of the banding patterns is seen. Regardless of the year, samples of endosomal regions are more similar to each other than to the cortex samples of the same individual. Replicate subsamples from one individual (May 2005) (c) show identical banding patterns and precise differences between endosome and cortex, as well as to several nearby seawater samples, which differ to some extent.

and cortex of one individual were apparently identical, slight variations were found between endosome as well as cortex samples from consecutive years (2003–2005) (Fig. 2b and c). Nevertheless, bacterial communities inhabiting the same sponge region (endosome or cortex) were more similar than populations from different regions (Fig. 2a and b). In contrast to the subsamples of a sponge individual (2005) that showed identical DGGE banding patterns, seawater samples from different nearby locations varied between each other to some extent (Fig. 2c). The clusters of DGGE banding patterns of endosome, cortex and seawater samples, respectively, were confirmed to be well separated by ANOSIM (R-value > 0.75).

Methods of diversity estimation

Comparison of the two regressions (Table 1) showed that rarefaction analysis using regression (2) resulted in higher estimated maximum OTU numbers a_2 as compared with a_1 of regression (1). a_2 is, in most cases, comparable with the richness estimation using the nonparametric estimator chao1, as proposed by Kemp & Aller (2004) (Table 1). Equality of parameters a_1 and a_2 and the statistics PRESS_1 and PRESS_2 of the two regressions could be rejected on a highly significant level ($P < 10^{-6}$) in both cases. We can therefore state that (i) Equation (2) fits significantly better than Equation (1) as a regression for fitting rarefaction curves and predicting total diversity, and that (ii) the total diversity a_1 calculated with the conventional Equation (1) is systematically lower than a_2 calculated with regression (2).

Diversity of sponge-associated bacteria

A total of 171 clone sequences were obtained (29–41 sequences for each clone library). Observed numbers of OTUs and the total diversity estimated by rarefaction analyses revealed high variability in the sponge-associated bacterial community (i) between sponge endosome and cortex, (ii) between sponge and ambient seawater and (iii) between the different sampling times. In the sponge samples from June 2004, in cortex and endosome, six and nine OTUs were identified, respectively (Table 1). By contrast, seawater collected at the same time displayed 27 identified OTUs (Table 1). *Tethya aurantium* sampled in April 2003 displayed

Table 1. Observed and estimated total bacterial diversity of phylotypes (OTUs) in the different sponge and seawater samples. Rarefaction analysis and the nonparametric richness estimator chao1 were used for diversity estimation. Rarefaction analysis was conducted with a commonly used regression (1) and a modified regression (2). In all cases regression (2) gave higher r^2 values and a higher expected diversity than regression (1). Except for the seawater clone library, chao1 coverage resembles total coverage estimated by the use of regression (2). Total diversity was best covered by the analysed clones for the clone library from the sponge cortex in 2004 (76–103% depending on method used)

			Rarefaction analysis (RA)						Chao1	
			Regression (1)			Regression (2)				
Clone library	n	OTU	a_1	r^2_{RA1}	C_{RA1}	a_2	r^2_{RA2}	C_{RA2}	S_{chao1}	C_{chao1}
Seawater 2004	41	27	46.2	0.99976	58%	56.5	0.99993	48%	88.2	31%
Sponge cortex total	66	30	41.1	0.99816	73%	67.7	0.99996	44%	59.0	51%
Sponge cortex 2003	37	26	49.5	0.99992	52%	56.6	0.99998	46%	60.0	43%
Sponge cortex 2004	29	6	5.8	0.97321	103%	7.9	0.99814	76%	6.7	90%
Sponge endosome total	65	21	23.0	0.99246	91%	36.1	0.99954	58%	35.5	59%
Sponge endosome 2003	33	13	14.8	0.99599	88%	20.5	0.99968	63%	20.6	63%
Sponge endosome 2004	32	9	9.1	0.99010	99%	11.8	0.99920	76%	12.4	73%

n, number of clones in clone library; OTU, number of phylotypes/OTU in clone library; *a*, asymptote of regression equation, giving the estimated total diversity; r^2, square of correlation-coefficient; *C*, OTU/estimated diversity, a measure of coverage of a clone library; Cchao1 = Observed phylotypes/predicted SChao1 = Coverage.

a higher diversity: 26 and 13 OTUs were identified in cortex and endosome, respectively (four-fold higher compared with cortex in 2004). The total number of OTUs obtained from the sponge cortex (30) was higher than each of the values calculated individually for 2003 (26) and 2004 (6).

Applying rarefaction analysis, regression (2) always showed higher r^2 values and led to a higher estimated total diversity (Fig. 3, Table 1). According to regression (1), the total bacterial diversity seems to be well covered by the gene libraries obtained from the sponge sampled in June 2004 (88–103%). However, rarefaction analysis using regression (2) demonstrated that these proportions are overestimated under regression (1). When applying regression (2), *c*. 48–76% of the diversity seems to be covered by the clone libraries in this study (Table 1). Only three phylotypes were obtained from endosome or cortex in both years. The majority of the sequences were found only in one of the years. Thus, the total diversity of endosome- and cortex-associated sequences (as determined by rarefaction analysis), respectively, is much higher if both years are included than if each year is considered separately. These differences in the diversity possibly demonstrate annual and seasonal variation in the bacterial communities.

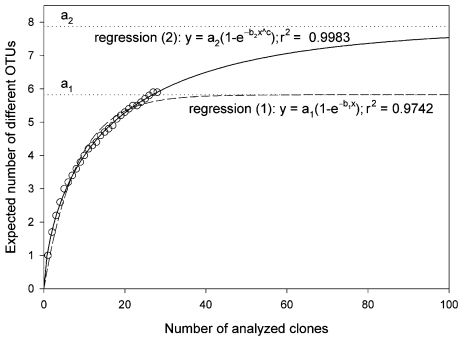

Fig. 3. Example analytical rarefaction curve plotted for one sponge-derived 16S rRNA gene clone library (sponge cortex 2004). The expected number of OTUs as determined by the analytical algorithm described by Hurlbert (1971) were plotted against the number of analysed clones (circles). Extrapolated regression curves (solid line and dashed line) are shown for the different regression Equations (1) and (2). The expected total diversity determined by the asymptotes (a_1/a_2) is indicated by dotted lines. Regression (1), which has been used in former studies (Webster *et al.*, 2004; Yakimov *et al.*, 2006), results in a lower expected total diversity compared with regression (2) ($a_1 < a_2$) with also lower values for the nonlinear coefficient of determination ($r_1^2 < r_2^2$).

Phylogenetic analysis

A high phylogenetic diversity was observed for the 171 bacterial sequences obtained from both sponge samples and surrounding seawater, including members of the *Alphaproteobacteria*, *Betaproteobacteria*, *Gammaproteobacteria* and *Deltaproteobacteria*, *Bacteroidetes*, *Verrucomicrobia*, *Planctomycetales*, *Gemmatimonadales*, *Acidobacteria*, *Actinobacteria*, *Spirochaeta* and *Cyanobacteria* (Table 2). However, the majority of sequences was affiliated with the *Proteobacteria* (38%), the *Cyanobacteria* (27%) and the *Bacteroidetes* (25%).

Some phylotypes were found in *T. aurantium* from both years. They form monophyletic clusters (i) related to the *Betaproteobacteria* (*Tethya-I*, Fig. 4a), (ii) affiliated with the *Cyanobacteria* (*Tethya-II*, Fig. 4b) and (iii) within the *Bacteroidetes* (*Tethya-III*, Fig. 4c). Within each of these

Table 2. List of phylogenetic affiliations of 16S rRNA gene clone sequences obtained from the cortex and endosome of *Tethya aurantium* sampled in 2003 and 2004 as well as surrounding seawater (2004)

Clone	Source	Length [bp]	Next relative	Acc.	Overlap [bp]	Identity	Phylogenetic affiliation
TAA-10-30v [1]	Cortex 2003	1498	Sponge clone L35 (*Latrunculia apicalis*)	AY321419	881	93%	*Betaproteobacteria*- related
TAA-5-01v [12]	Cortex 2004	1489	Sponge clone L35 (*Latrunculia apicalis*)	AY321419	882	94%	*Betaproteobacteria*- related
DGGE TA-Ia [2]	Cortex 03/04	142	Sponge clone HRV40 (*Halichondria panicea*)	UBZ88592	113	99%	*Betaproteobacteria*- related
TAA-10-50v [1]	Cortex 2003	1376	Mangrove bacterioplankton clone DS143	DQ234225	1376	96%	*Gammaproteobacteria, Oceanospirallales*
TAA-10-78v [1]	Cortex 2003	1393	Sponge clone E01-9c-26 (*Axinella verrucosa*)	AJ581351	1312	95%	*Gammaproteobacteria, Oceanospirallales*
TAA-10-33v [2]	Cortex 2003	1388	Uncultured bacterium clone A314926	AY907761	1216	93%	*Gammaproteobacteria*
TAA-10-62v [1]	Cortex 2003	1372	*Gammaproteobacterium* 17X/A02/237	AY576771	1375	91%	*Gammaproteobacteria*
TAA-10-90v [2]	Cortex 2003	1387	unc. sediment proteobacterium SIMO-2184	AY711550	810	93%	*Gammaproteobacteria*
TAA-10-60v [1]	Cortex 2003	1393	Uncultured bacterium clone SDKAS1_6	AY734243	1290	91%	*Gammaproteobacteria, Coxiella* group
TAA-10-18v [1]	Cortex 2003	1303	Marine *Alphaproteobacterium* clone MB11B07	AY033299	1313	99%	*Alphaproteobacteria*
TAA-5-11v [2]	Cortex 2004	1405	Seamount *Alphaproteobacterium* clone JdFBGBact_40	AF323257	1174	88%	*Alphaproteobacteria*
TAA-10-03v [1]	Cortex 2003	1367	Mucus bacterium 23	AY654769	1175	95%	*Alphaproteobacteria*
TAA-10-13v [1]	Cortex 2003	1335	Hypersaline bacterium clone E6aH10	DQ103609	765	92%	*Alphaproteobacteria*
TAA-10-23v [2]	Cortex 2003	1404	*Holophaga* sp. oral clone CA002	AF385537	1184	93%	*Deltaproteobacteria*
TAA-5-46v [1]	Cortex 2004	1435	*Synechococcus* sp. WH 8016	AY172834	1436	99%	*Cyanobacteria, Synechococcus* group
TAA-10-02v [3]	cortex 2003	1339	*Synechococcus* sp. WH 8016	AY172834	1322	99%	*Cyanobacteria, Synechococcus* group
TAA-10-19v [1]	Cortex 2003	1335	*Antithamnion* sp. plastid DANN	X54299	1335	95%	*Cyanobacteria,* chloroplasts
TAA-10-96v [3]	Cortex 2003	1387	*Tenacibaculum lutimaris* strain TF-42	AY661693	1303	98%	*Bacteroidetes, Flavobacteriaceae*
TAA-10-10v [4]	Cortex 2003	1368	*Flavobacteriaceae* bacterium CL-TF09	AY962293	1368	96%	*Bacteroidetes, Flavobacteriaceae*
TAA-10-14v [2]	Cortex 2003	1392	Unc. *Bacteroidetes* bacterium C319a-R8C-C8	AY678510	1384	97%	*Bacteroidetes, Flavobacteriaceae*
TAA-10-29v [1]	Cortex 2003	1386	*Flavobacteriaceae* str. SW334	AF493686	1252	96%	*Bacteroidetes, Flavobacteriaceae*
TAA-10-74v [1]	Cortex 2003	1390	Bacterium K2-15	AY345434	1390	90%	*Bacteroidetes, Flavobacteriaceae*
TAA-10-77v [1]	Cortex 2003	1381	Uncultured bacterium clone LC1408B-77	DQ270634	1180	91%	*Bacteroidetes, Flavobacteriaceae*
TAA-5-15v [3]	Cortex 2004	1430	*Bacteroidetes* bacterium PM13	AY548770	1201	89%	*Bacteroidetes, Flavobacteriaceae*
TAA-10-32v [1]	Cortex 2003	1385	*Microscilla furvescens*	AB078079	1340	91%	*Bacteroidetes, Flexibacteriaceae*
TAA-5-103v [10]	Cortex 2004	1375	*Microscilla furvescens*	AB078079	1301	91%	*Bacteroidetes, Flexibacteriaceae*
DGGE TA-II [2]	Cortex 03/04	137	*Bacteroidetes* clone GCTRA14_S	AY701461	135	97%	*Bacteroidetes, Flexibacteriaceae*
TAA-5-25v [1]	Cortex 2004	1485	*Flexibacter aggregans*	AB078038	1399	88%	*Bacteroidetes, Flexibacteriaceae*
TAA-10-06v [1]	Cortex 2003	1385	Uncultured marine eubacterium HstpL64	AF159640	876	92%	*Planctomycetales*
TAA-10-04v [1]	Cortex 2003	1387	Uncultured bacterium clone FS142-21B-02	AY704401	1183	90%	*Planctomycetales*

Continued

Table 2. Continued.

Clone	Source	Length [bp]	Next relative	Acc.	Overlap [bp]	Identity	Phylogenetic affiliation
TAA-10-09v [1]	Cortex 2003	1369	Uncultured *Pirellula* clone 6N14	AF029078	1369	97%	*Planctomycetales*
TAA-10-101v [1]	Cortex 2003	1419	sponge clone TK19 *(Aplysina aerophoba)*	AJ347028	1416	93%	*Gemmatimonadales*
TAA-10-43 [2]	Cortex 2003	1375	Unc. marine bacterium SPOTSFEB02_70m35	DQ009431	1357	92%	*Actinobacteria, Acidimicrobiaceae*
TAA-10-01v [1]	Cortex 2003	1382	Uncultured *Actinobacterium* clone Bol7	AY193208	1365	96%	*Actinobacteria*
TAI-8-03v [1]	Endosome 2003	1436	Sponge clone L35 (*Latrunculia apicalis*)	AY321419	881	94%	*Betaproteobacteria*- related
TAI-2-47f [12]	Endosome 2004	1436	Sponge clone L35 (*Latrunculia apicalis*)	AY321419	882	94%	*Betaproteobacteria*- related
DGGE TA-Ib [2]	endosome 03/04	142	Sponge clone HRV40 (*Halichondria panicea*)	UBZ88592	113	99%	*Betaproteobacteria*- related
TAI-2-153v [2]	Endosome 2004	1384	Sponge clone 34P16 (*Phyllospongia papyracea*)	AY845231	950	86%	*Gammaproteobacteria*
TAI-8-61v [1]	Endosome 2003	1370	Uncultured marine bacterium clone SPOTSAUG01_5m75	DQ009136	1370	99%	*Gammaproteobacteria*
TAI-8-75 [2]	Endosome 2003	864	Uncultured *Gammaproteobacterium* KTc1119	AF235120	860	99%	*Gammaproteobacteria*
TAI-8-99k [1]	Endosome 2003	462	Uncultured *Gammaproteobacterium* clone PI_4j5b	AY580744	438	100%	*Gammaproteobacteria*
TAI-8-76v [4]	Endosome 2003	1370	Uncultured marine bacterium clone SPOTSAPR01_5m185	DQ009135	1370	99%	*Gammaproteobacteria*
TAI-8-20v [2]	Endosome 2003	1388	Unidentified *Gammaproteobacterium* OM60	U70696	1389	99%	*Gammaproteobacteria*
TAI-8-64v [1]	Endosome 2003	1339	*Photobacterium phosphoreum* strain RHE-01	AY435156	1303	99%	*Gammaproteobacteria*
TAI-2-166v [5]	Endosome 2004	1443	*Cyanobacterium* 5X15	AJ289785	1443	99%	*Cyanobacteria, Synechococcus* group
TAI-8-58v [6]	Endosome 2003	1332	*Cyanobacterium* 5X15	AJ289785	1331	99%	*Cyanobacteria, Synechococcus* group
TAI-8-74v [9]	Endosome 2003	1340	*Synechococcus* so. Almo3	AY172800	1326	99%	*Cyanobacteria, Synechococcus* group
TAI-2-160v [6]	endosome 2004	1419	*Synechococcus* sp. RS9920	AY172830	1402	99%	*Cyanobacteria, Synechococcus* group
TAI-8-17v [3]	Endosome 2003	1372	*Flexibacter* sp. IUB42	AB058905	1375	95%	*Bacteroidetes, Flavobacteriaceae*
TAI-8-94v [1]	Endosome 2003	1380	Uncultured marine bacterium ZD0255	AJ400343	1381	96%	*Bacteroidetes, Flavobacteriaceae*
TAI-8-51v [1]	Endosome 2003	1388	Uncultured CFB group bacterium clone AEGEAN_179	AF406541	1368	97%	*Bacteroidetes, Flavobacteriaceae*
TAI-2-145v [1]	Endosome 2004	1438	Uncultured marine bacterium clone Chl1.12	DQ071033	1419	99%	*Bacteroidetes, Flavobacteriaceae*
TAI-2-81v [1]	Endosome 2004	1372	Uncultured marine bacterium clone SPOTSAPR01_5m235	DQ009115	1353	97%	*Bacteroidetes, Flavobacteriaceae*
TAI-2-123v [1]	Endosome 2004	1385	*Flexibacter aggregans* strain:IFO 15974	AB078038	1457	88%	*Bacteroidetes, Flexibacteriaceae*
TAI-2-130f [3]	Endosome 2004	1418	Uncultured marine eubacterium HstpL83	AF159642	1008	99%	*Planctomycetes*
TAI-2-28v [1]	Endosome 2004	1407	Uncultured Verrucomicrobia Arctic96BD-2	AY028221	1193	95%	*Verrucomicrobia*
TAI-8-67v [1]	Endosome 2003	1369	Uncultured bacterium clone ELB16-004	DQ015796	1369	98%	*Actinobacteria*
TAU-7-56k [1]	Seawater 2004	430	Uncultured *Gammaproteobacterium* clone SIMO-2629	DQ189604	367	99%	*Gammaproteobacteria*
TAU-7-53p [1]	Seawater 2004	937	Uncultured marine bacterium clone SPOTSOCT00_5m102	DQ009138	882	98%	*Gammaproteobacteria*

Continued

Table 2. Continued.

Clone	Source	Length [bp]	Next relative	Acc.	Overlap [bp]	Identity	Phylogenetic affiliation
TAU-7-30p [4]	Seawater 2004	835	uncultured *Gammaproteobacterium* CHAB-III-7	AJ240921	840	98%	*Gammaproteobacteria*
TAU-7-93 [1]	Seawater 2004	496	Uncultured *Gammaproteobacterium* OCS44	AF001650	495	99%	*Gammaproteobacteria*
TAU-7-25 [1]	Seawater 2004	407	Uncultured *Gammaproteobacterium* NAC11-19	AF245642	407	97%	*Gammaproteobacteria*
TAU-7-100v [1]	Seawater 2004	1509	Uncultured *Gammaproteobacterium* KTc1119	AF235120	1491	99%	*Gammaproteobacteria*
TAU-7-63p [1]	Seawater 2004	866	Uncultured bacterium clone MP104-1109-b35	DQ088799	843	99%	*Gammaproteobacteria*
TAU-7-71p [3]	Seawater 2004	866	Uncultured bacterium MabScd-NB	AB193929	833	99%	*Alphaproteobacteria*
TAU-7-36p [1]	Seawater 2004	858	Uncultured *Proteobacterium* clone SIMO-855	AY712392	748	99%	*Alphaproteobacteria*
TAU-7-38 [1]	Seawater 2004	414	Uncultured bacterium clone CD3B11	AY038391	410	97%	*Alphaproteobacteria*
TAU-7-44p [1]	Seawater 2004	862	Uncultured *Alphaproteobacterium* clone PI_4t1g	AY580547	809	95%	*Alphaproteobacteria*
TAU-7-79v [1]	Seawater 2004	1438	Unidentified eukaryote clone OM21 plastid 16S rRNA gene	U32671	1251	96%	*Cyanobacteria,* chloroplasts group
TAU-7-26p [2]	Seawater 2004	747	Environmental clone OCS50 chloroplast gene	AF001656	746	98%	*Cyanobacteria,* chloroplasts group
TAU-7-39p [1]	Seawater 2004	833	Unidentified haptophyte OM153	U70720	768	95%	*Cyanobacteria,* chloroplasts group
TAU-7-57p [1]	Seawater 2004	801	Uncultured diatom clone Hot Creek 8	AY168751	802	95%	*Cyanobacteria,* chloroplasts group
TAU-7-73p [1]	Seawater 2004	756	Unidentified eukaryote clone OM20	U32670	755	98%	*Cyanobacteria,* chloroplasts group
TAU-7-97p [3]	Seawater 2004	803	Environmental clone OCS20	AF001654	800	98%	*Cyanobacteria,* chloroplasts group
TAU-7-68v [4]	Seawater 2004	1436	Neoptilota densa plastid	DQ028877	1334	94%	*Cyanobacteria,* chloroplasts group
TAU-7-74p [1]	Seawater 2004	864	Environmental clone OCS162	AF001659	617	92%	*Cyanobacteria,* chloroplasts group
TAU-7-50p [1]	Seawater 2004	803	Uncultured *Bacteroidetes* bacterium clone SIMO-780	AY712317	580	96%	*Bacteroidetes, Flavobacteriaceae*
TAU-7-28p [2]	Seawater 2004	690	Uncultured *Bacteroidetes* bacterium clone CONW90	AY828420	582	99%	*Bacteroidetes, Flavobacteriaceae*
TAU-7-43 [1]	Seawater 2004	476	Uncultured *Bacteroidetes* bacterium clone CONW90	AY828420	457	95%	*Bacteroidetes, Flavobacteriaceae*
TAU-7-02v [1]	Seawater 2004	1490	Uncultured marine bacterium clone Chl1.12	DQ071033	1452	99%	*Bacteroidetes, Flavobacteriaceae*
TAU-7-69v [3]	Seawater 2004	1487	Unc. marine bacterium SPOTSAPR01_5m235	DQ009115	1468	97%	*Bacteroidetes, Flavobacteriaceae*
TAU-7-61p [1]	Seawater 2004	813	Unc. *Bacteroidetes* bacterium 3iSOMBO27	AM162576	817	96%	*Bacteroidetes, Flexibacteriaceae*
TAU-7-58 [1]	Seawater 2004	277	Uncultured bacterium gene for 16S rRNA, clone:JS624-8	AB121106	288	93%	*Spirochaetes*
TAU-7-55p [1]	Seawater 2004	804	*Bacillus* sp. C93	DQ091008	797	99%	*Firmicutes, Bacillus* group

Numbers in brackets indicate no. of sequences in the phylotype represented by listed clones.

clusters, sequences share > 99% similarity. Of special interest is cluster *Tethya–I*, which is represented by 26 clone sequences (19%) and was found in the cortex and endosome of all *T. aurantium* individuals. *Tethya-I* forms a monophyletic cluster with sponge-derived 16S rRNA gene sequences from different sponges from Antarctic (Webster *et al.*, 2004) and Australian waters (Taylor *et al.*, 2004), as well as the Mediterranean Sea (Althoff *et al.*, 1998). This sponge-specific monophyletic cluster is related to the *Betaproteobacteria* and branches deeply (dotted frame in Fig. 4a). In addition, the DGGE band TA-I, assigned to the sponge-specific cluster *Tethya-I*, was unique to all *T. aurantium*

samples but was not found in seawater. Moreover, no clone sequences belonging to the *Betaproteobacteria* were obtained from seawater in this study.

Within the *Cyanobacteria*, three phylotypes comprising 30 *Synechococcus* species sequences (22%) were obtained from *T. aurantium*-derived clone libraries. One of the phylotypes was found repeatedly in consecutive years (*Tethya-II*, Fig. 4b). *Synechococcus* species sequences were found mainly in the endosome samples (Table 2), but not in the surrounding seawater. All cyanobacteria-like sequences obtained from the surrounding seawater belonged to chloroplasts of different algae. Only one chloroplast sequence was also found in the sponge cortex in April 2003.

Within the *Bacteroidetes* one bacterial cluster (*Tethya-III*) of *Flexibacteriaceae* was repeatedly found in *T. aurantium* (Fig. 4c, Table 2). The sequences of the cluster shared highest similarity with *Microscilla furvescens* (AB078079, 91%) and were found in the cortex only. Additionally, DGGE band TA-II, present exclusively in cortex samples and absent from endosome and seawater, was assigned to this cluster (Fig. 4c). A further cluster of *T. aurantium*-derived *Flexibacteriacea* was found in both endosome and cortex in June 2004 samples (Fig. 4c). Similarity between the clusters was 90%. *Flexibacteriaceae* related (92%) to putative vertically transmitted sponge-symbionts (Enticknap *et al.*, 2006) were found in the sponge cortex from 2004 only (TAA-5-15v, Fig. 4c). All other *T. aurantium*-derived sequences within the *Bacteroidetes* belonged to the *Flavobacteriaceae* and *Saprospiraceae*, regardless of their origin from sponge cortex or endosome (Fig. 4c). All sequences showed a high degree of similarity to sequences retrieved from various marine environments (Fig. 4c, Table 2).

Thirty *T. aurantium*-derived 16S rRNA gene sequences (22%) were closely related to other sponge-derived 16S

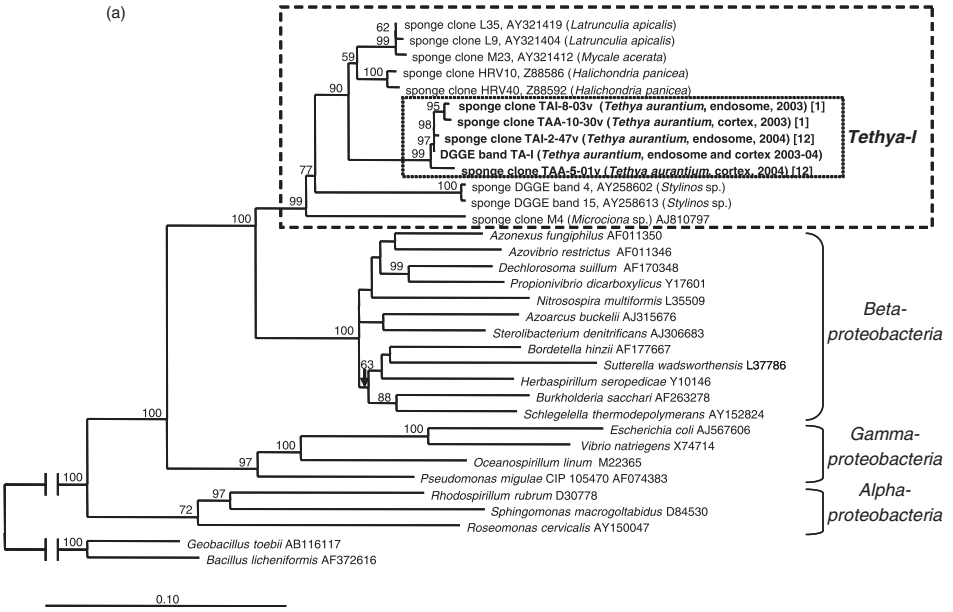

Fig. 4. Phylogenetic trees constructed from 16S rRNA gene sequences related to the *Betaproteobacteria* (a), *Cyanobacteria* (b) and *Bacteroidetes* (c). Sequences obtained from *Tethya aurantium* are shown in bold type. Adriatic seawater clone sequences are underlined. Numbers of represented clones in each OTU are given in brackets after the clone names. Clusters of *T. aurantium*-associated bacterial phylotypes found in both years (*Tethya-I*, *Tethya-II* and *Tethya-III*) are framed with dotted line. The new sponge-specific cluster related to the *Betaproteobacteria* is framed with a dashed line (a). All trees were generated using the maximum likelihood method. Tree (a) is based on sequences of 500–1500 bp length. The DGGE sequence (< 500) was added without changing the tree topology using the parsimony method in ARB. Trees (b) and (c) are based on almost complete sequences (b, ≥ 1000 bp; c, ≥ 1200 bp). Partial sequences ($< 1000/ < 1200$ bp) were added without changing the tree topology using the parsimony method in ARB and are indicated by dashed branches. The phylogenetic positions of partial sequences were verified by calculation of all length sequences separately. Bootstrapping analysis (100 datasets) was conducted. Values equal to or greater than 50% are shown. Bootstrap values in parentheses refer to tree calculations including short sequences. The scale bars indicate the number of substitutions per nucleotide position.

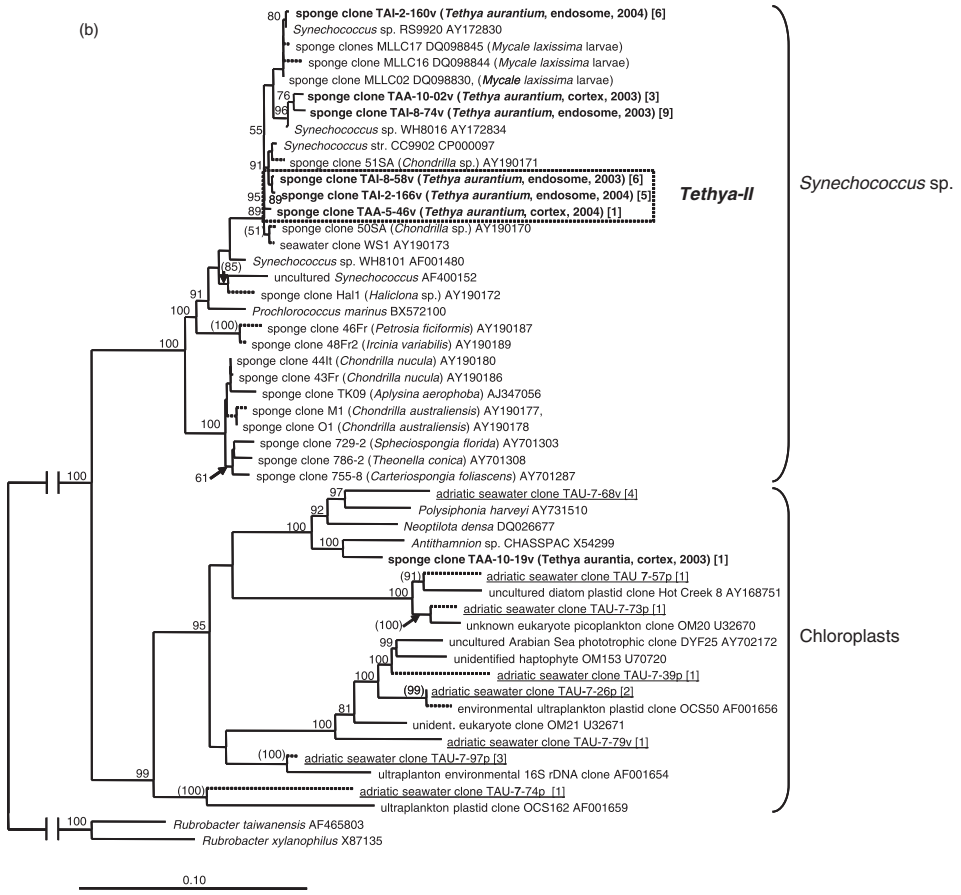

Fig. 4. Continued

rRNA gene sequences. Twenty-six of these belonged to cluster *Tethya-I*, with the remaining four sequences affiliated to the *Gemmatimonadales*, the *Gammaproteobacteria*, the *Actinobacteria* and the *Acidobacteria*: Clone TAA-10-101v, obtained from *T. aurantium* cortex in 2003, clustered monophyletically with the sponge-specific cluster 'uncertain-I' described by Hentschel *et al.* (2002) within the *Gemmatimonadales* (represented by sponge clone TK19, Table 2). Clone TAA-10-78v from the *T. aurantium* cortex (April 2003) was related to sequences obtained from sponges as well as other marine habitats within the *Gammaproteobacteria* (data not shown). BLAST search results showed closest association to sponge-associated bacteria (Table 2), but phylogenetic analysis could not identify monophyly of the sponge-derived gammaproteobacterial sequences. TAI-2-153v, representing two sequences obtained from the sponge endosome in 2004, was most similar to the *Phyllospongia papyracea*-associated *Gammaproteobacteria* clone 34P16 (Ridley *et al.*, 2005) (sequence similarity of 86%, Table 2). Again, phylogenetic analysis did not support monophyletic clustering of the sponge-derived sequences. *Actinobacteria* as well as *Acidobacteria* derived from sponges have been reported previously (Hentschel *et al.*, 2002; Imhoff & Stöhr, 2003; Kim *et al.*, 2005; Schirmer *et al.*, 2005) and sponge-specific clusters have been described (Hentschel *et al.*, 2002). *Tethya aurantium*-derived sequences TAI-8-

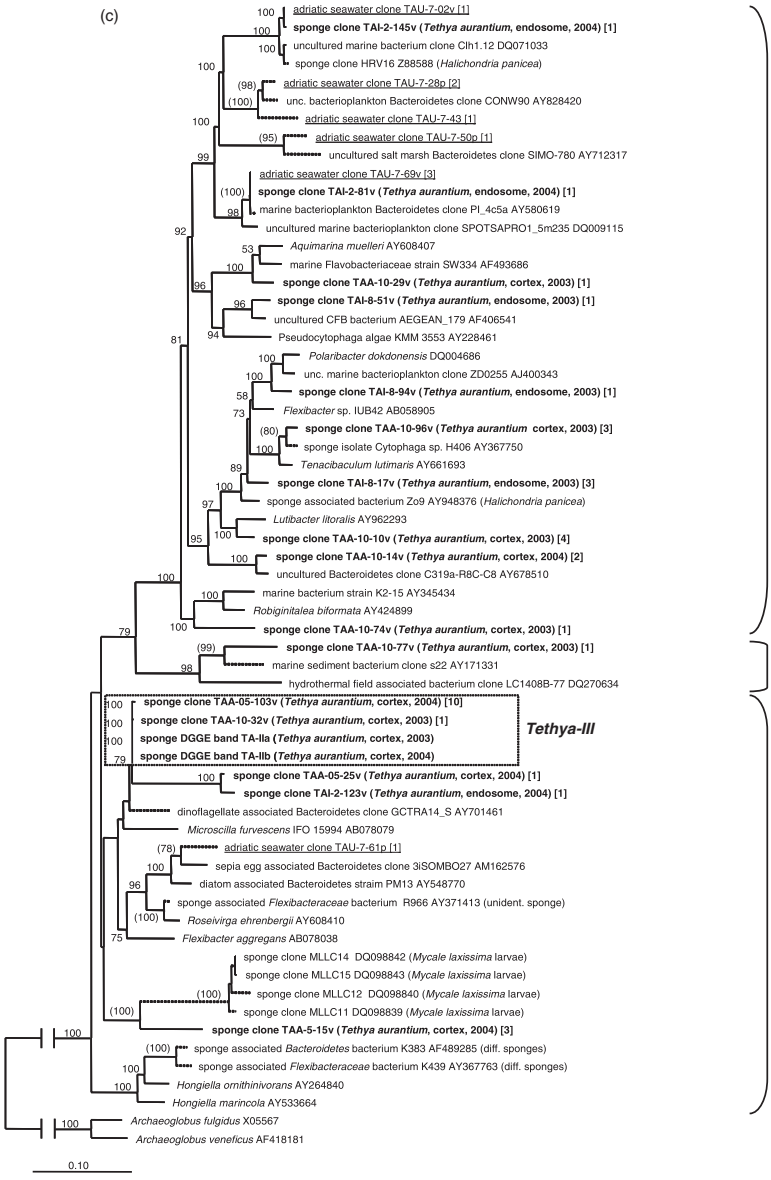

[a]Flav= *Flavobacteriaceae*, Sapr= *Saprospiraceae*, Flex= *Flexibacteriaceae*

Fig. 4. Continued

67v and TAA-10-43v showed similarities of 84–95% to different sponge-associated *Actinobacteria* sequences but did not group with any of the three described sponge-specific *Actinobacteria* clusters (Hentschel *et al*., 2002). TAA-10-23v, which represents two clones obtained from the *T. aurantium* cortex, showed < 90% sequence similarity to the sponge-specific cluster *Acido-I* (Hentschel *et al*., 2002) and did not cluster monophyletically with it.

Several sequences obtained from *T. aurantium* were not specifically related to sequences found in sponges, but were either closely related to seawater-derived bacteria or to bacteria associated with other marine macroorganisms (Vergin *et al*., 1998; Cho & Giovannoni, 2004; Brown *et al*., 2005) [i.e. TAI-8-61v, TAI-8-64v, TAI-8-20v (*Gammaproteobacteria*) and TAI-2-130v, TAA-10-09v (*Planctomycetales*); Table 2]. Bacteria affiliated with the *Gammaproteobacteria* (TAU-7-100v/TAI-8-75p) and the *Flavobacteriaceae* (*Bacteroidetes*) (TAI-2-145v/TAU-7-02v and TAI-2-81v/TAU-7-69) were found in both *T. aurantium* endosome and seawater in this study. No sequence obtained from the sponge cortex showed similarity to seawater-derived sequences obtained in this study.

Alphaproteobacteria were exclusively found in the *T. aurantium* cortex and in ambient seawater in June 2004 (Table 2). The sponge-derived sequences were related to bacterioplankton-derived sequences (Suzuki *et al*., 2001), coral mucus-associated bacteria (O. Koren & E. Rosenberg, unpublished data, GenBank accession no. AY654769) and a filamentous bacterium from a wastewater treatment plant (Levantesi *et al*., 2004). *Alphaproteobacteria* closely related to those found in seawater in this study (TAU-7-44p and TAU-7-38) have been obtained from sponges (*Halichondria panicea* and *Halichondria okadai*) previously (Althoff *et al*., 1998; I. Okano *et al*., unpublished data, GenBank accession no. AB054143).

Discussion

Although sponges do not possess organs or real tissues, cortex and endosome are clearly differentiated with respect to structure and function. For the first time, our studies on *Tethya aurantium* have revealed that they also differ in their bacterial communities. Distinct phylotypes, represented by DGGE bands and 16S rRNA gene clone sequences, were affiliated with the different regions of the sponge.

Tethya aurantium supports a relatively low diversity of specifically associated bacteria. Only three bacterial phylotypes were found in sponge specimens from both years investigated. For diversity estimation we applied rarefaction analysis in combination with two nonlinear regressions. The commonly used regression (1) was shown to underestimate systematically the total diversity, while regression (2) results in estimates comparable with those from chao1. Regression (2) was demonstrated to be significantly better suited as a regression for fitting rarefaction curves and predicting total diversity, and therefore is recommended to be used for diversity estimation of clone libraries in future studies. Under application of the more conservative regression (2), rarefaction analysis displays only two (cortex) and four (endosome) expected additional bacterial phylotypes (OTUs) not identified in this study for the *T. aurantium* specimen from 2004.

One characteristic cluster closely related to the *Betaproteobcteria* (cluster *Tethya-I*) is associated with both endosome and cortex of *T. aurantium*. *Betaproteobacteria*, with the exception of ammonium oxidizers (Voytek & Ward, 1995), are not abundant in open oceans (Giovannoni & Rappé, 2000), but are characteristic of freshwater habitats (Methe *et al*., 1998; Schweitzer *et al*., 2001) and have also been observed in coastal waters (Rappe *et al*., 1997; Fuhrman & Ouverney, 1998). Nonetheless, *Betaproteobacteria*-affiliated bacteria have previously been found in sponges by culture-independent methods (Althoff *et al*., 1998; Webster *et al*., 2001, 2004; Thoms *et al*., 2003; Taylor *et al*., 2004). In *Rhopaloides odorabile*, they were located intracellularly in some cases by fluorescence *in situ* hybridization (Webster *et al*., 2001). *Tethya-I* clusters monophyletically with those other sponge-derived sequences (Althoff *et al*., 1998; Webster *et al*., 2004; Taylor *et al*., 2004, 2005), forming a sponge-specific monophyletic cluster (Fig. 4a). Our studies indicate that this cluster branches deeply within the *Betaproteobacteria*, but its exact phylogenetic affiliation remains uncertain. Phylogenetic analysis using the backbone tree and the parsimony method implemented in the ARB program (Ludwig *et al*., 2004) demonstrated a consistent affiliation with the *Betaproteobacteria*, although within this group the phylogenetic position of the *Tethya-I* cluster largely depends on the (DNA)-filter used. By contrast, complete phylogenetic calculations including a reasonable number of representatives of the *Betaproteobacteria*, *Gammaproteobacteria* and *Alphaproteobacteria*, using the ML method (Felsenstein, 1981), placed the sponge-specific cluster outside the known *Betaproteobacteria* (Fig. 4a).

Finding of *Tethya-I*-related sequences in *Halichondria panicea* from the Adriatic Sea but not in individuals from the North Sea or the Baltic Sea (Althoff *et al*., 1998) possibly indicates a synergistic sponge–microbe association. Yet, the occurrence of members of the *Betaproteobacteria*-related sponge-specific cluster is not limited to the Mediterranean Sea, as formerly unaffiliated sequences obtained from the Antarctic sponges *Latrunculia apicalis* and *Mycale acerata* (Webster *et al*., 2004) can now be assigned to the cluster. As *Betaproteobacteria* are abundant in freshwater habitats (Methe *et al*., 1998; Schweitzer *et al*., 2001) a freshwater origin cannot be excluded for the *T. aurantium*-derived sequences obtained from the river-fed Limksi kanal.

However, no *Betaproteobacteria* were found in the seawater surrounding the *T. aurantium* habitat and furthermore no freshwater-derived bacteria closely related to the *Tethya-I* cluster have been described.

Cyanobacterial associations in sponges have been known for many years. Within the *Synechococcus* group one specifically sponge-associated cluster and several additional sponge-associated *Cyanobacteria* have been identified (Steindler *et al.*, 2005). Besides symbiotic associations, the genus *Synechococcus* is also known as a member of marine picoplankton communities and serves as food for different filter-feeding animals, including sponges (Pile *et al.*, 1996). For *T. aurantium* no cyanobacterial associations have been reported in the literature. Interestingly, we found *Synechococcus* species sequences making up a major part of the endosome-derived clone library ($n = 26\%$, 39%) (Fig. 4b, Table 2). They represent three closely related phylotypes, only distantly related to the sponge-specific group of *Synechococcus* species strains. They show high sequence similarity to several cultured and uncultured *Synechococcus* strains, also including sponge- and sponge-larvae-associated uncultured strains obtained from *Chondrilla* sp. and *Mycale laxissima* (Usher *et al.*, 2004; Enticknap *et al.*, 2006). The close relationship to putative vertically transmitted sponge-associated *Synechococcus* strains indicates constant and obligate association to sponges. However, unlike the *T. aurantium*-derived sequences in this study, the closely related cyanobacterial symbionts from *Chondrilla* sp. were also found in seawater. It was hypothesized that these *Cyanobacteria* have become symbiotic with sponges relatively recently (Usher *et al.*, 2004). Owing to the close phylogenetic relationship to planktonic *Synechococcus* strains, a seawater origin cannot be excluded for the *T. aurantium*-associated strains either. *Cyanobacteria* in sponges have generally been found in the thin (few millimetres) outer tissue regions, where light energy is available for photosynthesis. The endosome of *T. aurantium* is covered by a thick and dense cortex region, but spicule bundles might function as a natural light conductor, similar to fibre-optic systems, as was postulated for the growth of the sponge-associated green alga *Ostreobium* sp. in *Tethya seychellensis* (Gaino & Sará, 1994).

A specifically cortex-associated bacterial cluster was identified within the division *Bacteroidetes*, affiliated with the family *Flexibacteriaceae* (clone cluster *Tethya-III* and DGGE band TA-II, Fig. 2). Although several previous studies have demonstrated *Bacteroidetes* belonging to the family *Flavobacteriaceae* to be associated with sponges (Webster *et al.*, 2001, 2004; Lafi *et al.*, 2005), only very recently have sponge-associated *Flexibacteriaceae* been obtained from sponge larvae by culture-independent methods (Enticknap *et al.*, 2006). These putative vertically transmitted sponge symbionts are closely related to sequences obtained from *T. aurantium* cortex in 2004 and distantly related to cluster *Tethya-III* found in both years. Cluster *Tethya-III* has been observed in sponges for the first time in this study. The bacteria were not detected in the ambient seawater and in the sponge endosome. Given the occurrence in the sponge cortex exclusively and presence in specimens from consecutive years as well as the phylogenetically relatively large distance ($< 91\%$) to known sequences, we assume specific association between the *Microscilla*-like bacteria and *T. aurantium*.

As sponges are filter-feeding animals, a seawater origin of sponge-derived bacterial sequences cannot be excluded despite repeated washing steps in sterile seawater prior to DNA extraction. Several sequences obtained from seawater in this study share high similarity with clone sequences found in both *T. aurantium* and other sponges. Thus, some of the endosome-associated bacterial sequences may solely resemble DNA of ambient seawater bacteria ingested in the choanocyte chambers. Additionally, the high variability of different phylotypes observed either implies seasonal differences in the sponge-associated bacterial communities or possibly reflects seasonal microbial population dynamics in the ambient seawater. The similarity between the sponge endosome-associated bacterial community and the ambient seawater bacterioplankton as demonstrated in DGGE and phylogenetic analysis again emphasizes the need to differentiate between sponge-specific and merely ingested bacteria.

Hentschel *et al.* (2002) found 70% of all sponge-derived sequences clustering together in different phylogenetic clades. By contrast, a minor fraction (22%) of the *T. aurantium*-derived sequences were closely related to other sponge-associated bacteria. Apart from cluster *Tethya–I* related to the *Betaproteobacteria*, only two additional sequences obtained from *T. aurantium* cluster with other known sponge-derived sequences. The monophyly of the sponge-specific cluster indicates common ancestry for members of this group. Furthermore, limitation of these bacteria to associations with the phylum Porifera can be hypothesized. However, because abundance and diversity of bacteria associated with different sponges depends to a large extent on the sponge species and possibly on seasonal influences, a uniform specifically sponge-associated bacterial community as proposed by Hentschel *et al.* (2002) probably does not exist.

We suggest a specific association of both the *Betaproteobacteria*-related cluster *Tethya–I* and the *Flexibacteriaceae* cluster *Tethya-III* with the sponge *T. aurantium*. The new cluster of specifically associated *Flexibacteriaceae* has so far been exclusively found in *T. aurantium* and its presence in sponges of other taxonomic affiliation and geographical regions remains to be investigated. The unusual association of *Synechococcus* species strains with the *T. aurantium*

endosome and the putative light conduction by sponge spicule bundles will be studied in future research.

Acknowledgements

We gratefully acknowledge the help of R. Batel and the personnel at the Ruder Boskovic Institut (Rovinj, Croatia) and F. Brümmer (University of Stuttgart, Germany) during sampling of the sponges. This work was supported by the German Federal Ministry of Education and Research (bmb+f) as part of the Kompetenz-Zentrum BIOTECmarin (grant no. 03F0345B)

References

Althoff K, Schütt C, Steffen R, Batel R & Müller WEG (1998) Evidence for a symbiosis between bacteria of the genus *Rhodobacter* and the marine sponge *Halichondria panicea*: harbor also for putatively toxic bacteria? *Mar Biol* **130**: 529–536.

Altschul SF, Gish W, Miller W, Myers EW & Lipman DJ (1990) Basic local alignment search tool. *J Mol Biol* **215**: 403–410.

Brown MV, Schwalbach MS, Hewson I & Fuhrman JA (2005) Coupling 16S-ITS rDNA clone libraries and automated ribosomal intergenic spacer analysis to show marine microbial diversity: development and application to a time series. *Environ Microbiol* **7**: 1466–1479.

Brümmer F, Calcinai B, Götz M, Leitermann F, Nickel M, Schillak L, Sidri M & Zucht W (2004) Overview on the sponge fauna of the Limski kanal, Croatia, Northern Adriatic Sea. *Boll Musei Institut Biol 2004 (Genova)* **68**: 219–227.

Burja AM & Hill RT (2001) Microbial symbionts of the Australian great barrier reef sponge, *Candidaspongia flabellata*. *Hydrobiologia* **461**: 41–47.

Burja AM, Webster NS, Murphy PT & Hill RT (1999) Microbial symbionts of great barrier reef sponges. *Mem Queensl Mus* **44**: 63–75.

Burton M (1928) A comparative study of the characteristics of shallow-water and deep-sea sponges, with notes on their external form and reproduction. *J Queckett Microsc Club Ser 2* **16**: 49–70.

Cho JC & Giovannoni SJ (2004) Cultivation and growth characteristics of a diverse group of oligotrophic marine *Gammaproteobacteria*. *Appl Environ Microbiol* **70**: 432–440.

Clarke KR (1993) Non-parametric multivariate analysis of changes in community structure. *Australian Journal of Ecology* **18**: 117–143.

Clarke KR & Gorley RN (2001) *PRIMER v5: User Manual/ Tutorial, PRIMER-E*. Plymouth UK.

Clarke KR & Warwick RM (1994) Similarity-based testing for community pattern–the 2-way layout with no replication. *Mar Biol* **118**: 167–176.

Enticknap JJ, Kelly M, Peraud O & Hill RT (2006) Characterization of a culturable alphaproteobacterial symbiont common to many marine sponges and evidence for vertical transmission via sponge larvae. *Appl Environ Microbiol* **72**: 3724–3732.

Felsenstein J (1981) Evolutionary trees from DNA-sequences–a maximum-likelihood approach. *J Mol Evol* **17**: 368–376.

Fuhrman JA & Ouverney CC (1998) Marine microbial diversity studied via 16S rRNA sequences: cloning results from coastal waters and counting of native archaea with fluorescent single cell probes. *Aquat Ecol* **32**: 3–15.

Gaino E & Sará M (1994) Siliceous spicules of *Tethya seychellensis* (*Porifera*) support the growth of a green-alga – a possible light conducting system. *Mar Ecol Prog Ser* **108**: 147–151.

Giovannoni SJ & Rappé MS (2000) Evolution, diversity, and molecular ecology of marine prokaryotes. *Microbial Ecology of the Oceans* (Kirchman DL, ed), pp. 47–84. Wiley-Liss, New York.

Guindon S & Gascuel O (2003) A simple, fast, and accurate algorithm to estimate large phylogenies by maximum likelihood. *Syst Biol* **52**: 696–704.

Guindon S, Lethiec F, Duroux P & Gascuel O (2005) PHYML Online–a web server for fast maximum likelihood-based phylogenetic inference. *Nucleic Acids Res* **33**: W557–W559.

Hentschel U, Hopke J, Horn M, Friedrich AB, Wagner M, Hacker J & Moore BS (2002) Molecular evidence for a uniform microbial community in sponges from different oceans. *Appl Environ Microbiol* **68**: 4431–4440.

Hinde R, Pironet F & Borowitzka MA (1994) Isolation of *Oscillatoria spongeliae*, the filamentous cyanobacterial symbiont of the marine sponge *Dysidea herbacea*. *Mar Biol* **119**: 99–104.

Hooper NJA & van Soest RWM (2002) *Systema Porifera: A Guide to the Classification of Sponges*. Kluwer Academic/Plenum Publishers, New York.

Hurlbert S (1971) The nonconcept of species diversity: a critique and alternative parameters. *Ecology* **52**: 577–586.

Imhoff JF & Stöhr R (2003) Sponge-associated bacteria: general overview and special aspects of bacteria associated with *Halichondria panicea*. *Sponges (Porifera)* (Müller WEG, ed), pp. 35–56. Springer Verlag, Berlin.

Kemp PF & Aller JY (2004) Estimating prokaryotic diversity: when are 16S rDNA libraries large enough? *Limnol Oceanogr-Meth* **2**: 114–125.

Kim TK, Garson MJ & Fuerst JA (2005) Marine actinomycetes related to the *Salinospora* group from the great barrier reef sponge *Pseudoceratina clavata*. *Environ Microbiol* **7**: 509–518.

Koellner T, Hersperger AM & Wohlgemuth T (2004) Rarefaction method for assessing plant species diversity on a regional scale. *Ecography* **27**: 532–544.

Kuzmanovic N (1985) *Preliminarna Istrazivanja Dinamike Vodenih Masa Limskog Kanala (Zavrsni Izvjestaj)*. Rep. "Institut Ruder Boskovic", Rovinj, Croatia.

Lafi F, Garson M & Fuerst J (2005) Culturable bacterial symbionts isolated from two distinct sponge species (*Pseudoceratina clavata* and *Rhabdastrella globostellata*) from the great barrier reef display similar phylogenetic diversity. *Microb Ecol* **50**: 213–220.

Lane DL (1991) 16S/23S rRNA sequencing. *Nucleic Acid Techniques in Bacterial Systematics* (Stackebrandt E & Goodfellow M, eds), pp. 115–175. John Wiley & Sons, New York.

Levantesi C, Beimfohr C, Geurkink B, Rossetti S, Thelen K, Krooneman J, Snaidr J, van der Waarde J & Tandoi V (2004) Filamentous *Alphaproteobacteria* associated with bulking in industrial wastewater treatment plants. *Syst Appl Microbiol* **27**: 716–727.

Ludwig W, Strunk O, Westram R *et al*. (2004) ARB: a software environment for sequence data. *Nucleic Acids Res* **32**: 1363–1371.

Maidak BL, Cole JR, Parker CT *et al*. (1999) A new version of the RDP (ribosomal database project). *Nucleic Acids Res* **27**: 171–173.

Manz W, Arp G, Schumann-Kindel G, Szewzyk U & Reitner J (2000) Widefield deconvolution epifluorescence microscopy combined with fluorescence in situ hybridization reveals the spatial arrangement of bacteria in sponge tissue. *J Microbiol Meth* **40**: 125–134.

Methe BA, Hiorns WD & Zehr JP (1998) Contrasts between marine and freshwater bacterial community composition: analyses of communities in Lake George and six other Adirondack lakes. *Limnol Oceanogr* **43**: 368–374.

Muyzer G, Dewaal EC & Uitterlinden AG (1993) Profiling of complex microbial populations by denaturing gradient gel electrophoresis analysis of polymerase chain reaction-amplified genes coding for 16S ribosomal-RNA. *Appl Environ Microbiol* **59**: 695–700.

Petri R & Imhoff JF (2001) Genetic analysis of sea-ice bacterial communities of the Western Baltic Sea using an improved double gradient method. *Polar Biol* **24**: 252–257.

Pile AJ, Patterson MR & Witman JD (1996) *In situ* grazing on plankton $< 10\,\mu m$ by the boreal sponge *Mycale lingua*. *Mar Ecol Prog Ser* **141**: 95–102.

Rappe MS, Kemp PF & Giovannoni SJ (1997) Phylogenetic diversity of marine coastal picoplankton 16S rRNA genes cloned from the continental shelf off Cape Hatteras, North Carolina. *Limnol Oceanogr* **42**: 811–826.

Ridley CP, Faulkner DJ & Haygood MG (2005) Investigation of *Oscillatoria spongeliae*-dominated bacterial communities in four dictyoceratid sponges. *Appl Environ Microbiol* **71**: 7366–7375.

Sará M (1987) A study on the genus *Tethya* (*Porifera, Demospongiae*) and new perspectives in sponge systematics. *Taxonomy of Porifera*, *G13* (Vacelet J & Boury-Esnault N, eds), pp. 205–225. Springer, Berlin.

Schirmer A, Gadkari R, Reeves CD, Ibrahim F, DeLong EF & Hutchinson CR (2005) Metagenomic analysis reveals diverse polyketide synthase gene clusters in microorganisms associated with the marine sponge *Discodermia dissoluta*. *Appl Environ Microbiol* **71**: 4840–4849.

Schweitzer B, Huber I, Amann R, Ludwig W & Simon M (2001) *Alpha-* and *Betaproteobacteria* control the consumption and release of amino acids on lake snow aggregates. *Appl Environ Microbiol* **67**: 632–645.

Steindler L, Huchon D, Avni A & Ilan M (2005) 16S rRNA phylogeny of sponge-associated cyanobacteria. *Appl Environ Microbiol* **71**: 4127–4131.

Suzuki MT, Beja O, Taylor LT & DeLong EF (2001) Phylogenetic analysis of ribosomal RNA operons from uncultivated coastal marine bacterioplankton. *Environ Microbiol* **3**: 323–331.

Taylor MW, Schupp PJ, Dahllof I, Kjelleberg S & Steinberg PD (2004) Host specificity in marine sponge-associated bacteria, and potential implications for marine microbial diversity. *Environ Microbiol* **6**: 121–130.

Taylor MW, Schupp PJ, de Nys R, Kjelleberg S & Steinberg PD (2005) Biogeography of bacteria associated with the marine sponge *Cymbastela concentrica*. *Environ Microbiol* **7**: 419–433.

Thoms C, Horn M, Wagner M, Hentschel U & Proksch P (2003) Monitoring microbial diversity and natural product profiles of the sponge *Aplysina cavernicola* following transplantation. *Mar Biol* **142**: 685–692.

Tuma RS, Beaudet MP, Jin XK, Jones LJ, Cheung CY, Yue S & Singer VL (1999) Characterization of SYBR gold nucleic acid gel stain: a dye optimized for use with 300-nm ultraviolet transilluminators. *Anal Biochem* **268**: 278–288.

Usher KM, Fromont J, Sutton DC & Toze S (2004) The biogeography and phylogeny of unicellular cyanobacterial symbionts in sponges from Australia and the Mediterranean. *Microb Ecol* **48**: 167–177.

Vacelet J (1970) Description de cellules a bactéries intranucléaires chez des éponges *Verongia*. *J Microsc-Paris* **9**: 333–346.

Vacelet J (1971) Étude en microscopie électronique de l'association entre une cyanophycée chroococcale et une éponge du genre *Verongia*. *J Microsc-Paris* **12**: 363–380.

Vacelet J (1975) Étude en microscopie électronique de l'association entre bactéries et spongiaires du genre *Verongia* (Dictyoceratida). *J Microscopie Biol Cell* **23**: 271–288.

Vacelet J & Donadey C (1977) Electron microscope study of the association between some sponges and bacteria. *J Exp Mar Biol Ecol* **30**: 301–314.

Vergin KL, Urbach E, Stein JL, DeLong EF, Lanoil BD & Giovannoni SJ (1998) Screening of a fosmid library of marine environmental genomic DNA fragments reveals four clones related to members of the order Planctomycetales. *Appl Environ Microbiol* **64**: 3075–3078.

Voytek M & Ward B (1995) Detection of ammonium-oxidizing bacteria of the beta-subclass of the class *Proteobacteria* in aquatic samples with the PCR. *Appl Environ Microbiol* **61**: 1444–1450.

Webster NS & Hill RT (2001) The culturable microbial community of the great barrier reef sponge *Rhopaloeides odorabile* is dominated by an *Alpha-Proteobacterium*. *Mar Biol* **138**: 843–851.

Webster NS, Wilson KJ, Blackall LL & Hill RT (2001) Phylogenetic diversity of bacteria associated with the marine sponge *Rhopaloeides odorabile*. *Appl Environ Microbiol* **67**: 434–444.

Webster NS, Negri AP, Munro MMHG & Battershill CN (2004) Diverse microbial communities inhabit Antarctic sponges. *Environ Microbiol* **6**: 288–300.

Wilkinson CR (1978) Microbial associations in sponges. III. Ultrastructure of the *in situ* association in coral reef sponges. *Mar Biol* **1978**: 177–185.

Yakimov MM, Cappello S, Crisafi E, Tursi A, Savini A, Corselli C, Scarfi S & Giuliano L (2006) Phylogenetic survey of metabolically active microbial communities associated with the deep-sea coral *Lophelia pertusa* from the Apulian plateau, Central Mediterranean Sea. *Deep-Sea Res Pt I* **53**: 62–75.

Declaration of Academic Integrity / Selbstständigkeitserklärung

With this statement I declare that I have independently completed the above thesis, except for scientific consulting by my supervisor Prof. Dr. Karin Lochte. The thoughts taken directly or indirectly from external sources are properly marked as such. This thesis was not previously submitted to another academic institution.

Hiermit erkläre ich, dass ich diese Arbeit selbstständig verfertigt habe, abgesehen von der wissenschaftlichen Beratung durch meine Betreuerin Prof. Dr. Karin Lochte. Alle direkten und indirekten Zitate aus externen Quellen sind als solche gekennzeichnet. Auf der Grundlage dieser Arbeit wurde noch kein Promotionsversuch an einer anderen akademischen Einrichtung unternommen.

Kiel, …….